

0058369

Department of Energy
Richland Operations Office
P.O. Box 550
Richland, Washington 99352

NOV 12 2002

03-WMD-0031

Ms. Jane Hedges
Cleanup Section Manager
Nuclear Waste Program
State of Washington
Department of Ecology
1315 W. Fourth Avenue
Kennewick, Washington 99336

RECEIVED
NOV 11 2002
DEC 03 2002
EDMC

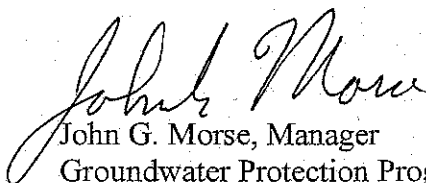
Dear Ms. Hedges:

TRANSMITTAL OF FISCAL YEAR (FY) 2002 STATUS REPORT FOR ITP# FT10WE21
TASK M - DEVELOPMENT OF A GEOCHEMICAL MODEL FOR URANIUM
TRANSPORT IN UNSATURATED AND SATURATED SEDIMENTS AT THE 200-WEST
AREA U.S. DEPARTMENT OF ENERGY HANFORD SITE, WA

Attached is the subject document for your information. The purpose of this report is to describe the activities accomplished by MSE Technology Applications, Inc. and to provide a year-end status for FY 2002 for the subject task. The objective of this task is to develop a conceptual geochemical model to quantify the mobility of uranium in the unsaturated and saturated soils associated with the 216-U1/U2 Cribs in the 200-West Area.

If you have any questions, please contact me, or you may contact Arlene Tortoso, Waste Management Division, on (509) 373-9631.

Sincerely,


John G. Morse, Manager
Groundwater Protection Program

WMD:ACT

Attachment

cc w/attach:
N. Ceto, EPA
D. Goswami, Ecology
D. Maddox, EM-40
J. Price, Ecology
Administrative Record (200-UP-1 OU)

cc w/o attach:
S. W. Petersen, FHI

FY02 Status Report for

TTP# FT10WE21 Task M

**Development of a Geochemical Model
for Uranium Transport in Unsaturated and
Saturated Sediments at the 200-West Area
U.S. Department of Energy Hanford Site, WA**

Prepared by:

MSE Technology Applications, Inc.
200 Technology Way
P.O. Box 4078
Butte, Montana 59702

September 30, 2002

**FY02 Status Report for
TTP# FT10WE21
Task M – Development of a
Geochemical Model for Uranium
Transport in the Unsaturated and
Saturated Sediments at the 200-West
Area of the Department of Energy
Hanford Site, Washington**

Prepared by:

MSE Technology Applications, Inc.
200 Technology Way
P.O. Box 4078
Butte, Montana 59702

September 30, 2002

EXECUTIVE SUMMARY

This year-end status report fulfills the fiscal year 2002 (FY02) Milestone M2-03 for TTP #FT10WE21 "Subsurface Contaminant and In Situ Remediation Projects, Subtask M". MSE Technology Applications (MSE) is funded by the Subsurface Contaminants Focus Area (SCFA) and the U.S. Department of Energy (DOE) under TTP #FT10WE21 to contribute to fulfilling needs identified by the Hanford Science and Technology Coordination Group (STCG).

MSE is focusing the efforts of the work in the 200 West Area of the Hanford Site where a plume of uranium exists in the 200-UP-1 Groundwater Operable Unit. The objective of this project is to develop a conceptual geochemical model to quantify the mobility of uranium in the unsaturated and saturated soils associated with the 216-U1/U2 Cribs in the 200 West Area of the Hanford Site, producing an acceptable correlation between predicted and observed concentrations of uranium in the groundwater.

The distribution of contaminants such as uranium in the soil profile depends on the physical properties of the waste stream, which provides the transport medium (i.e., water), and the chemical properties of the contaminant, which affect contaminant-soil interactions. Other characteristics affecting the contaminant soil interaction include the geologic and geochemical properties of the soil column and the composition of soil moisture and soil gases.

The activities accomplished during FY02 are described in this report. Laboratory analyses completed in FY02 include analyses of the soil and soil gas samples obtained during the drilling of well 299-W19-43; and completion of the laboratory batch testing for model calibration. Geochemical modeling activities completed include the incorporation of data and information from the field measurements and laboratory analyses into the geochemical model and completion of first iteration of the geochemical model. In addition, a summarization of inventory of the wastes disposed of in the 216-U1/U2 Cribs was prepared and the procurement process for the validation for the geochemical model was initiated. The available results from these activities are presented in this report.

The geochemical model parameters, sensitivity analysis of uranyl (UO_2^{+2}) adsorption modeled by MINEQL+© v. 4.5, calibration batch testing, and initial geochemical modeling results are discussed in this report. The geochemical model considers UO_2^{+2} is adsorbed to specific sorbing sites, typically composed of metal oxide or hydroxide coatings on the soil matrix.

The primary sorbents of uranium are Fe(III) and Al oxyhydroxides, clays, zeolites, phosphate minerals, and organic matter (Langmuir, 1997). Previous studies have indicated that iron-hydroxide surface sites (=FeOH) dominate UO_2^{+2} complexation in Hanford soils (Barnett et al., 2002). Consequently, MSE assumed that the primary sorbent of UO_2^{+2} in the soils was =FeOH .

MSE chose to use a diffuse layer surface complexation model for the geochemical modeling efforts. The parameters required for the diffuse layer model include: the concentration of available sorbing sites in a given volume of the soil matrix; the surface area of the sorbents exposed to the groundwater; and the thermodynamic equilibrium constants for reactions involving the surface sites and aqueous components. The remaining parameters used in the geochemical modeling of UO_2^{+2} adsorption included aqueous component concentrations, CO_2 concentrations, and thermodynamic constants. Results of the sensitivity analysis of UO_2^{+2} adsorption were used to determine which model parameters affected UO_2^{+2} adsorption most.

Calibration of the geochemical model will be completed through a series of laboratory batch tests to compare the measured sorption of UO_2^{+2} to the adsorption predicted by the geochemical model. Initial laboratory batch tests were conducted to provide calibration data. Input parameters for the geochemical model will be adjusted within reasonable bounds in order to produce an acceptable correlation between the

predicted and measured data. Because the sorption of uranium to soils is pH dependent, the model results are presented as plots of uranium sorption a function of pH.

The results of the initial geochemical model as compared to the results from the batch testing are presented in this report. The results are presented as plots of the percent of uranium adsorbed as a function of the pH under which the adsorption occurred for both the model predictions and observed data from the batch tests. The goodness-of-fit between the observed and predicted UO_2^{+2} adsorption data was evaluated quantitatively and qualitatively.

Discrepancies between the model and laboratory results may be attributed to several factors including over/under estimation of available adsorption sites, errors in thermodynamic constants, and inclusion and/or exclusion of specific chemical reactions. While the RMSE values for the models indicate poor agreement between the modeled and observed values for adsorption, the general shape of the modeled and observed sorption curves in most cases is promising. The results of this preliminary effort will be reexamined, several batch tests rerun and the batch test procedure reviewed to ensure that the modeled geochemical conditions reflected those of the batch test.

CONTENTS

EXECUTIVE SUMMARY.....	II
CONTENTS	IV
FIGURES	VI
PLATES	VI
TABLES	VII
LIST OF ACRONYMS	VIII
1 INTRODUCTION.....	1-1
1.1 BACKGROUND	1-1
1.1.1 Previous Investigations	1-1
1.1.2 Remedial Action Objectives	1-2
1.1.3 Conceptual Site Model.....	1-2
1.2 PROJECT OBJECTIVE	1-4
1.3 SCOPE	1-4
1.4 PROJECT SCHEDULE.....	1-5
1.5 PROJECT PARTICIPANTS	1-5
1.6 REPORT ORGANIZATION.....	1-5
2 DESIGN APPROACH.....	2-1
2.1 THE GEOCHEMICAL MODEL	2-1
2.1.1 Surface Complexation Parameters.....	2-2
2.1.2 Significance of Carbon Dioxide to Uranium Mobility in Vadose Zone..	2-2
2.2 EXPERIMENTAL APPROACH.....	2-3
3 FISCAL YEAR 2001 ACTIVITIES.....	3-1
3.1 PLANNING DOCUMENT PREPARATION.....	3-1
3.2 WELL 299-W19-43 DRILLING AND SOIL SAMPLING	3-2
3.2.1 Soil Chemical and Physical Properties	3-3
3.2.2 Porewater Chemistry.....	3-3
3.3 SOIL GAS INVESTIGATION.....	3-3
3.3.1 Summary of CPT Soil Gas Sampling	3-3
3.4 GEOPHYSICAL LOGGING.....	3-4
4 FISCAL YEAR 2002 ACTIVITIES.....	4-1
4.1 LABORATORY AND FIELD MEASUREMENTS	4-1
4.2 PRELIMINARY GEOCHEMICAL MODEL AND SENSITIVITY ANALYSIS.....	4-1
4.3 GEOCHEMICAL MODEL CALIBRATION AND VALIDATION.....	4-2
4.4 216-U1/U2 CRIBS WASTE DISPOSAL INVENTORY.....	4-2
5 FISCAL YEAR 2003 ACTIVITIES.....	5-1
6 FISCAL YEAR 2004 ACTIVITIES.....	6-1
7 RESULTS	7-1
7.1 FIELD OBSERVATIONS OF LITHOLOGY.....	7-1
7.1.1 Hanford formation	7-1
7.1.1.1 Hanford Unit 1	7-1
7.1.1.2 Hanford Unit 2	7-1

7.1.2	Plio-Pleistocene Unit	7-2
7.1.2.1	Palouse Soil.....	7-2
7.1.2.2	Caliche	7-2
7.1.3	Ringold Formation	7-3
7.1.3.1	Upper Ringold.....	7-3
7.1.3.2	Unit E Gravels.....	7-3
7.2	GEOPHYSICAL LOGGING DATA	7-4
7.2.1	General Geophysical Log Observations	7-4
7.2.2	Hanford Unit Geophysical Log Responses.....	7-5
7.2.3	Plio-Pleistocene Geophysical Log Responses	7-5
7.2.4	Upper Ringold Geophysical Log Responses	7-5
7.3	LABORATORY ANALYSES OF SOIL SAMPLES	7-6
7.3.1	Physical Properties and Soil Chemistry	7-6
7.3.1.1	Bulk Density and Particle Density	7-6
7.3.1.2	Particle Size Analysis	7-7
7.3.1.3	Elemental Composition of Soil from X-Ray-Florescence (XRF).....	7-7
7.3.1.4	Bulk Mineralogy from X-Ray Diffraction (XRD).....	7-7
7.3.1.5	Soil Carbon Content.....	7-7
7.3.2	Soil Moisture and Sediment-Water Extract Chemistry	7-14
7.3.2.1	Soil Moisture.....	7-14
7.3.2.2	Sediment-Water Extract pH, Eh, Conductivity, and Alkalinity.....	7-15
7.3.2.3	Carbon Concentrations of Sediment-Water Extract	7-15
7.3.2.4	Cations and Anions of Sediment-Water Extract.....	7-15
7.4	PETROGRAPHIC ANALYSIS OF SOIL SAMPLES.....	7-18
7.4.1	Hanford Soils	7-19
7.4.2	Plio-Pleistocene Unit	7-19
7.4.3	Ringold Soils.....	7-19
7.5	CITRATE-BICARBONATE-DITHIONITE (CBD) EXTRACT RESULTS.....	7-19
7.6	CARBON DIOXIDE SAMPLING RESULTS	7-20
7.6.1	Calculated pH Values	7-21
8	GEOCHEMICAL MODELING EFFORTS	8-1
8.1	SENSITIVITY ANALYSIS FOR URANIUM SORPTION.....	8-1
8.1.1	Surface Site Concentration	8-2
8.1.2	UO ₂ ⁺² Concentrations in Solution.....	8-3
8.1.3	Effect of CO ₂ Concentrations on Sorption.....	8-4
8.1.4	Effects of Ions in Solution	8-6
8.2	BATCH TESTS FOR MODEL CALIBRATION	8-9
8.2.1	Batch Test Solid Phase.....	8-10
8.2.2	Batch Test Aqueous Phase.....	8-10
8.2.3	Batch Test Gas Phase.....	8-11
8.2.4	Batch Testing	8-12
8.3	GEOCHEMICAL MODELING OF BATCH TESTS.....	8-13
8.3.1	Aqueous Component Concentrations	8-14
8.3.2	Carbon Dioxide Concentrations.....	8-14
8.3.3	Thermodynamic Data.....	8-14
8.3.4	Surface Complexation Sorbent Data.....	8-15

8.3.5	Surface Complexation Reactions.....	8-16
9	INITIAL GEOCHEMICAL MODEL EVALUATION.....	9-1
9.1	BATCH TEST RESULTS.....	9-1
9.2	INITIAL GEOCHEMICAL MODEL RESULTS.....	9-2
10	MODEL PARAMETER OPTIMIZATION/CALIBRATION STATUS	10-1
11	MODEL VALIDATION STATUS	11-1
12	PROJECTED OUT YEAR ACTIVITIES	12-1
12.1	FY03	12-1
12.2	FY04	12-1
13	REFERENCES.....	13-1
APPENDIX A DURATEK GEOPHYSICAL LOGGING REPORTS.....		I
PLATES.....		XVII

FIGURES

Figure 1-1.	Conceptual site model.....	1-3
Figure 3-1.	Location of new well (from BHI, 2001b).	3-2
Figure 7-1.	A schematic diagram showing the CO ₂ concentration measurement system and process.	7-21
Figure 7-2.	Plot of uranium sorption and frequency of pH values from CO ₂ data and laboratory measurements.....	7-23
Figure 8-1.	UO ₂ ⁺² adsorption versus total Fe concentration and at a constant pH and constant UO ₂ ⁺² concentration.....	8-3
Figure 8-2.	UO ₂ ⁺² adsorption versus total UO ₂ ⁺² concentration at constant pH and constant total Fe(III).	8-4
Figure 8-3.	Effects of Log pCO ₂ values on total percent UO ₂ ⁺² adsorption as a function of pH.	8-5
Figure 8-4.	Effects on total percent UO ₂ ⁺² adsorption from the addition of Mg ⁺² to the solution.	8-6
Figure 8-5.	Effects on total percent UO ₂ ⁺² adsorption from the addition of F ⁻ to the solution.	8-7
Figure 8-6.	Effects on total percent UO ₂ ⁺² adsorption from the addition of PO ₄ ⁻³ to the solution.	8-8
Figure 8-7.	Effects on total percent UO ₂ ⁺² adsorption from the addition of SO ₄ ⁻² to the solution.	8-9
Figure 8-8.	CO ₂ monitoring measurements acquired during the calibration batch tests.	8-12
Figure 8-9.	Batch testing laboratory setup at MSE.....	8-13
Figure 9-1.	Geochemical modeling and batch test results for MSE-CORE-101B.....	9-3
Figure 9-2.	Geochemical modeling and batch test results for MSE-CORE-104B.....	9-4
Figure 9-3.	Geochemical modeling and batch test results for MSE-CORE-106B.....	9-5
Figure 9-4.	Geochemical modeling and batch test results for MSE-CORE-112B.....	9-6
Figure 9-5.	Geochemical modeling and batch test results for MSE-CORE-119B.....	9-7

PLATES

Plate 1. Lithologic Data

- Plate 2. Sediment Mineralogy
- Plate 3. Groundwater Geochemical Data
- Plate 4. Petrographic Analysis Data

TABLES

Table 3-1. Soil Chemical and Physical Property Measurements	3-5
Table 3-2. Porewater Chemistry Measurements	3-5
Table 3-3. Soil Gas Sample Intervals	3-6
Table 3-4. Gamma-emitting isotopes addressed in addition to standard K, U, and Th isotopes.....	3-6
Table 7-1. Laboratory analytical results for soil chemistry and physical properties	7-9
Table 7-2. Laboratory analytical results for soil particle size measurements	7-10
Table 7-3. Bulk chemical analysis of soils from XRF	7-11
Table 7-5. Bulk mineralogical results from XRD analysis of soils	7-12
Table 7-7. Bulk mineralogical results from XRD analysis of clay fraction in soils	7-13
Table 7-8. Laboratory analytical results for soil carbon content	7-14
Table 7-9. Soil moisture data.....	7-16
Table 7-10. Laboratory results of sediment-water extract chemistry and physical properties.....	7-17
Table 7-11. Laboratory results for cation concentrations in the sediment-water extracts.....	7-18
Table 7-12. Laboratory results for the anion concentrations in the groundwater	7-18
Table 7-13. Laboratory results from citrate-bicarbonate-dithionate analysis	7-20
Table 7-14. Calculated pH values compared to laboratory pH measurements	7-22
Table 8-1. Summary of soil samples used in model calibration batch tests.....	8-10
Table 8-2. Measured uranium concentrations in initial batch test solutions	8-11
Table 8-3. Subsurface and batch test CO ₂ concentrations.....	8-12
Table 8-4. Aqueous component concentrations used in the initial geochemical model	8-14
Table 8-5. Soil $\equiv\text{FeOH}$ concentration values for geochemical model	8-15
Table 9-1. Results of uranium adsorption batch tests	9-1

LIST OF ACRONYMS

ARA	Applied Research Associates, Inc.
ASTM	American Standards Testing and Materials
BET	Brunauer, Emmett, and Teller
BHI	Bechtel Hanford, Inc.
CBD	citrate-bicarbonate-dithionite
CO ₂	Carbon Dioxide
Cps	counts per second
CPT	Cone Penetrometer Test
DOE	Department of Energy
DOE-RL	DOE-Richland
DOE-WETO	DOE-Western Environmental Technology Office
DOW	Description of Work
DQO	Data Quality Objective
EGM	ethylene glycol monoethyl ether
EPA	Environmental Protection Agency
ERC	Environmental Restoration Contractor
ETF	Effluent Treatment Facility
FHI	Fluor Hanford Inc.
ft-bgs	feet below ground surface
FY	fiscal year
MCL	Maximum Contaminant Level
MOU	Memorandum of Understanding
MSE	MSE Technology Applications, Inc.
MTCA	Model Toxics Control Act
PNNL	Pacific Northwest National Laboratory
ppm	parts per million
QAPP	Quality Assurance Project Plan
RAO	Remedial Action Objective
ROD	Record of Decision
SAP	Sampling and Analysis Plan
SCFA	Subsurface Containment Focus Area
STCG	Science and Technology Coordination Group
STR	Subcontractor Technical Representative
WHC	Westinghouse Hanford Company
UO ₂ ⁺²	uranyl
XRF	x-ray-florescence
XRD	x-ray diffraction
≡FeOH	iron-hydroxide surface sites

1 INTRODUCTION

This year-end status report update fulfills the fiscal year 2002 (FY02) Milestone M2-03 for TTP #FT10WE21 "*Subsurface Contaminant and In Situ Remediation Projects, Subtask M*". MSE Technology Applications (MSE) is funded by the Subsurface Contaminants Focus Area (SCFA) and the U.S. Department of Energy (DOE) under TTP #FT10WE21 to contribute to the following needs identified by the Hanford Science and Technology Coordination Group (STCG).

- 1) RL-SS28 "*Understand, Quantify, and Develop Descriptions of Reactions and Interactions between Contaminants of Concern and Vadose Zone Sediments*"; and
- 2) RL-SS32, "*Understand and Quantify the Relationship Between Contaminant Sources, Vadose Zone Plume Properties, and Groundwater Plume Properties at Hydrologic Boundaries with a Focus on the Groundwater-Vadose Zone Interface*".

The work addressed by these needs is considered critical to the success of the Accelerated Cleanup: Paths to Closure (ACPC). Other needs that this work may feed into include RL-SS12, "*Cost-Effective, In-situ Remediation of the Vadose Zone of One or More of the Following Radionuclides: Uranium, Plutonium, Cesium, Cobalt, or Strontium-90*"; and RL-SS16, "*In-situ Characterization to Determine the Extent of Soil Contamination of One or More of the Following Radionuclides: Uranium, Plutonium, Cesium, Cobalt, or Strontium-90*".

RL-SS12 and RL-SS16 are remediation needs that address general technology gaps in characterization, monitoring, and remediation. These specific needs call for application of innovative technologies, which can also include novel combinations of existing technologies.

1.1 BACKGROUND

MSE is focusing the efforts of the work in the 200 West Area of the Hanford Site where a plume of uranium exists in the 200-UP-1 Groundwater Operable Unit. The contaminated groundwater is primarily associated with discharges to the U1 and U2 cribs in the 200-Area. Currently, a pump and treat system is in place at the site that is designed to reduce the contaminant mass within the plume and minimize migration of uranium and technetium-99 from the 200 West Area. Analytical data from monitoring wells located within and around the contaminated groundwater indicate the pump and treat system is effectively removing the technetium-99 from the groundwater, however, it is not removing enough uranium from the groundwater to meet the compliance requirements for the site. The purpose of the study is to focus on uranium and how it interacts with the soil in terms of adsorption to the soil matrix.

Technetium-99, nitrate, and carbon tetrachloride are also present within 200-UP-1 Operable Unit in concentrations above the maximum concentration limit (MCL) for drinking water under the Safe Drinking Water Act. These contaminants have been adequately addressed by the pump and treat system, or are being addressed by other remedial systems and are not of specific concern at this site. However, other contaminants that may be present at the site may be considered from the standpoint of the impact they may have on the mobility of the uranium.

The remedial action objective (RAO) for uranium in the groundwater, as stated in the Interim Action Record of Decision for the 200-UP-1 Operable Unit (EPA, February 1997), at the site is 480 micrograms per liter ($\mu\text{g/L}$). This value corresponds to 10 times the cleanup level for uranium under the Washington State Department of Ecology's Model Toxics Control Act (MTCA).

1.1.1 Previous Investigations

Previous investigations at the site include:

- 1) U1/U2 Uranium Plume Characterization (WHC June 1, 1988);
- 2) 200 West Area Limited Field Investigation (BHI March 1995);
- 3) Waste Site Grouping for 200 Areas Soil Investigations (DOE/RL January 1, 1997); and
- 4) 200 Areas Remedial Investigation/Feasibility Study (DOE/RL April 1, 1999).

1.1.2 Remedial Action Objectives

The remedial action objective (RAO) for uranium in the groundwater, as stated in the *Interim Action Record of Decision for the 200-UP-1 Operable Unit* (EPA, February 1997), at the site is 480 micrograms per liter ($\mu\text{g/L}$). This value corresponds to 10 times the cleanup level for uranium under the Washington State Department of Ecology's *Model Toxics Control Act* (MTCA).

In FY99, the average uranium concentration in extraction well 299-W19-39 was 210 $\mu\text{g/L}$. Uranium concentrations have ranged from 275 $\mu\text{g/L}$ in 1997 to 210 $\mu\text{g/L}$ at the end of FY99 in the extraction well. Downgradient, in well 299-W19-40, the uranium concentration was approximately 200 $\mu\text{g/L}$. However, concentrations of uranium within the plume exceed the RAO.

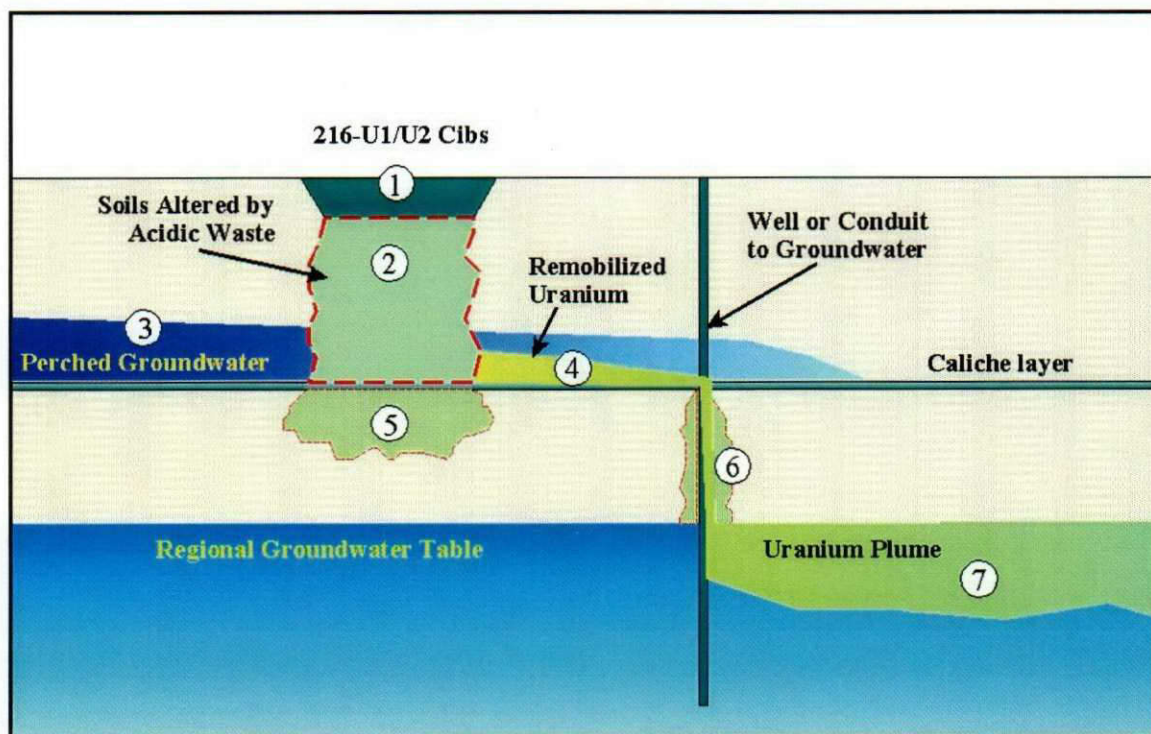
1.1.3 Conceptual Site Model

The following description of the distribution of uranium contamination at the site is taken from the *Interim Action Record of Decision (ROD) for the 200-UP-1 Operable Unit* (EPA, February, 1997).

The 200 West Area is an operational area of approximately 5.1 square kilometers (1.97 square miles) where spent nuclear fuel was processed in four main facilities: U Plant (primarily uranium recovery); Z Plant (primarily plutonium separation and recovery); and S and T Plants (primarily uranium and plutonium separation from irradiated fuel rods).

Contamination in the 200-UP-1 Operable Unit resulted from historic discharges of process water from the UO3 Plant to five primary liquid waste disposal sites (cribs). The predominant contaminants were uranium and technetium-99. The major portion of discharge to the soil column was via two cribs (216-U1 and 216-U2) between 1951 and 1968, which transported the mobile constituents, particularly technetium-99, to the water table. However, most of the uranium discharged to the cribs was retained in the upper 20 meters (66 feet) of the soil column. During the final years of the cribs operation (1966 through 1968), small volumes of highly acidic decontamination wastes were discharged, which resulted in the dissolution and transport of part of the previously deposited autunite (uranium phosphate). Low concentrations of uranium were detected in the groundwater monitoring wells near 216-U1/U2 during this period. The majority of dissolved uranium was distributed throughout the soil column beneath the crib with the largest concentration deposited above a caliche layer at about 50 meters (164 feet) depth. During 1984, large volumes of cooling water were discharged to the adjacent 216-U16 crib, which reportedly resulted in transport of uranium to the groundwater. This history and the contaminant flow path are captured in Figure 1-1, generated by MSE to facilitate the understanding of the site.

Conceptual Model for Uranium Transport to the Groundwater from the 216-U1/U2 Cribs 200 West Area, Hanford Site



- ① Dilute acidic liquid waste containing uranium was disposed to the ground through the 216-U1/U2 cribs from 1957 until 1968. The uranium was immobilized in the soil by the formation of an insoluble carbonate-phosphate compound.
- ② From 1966 through 1968, the pH of the waste stream decreased and the uranium was re-mobilized and deposited deeper into the soils, possibly to a caliche layer. The more acidic waste stream may have also altered the soils directly below the cribs.
- ③ In the early 1980's, cooling water was discharged to a crib (216-U16) located south of the 216-U1/U2 cribs, creating a perched water table on the caliche layer.
- ④ This perched water may have been responsible for transporting the more mobile uranium to a vertical conduit, such as a well or thin spot in the caliche layer.
- ⑤ Some of the uranium may have permeated to the soil below the caliche layer beneath the 216-U1/U2 cribs.
- ⑥ The mobile uranium traveled down the vertical conduit to the regional groundwater table. As it traveled, the uranium may have permeated into the soils surrounding the conduit.
- ⑦ Upon reaching the water table, the uranium spread out and formed the uranium plume found at the site.

Figure 1-1. Conceptual site model.

During 1985 uranium concentrations in the groundwater abruptly increased from 166 to 72,000 pCi/L. Limited pump and treat activities were initiated in 1985 to recover the uranium from the groundwater using ion exchange. During the six months of pump and treat, about 687 kilograms (1,500 pounds) of uranium were recovered and the concentration in well 199-W19-3 was reduced to 1,700 pCi/L.

From September 1995 to February 1997, the Phase I pump-and-treat injection operations operated using a single extraction well and a single injection well. Operations were halted from February 8, 1997 to March 30, 1997.

On February 25, 1997, an interim action ROD was issued for the 200-UP-1 pump-and-treat operations. The selected remedy consisted of pumping and treating the highest concentration zone of the uranium and technetium-99 plumes. Before the interim action ROD, groundwater was treated onsite using ion-exchange technology and granular activated carbon. Since starting Phase II of the operations in March 1997, groundwater is transported to the Effluent Treatment Facility (ETF). Once treated, the groundwater is discharged to the state-approved land disposal site north of the 200 West Area.

In addition to the uranium and technetium-99 plumes, nitrate and carbon tetrachloride are also present within 200-UP-1 Operable Unit in concentrations above the MCL for drinking water. Nitrate contamination resulted from discharges of neutralized nitric acid to various cribs located in the U Plant and S Plant areas. The source for the carbon tetrachloride is believed to be upgradient and outside the 200-UP-1 Operable Unit, and associated with the Z Plant disposal sites. The extent of carbon tetrachloride and nitrate contaminant plumes are much larger compared to uranium and technetium-99 plumes. Carbon tetrachloride contamination in the groundwater is found throughout the entire 200 West Area. A small amount of carbon tetrachloride was used as a degreasing agent in the 200 Area. The nitrate plume extends from west of the 200 Area to the Columbia River. The nitrate plume is much larger and coalesces with other nitrate contaminant plumes from a number of 200 West Area facilities.

The leading edge of the uranium plume has migrated beyond the 200 West Area boundaries. The combined uranium and technetium-99 plume covers an area of approximately 0.5 square kilometers (0.2 square miles).

1.2 PROJECT OBJECTIVE

The objective of this project is to develop a conceptual model of uranium mobility in the unsaturated and saturated soils associated with the 216-U1/U2 Cribs in the 200 West Area of the Hanford Site, producing an acceptable correlation between predicted and observed concentrations of uranium in the groundwater.

1.3 SCOPE

The scope of the project includes the following tasks:

1. Sampling of the soil and porewater for analysis of chemical and physical properties to develop a surface complexation model for the site. This will be used to determine the variation in the partitioning of the uranium between the soil and porewater for the site soil profile.
2. Using the surface complexation model, new partitioning relationships for potential contaminant transport paths at the site will be developed.
3. The new partitioning relationships will be used to simulate uranium transport for each potential transport path including its source.
4. The model providing the best fit of the simulated results with observed data will be used to update the conceptual model of uranium transport at the site.

The majority of the data that are being used for developing the geochemical model were obtained from analysis of soil and porewater samples acquired during the installation of well 299-W19-43 in FY01 within the UP-1 Operable Unit. Other data sources include soil samples from the Hanford core library, data obtained from a cone penetrometer test (CPT) conducted near the location of well 299-W19-43, and information obtained from previous documentation on the cribs of concern and their waste inventory.

The sampling effort, coordinated in conjunction with Bechtel Hanford, Inc. (BHI), the organization responsible for work in this area before July 1, 2002, followed site work requirements and protocols. BHI, as representative of the host site, assumed responsibility for coordination of in-kind and direct sampling support for this effort, and therefore provided the EM-40 cost sharing. The host site also provided support in the areas of site interface and documentation requirements.

1.4 PROJECT SCHEDULE

The project will be completed over a four-year period. The sampling was completed, and the laboratory analysis initiated during FY01. During FY02, the laboratory analyses and the stratigraphic, lithologic, and geochemical profiles for the site were completed. Also in FY02, the first iteration of a geochemical model and the laboratory batch tests for model calibration were completed. In FY03, the calibration of the geochemical model will be completed and the model will be validated. Once this is completed, the conceptual model will be refined and recommendations for remedial alternatives will be presented. This status report was initially prepared at the end of FY01, updated at the end of FY02, and will be updated again in FY03. A final closeout report for the project will be prepared at the end of FY04.

1.5 PROJECT PARTICIPANTS

The project participants have been MSE, BHI, Fluor Hanford Inc. (FHI), DOE-Richland Office (DOE-RL), and the Washington State Department of Ecology (Ecology). The roles and responsibilities of each party are defined in the project management plan (MSE, 2001a) and the Memorandum of Understanding (MOU) (BHI, 2001a).

1.6 REPORT ORGANIZATION

This report is organized to capture the efforts completed during FY01 and FY02, and to provide sufficient background of the project to support these efforts. The report includes a summary of the project design and approach followed by a review of the activities completed during FY01 and FY02, and the results of these activities. Also included are the projected out year activities for the project.

2 DESIGN APPROACH

The distribution of contaminants such as uranium in the soil profile depends on the physical properties of the waste stream, which provides the transport medium (i.e., water), and the chemical properties of the contaminant, which affect contaminant-soil interactions. Other characteristics affecting the contaminant soil interaction include the geologic and geochemical properties of the soil column and the composition of soil moisture and soil gases. Contaminant soil interaction is generally described in terms of the following processes:

1. Adsorption and desorption including ion exchange;
2. Precipitation and dissolution;
3. Filtration and remobilization of colloids and suspended particles; and
4. Diffusion into micro-pores within mineral grains.

Of these, adsorption and desorption of the contaminant to the soil matrix are probably the dominant processes for site conditions. As such, the project has been designed to understand controls on these processes. Precipitation and dissolution are also expected to influence uranium mobility, and will be investigated during the project. The other processes listed will be addressed to determine their relative importance. However, they are not expected to be important to the mobility of uranium at the site.

2.1 THE GEOCHEMICAL MODEL

A geochemical model of the site will be developed to describe the mobility of uranium in unsaturated and saturated zones for the existing site conditions. To provide the best geochemical model, both the unsaturated and saturated zones must be characterized. The unsaturated zone is important because uranium is likely still bound in the soil. Consequently, the unsaturated zone is a potential continuing contaminant source. Likewise, the saturated zone is important because it is the primary focus of the current remedial action (pump-and-treat).

The geochemical model will be used to enhance the current conceptual model of the site. The conceptual model is the basis for developing flow and transport models, which serve to evaluate potential remedial options for the site. It is imperative to study and understand the entire mobility system, including the contaminant source, vadose zone transport and adsorption processes, and the saturated zone transport and adsorption processes. Concentrating on just one of these could potentially lead to the implementation of a remedial action that will ultimately fail. By characterizing and understanding the entire process, future modeling of the uranium mobility will be significantly more detailed and as a result, a more successful remedial system can be designed.

Developing the geochemical model will require going beyond empirical adsorption isotherm models, which cannot be extrapolated to conditions that differ from those considered in model parameterization. Surface complexation adsorption models can allow such extrapolation (Langmuir, 1997), and so may be used to predict uranium adsorption/desorption under conditions that might be encountered during various remediation scenarios outside those studied.

The use of surface complexation models requires an understanding of the chemical and physical properties of the soil, porewater (unsaturated zone), groundwater (saturated zone), and the waste stream. Surface complexation models take into account changes in adsorption as a function of pH and concentrations of competing ions and complexed species; and therefore are well suited to conditions of changing pH and soil/groundwater chemistry. Such variable conditions are expected at the site, due to the variable nature of the waste stream. Additionally, remedial options for the site may also require consideration of the effects of changing soil/groundwater chemistry, including pH, on uranium mobility.

Once the geochemistry of the system is understood, both laboratory experiments and complexation modeling can be undertaken to describe the mobility of the uranium in the unsaturated and saturated sediments. This approach will allow a better understanding of the movement of uranium from the vadose zone to the groundwater. Moreover, the mobility of uranium in the groundwater will be better understood. The detailed characterization of the unsaturated and saturated zones, with respect to uranium mobility, will permit a more precise evaluation of various remediation options for the site. Results from the surface complexation model will be validated through additional laboratory analysis on the unsaturated and saturated zone soil samples acquired from the borehole.

2.1.1 Surface Complexation Parameters

The following discussion of surface-complexation model parameters is from Langmuir (1997). There are several surface complexation-modeling schemes. The three most common are the diffuse layer model, the constant capacitance model, and the triple layer model. All yield the same general solutions, however, the diffuse layer model requires the least number of parameters to execute. All of the models require the concentration of available sorbing sites in a given volume of the soil matrix, which is a function of the surface area of sorbents exposed to the porewater solution and the surface charge density of the sorbents. The concentration of available sorbing sites is typically expressed as the number of moles of sorbing sites in contact with a liter of solution. The concentration of sorbing sites is determined from the following relationship (Langmuir, 1997).

$$\Gamma_{SOH} \text{ (mol} \cdot \text{sites / L)} = \frac{N_s \text{ (site / m}^2\text{)} \times S_A \text{ (m}^2 \text{ / g)} \times C_s \text{ (g / l)}}{N_A \text{ (sites / mole} \cdot \text{sites)}} \quad \text{Equation 1}$$

Where: Γ_{SOH} is the concentration of sorbing surface sites, measured in moles of monovalent sites exposed to a liter of solution, N_s is the surface site density, S_A is the surface area per weight of sorbent, C_s is the weight of sorbent in contact with a liter of solution, and N_A is Avogadro's number of sorbent sites per moles of sites.

The primary sorbents of uranium are Fe(III) and Al oxyhydroxides, clays, zeolites, phosphate minerals, and organic matter. The relative importance of sorbents can be determined through physical and optical examination including a particle size determination and chemical and mineralogical analysis of the soils. The model also requires equilibrium, or so-called intrinsic constants, that describe the adsorption and desorption of protons, and important cations, ligands and metal complexes. Measured and estimated intrinsic constants are available for a wide range of adsorption reactions on different mineral surfaces, as are other properties including mineral surface areas and surface charge densities (Dzombak and Morel, 1990; Langmuir, 1997). These values will be reexamined and possibly refined through the analytical work in FY03. Many researchers have noted that any of the surface complexation models do equally well in general at modeling and predicting the adsorption behavior of uranium and other metals accurately (Turner, 1995). For this reason, and because the diffuse layer model is the simplest of these models to parameterize and apply, it has been chosen for this study.

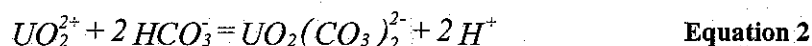
2.1.2 Significance of Carbon Dioxide to Uranium Mobility in Vadose Zone

Literature indicates that the concentration of CO_2 within the unsaturated zone may vary as much as one hundred fold of the CO_2 concentration in the atmosphere above grade, where it occurs at the level of approximately 330 parts per million (ppm). Concentration of CO_2 controls the uranium mobility because the uranyl ion (UO_2^{+2}) adsorption in soil is pH dependent, and the pH depends on concentration of CO_2 ; the higher the CO_2 concentration, the lower the pH. Experiments show that uranyl adsorption by ferric oxides increases with a pH of up to 6 or 7, and then decreases with the uranium being desorbed, i.e., mobilized at higher pHs. In other words, uranyl is most mobile at low and high pH values and tends to be adsorbed if pH is close to neutral.

Although similar principles control the mobility of uranium in the saturated zone, the analytical approach to groundwater sampling is slightly different. Measurement of the groundwater pH is a routine procedure

involving a direct measurement. However, for the unsaturated zone there is no cost-effective method to measure the pH of soil moisture at depth. Consequently, values of pH must be calculated from the measured values of CO_2 .

The mobility of hexavalent uranium [U(VI)] in unsaturated zone waters usually depends on its occurrence as carbonate complexes, which make uranium highly mobile. When U(VI) is in the form of a carbonate complex, it is poorly adsorbed and its minerals become orders of magnitude more soluble than if it occurs as an uncomplexed free UO_2^{2+} . Important carbonate complexes include UO_2CO_3^0 , $\text{UO}_2(\text{CO}_3)_2^{-2}$, and $\text{UO}_2(\text{CO}_3)_3^{-4}$. The carbonate complexes dominate the chemistry of U(VI) in most natural waters above pH 5-6. Their occurrence and abundance depend on both the pH and alkalinity of the water, as can be seen by the reaction forming the dicarbonate complex which may be written:

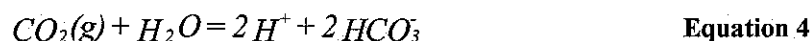


The equilibrium constant for this reaction is:

$$K_{eq} = \frac{(\text{UO}_2(\text{CO}_3)_2^{-2})(\text{H}^+)^2}{(\text{UO}_2^{2+})(\text{HCO}_3^-)^2} \quad \text{Equation 3}$$

These expressions show that an increase in alkalinity or pH favors formation of the complex.

It is possible to extract unsaturated zone moisture and analyze it to determine the alkalinity, but there is no cost-effective way to measure the pH of soil moisture at depth. However, the pH of unsaturated zone waters depends on the CO_2 pressure in the unsaturated zone air, as is evident in the following reaction:



For which:

$$K_{eq} = \frac{(P_{\text{CO}_2})}{[\text{H}^+]^2 [\text{HCO}_3^-]^2} \quad \text{Equation 5}$$

The CO_2 pressure of unsaturated zone air cannot be assumed equal to its value of about 0.0003 bars found in atmospheric air. In fact, its pressure at depth is likely to be 10 to 100 times greater (cf. Langmuir, 1997, p. 158). Nevertheless, if the partial pressure of CO_2 gas in the unsaturated zone air and the alkalinity of the water are measured, the pH of soil moisture can be computed through Equation 5. The computed pH and measured alkalinity permit the calculation of concentrations of carbonate complexes through Equation 3, thereby making it possible to estimate the solubility of U(VI) and its tendency to be adsorbed. In other words, the measured alkalinity and CO_2 pressure permit estimating the mobility of uranium in the unsaturated zone, provided other geochemical information, e.g., sorption sites, etc., is available.

MSE proposed to focus soil-sampling activities in the Plio-Pleistocene unit, specifically the caliche layer often present in the unit. Sampling was concentrated in this zone in an attempt to quantify the impact of the caliche layer on CO_2 concentration in the formation air (MSE, 2001b).

2.2 EXPERIMENTAL APPROACH

The results of the diffuse layer model are typically expressed in terms of the concentration of sorbate in the porewater and the amount adsorbed to a given surface area of soil material. If the effective surface area of a weight of sorbent material is known, partitioning relationships can be derived from these results

(Langmuir, 1997; Pabalan et al., 1998). The power of the surface complexation approach is that the partitioning relationships can be developed for various soil conditions that currently exist at the site, and for different conditions that might arise during remedial efforts. The result is a dynamic model for predicting uranium mobility at the site, which may then be used to:

1. Target the remedial action to the most probable subsurface region that has been the main contributor to the groundwater plume.
2. Select an appropriate remedial action to stabilize or remove the contaminant source.
3. Evaluate options to meet the remedial action objectives for the uranium plume in the groundwater.

The investigative approach is primarily based on the assumption that the stratigraphy defined in nearby boreholes is locally consistent and representative of the project site. This assumes that the soils sampled during the well installation and samples taken from existing core(s) are representative of the condition of the soils below the cribs before the disposal of waste to the cribs.

Additionally, it is assumed that the waste stream history is sufficiently well known such that when combined with the geochemical and conceptual models, the mass of uranium that is still being recharged to the groundwater from the soil column can be estimated.

3 FISCAL YEAR 2001 ACTIVITIES

The activities completed during FY01 are described in this section. These include development of project planning documents, installation of well 299-W19-43 from which soil and soil gas samples were obtained for analysis, acquisition of borehole geophysical data from well 299-W19-43, and completion of a additional soil gas sampling using a CPT. The laboratory analysis of the samples obtained during the drilling was also initiated.

3.1 PLANNING DOCUMENT PREPARATION

Early in FY01, MSE and BHI worked together to better focus the project efforts and to plan the project objectives to meet the Hanford site need of quantifying the mobility of uranium in the unsaturated and saturated soils associated with the 216-U1/U2 Cribs in the 200 West Area. In addition to conference calls for the project coordination, several planning meetings were held at the Hanford Site and the data quality objective (DQO) process was initiated to identify the project issues and focus the project goals.

Representatives from MSE, BHI, DOE Western Environmental Technology Office (DOE-WETO), DOE Richland Office (DOE-RL), Washington State Department of Ecology, Pacific Northwest National Laboratory (PNNL), and CH2M Hill Hanford, Inc. were involved in the initial project planning and DQO process.

From those initial planning meetings and the subsequent weekly conference calls, the following planning documentation was developed by MSE in support of the project:

- *Data Quality Objectives Summary Report for Development of a Conceptual Geochemical Model for Uranium Transport in the Unsaturated and Saturated Sediments at the 200 West Area of the DOE Hanford Site, Washington* (MSE, 2001c);
- *Multi-Year Implementation and Project Management Plan for Development of a Conceptual Geochemical Model for Uranium Transport in the Unsaturated and Saturated Sediments at the 200 West Area of the DOE Hanford Site, Washington* (MSE, 2001a);
- *Sampling and Analysis Plan (SAP) for Development of a Conceptual Geochemical Model for Uranium Transport in the Unsaturated and Saturated Sediments at the 200 West Area of the DOE Hanford Site, Washington* [including the Quality Assurance Project Plan (QAPP)] (MSE, 2001b);
- *Memorandum of Understanding (MOU) Between MSE Technology Applications, Inc., and Bechtel Hanford, Inc. For Site Access and Quality Assurance, Environmental, Health, and Safety Oversight* (BHI, 2001a);
- *Health and Safety Plan for Carbon Dioxide Sampling of the Borehole at the 200 West Area of the Hanford Site in Support of the Uranium Mobility Study in the 200 West Area of the Hanford Site* (MSE, 2001d); and
- *Description of Work: Soil Gas CO₂ Concentration and Soil Moisture Investigation at 200 West Area Hanford Site for the UP-1 Uranium Mobility Investigation* (MSE, 2001e).

Each of these documents was developed according to BHI requirements for conducting fieldwork on the Hanford Site and reviewed by BHI. DOE-RL and Ecology reviewed the Data Quality Objectives Summary Report, and the SAP. DOE-RL also reviewed the Multi-Year Implementation and Project Management Plan and the Description of Work for the soil gas sampling. In addition to the preliminary planning meetings, MSE, BHI, and DOE-RL participated in several supplementary meetings to further plan and finalize the field sampling efforts, field logistics, and support activities.

3.2 WELL 299-W19-43 DRILLING AND SOIL SAMPLING

In an effort to expedite the removal of uranium and technetium from the groundwater in 200-UP-1 OU, DOE-RL and Ecology agreed to convert former injection well 299-W19-36 into an extraction well. As a result of this action, a new groundwater monitoring well (299-W19-43) was needed in close enough proximity to well 299-W19-36 to monitor extraction well performance, hydraulic conditions, and contaminant concentrations. Existing groundwater monitoring wells 299-W19-28, 299-W19-29, and 299-W19-34A were considered to meet this objective; however, wells 299-W19-28 and 299-W19-29 have recently gone dry, and well 299-W19-34A is screened too deep (top of screen is approximately 60 ft below the water table) in the aquifer to effectively monitor extraction well performance (BHI, 2001b).

Cable-tool drilling methods were used to advance borehole 299-W19-43 to a total depth of 296 feet from July 2, 2001 through July 20, 2001. The location of the borehole is shown in Figure 3-1. The installation and sampling of the well was completed by BHI. The sampling followed the MSE Sampling and Analysis Plan (MSE, 2001b) prepared for the project.

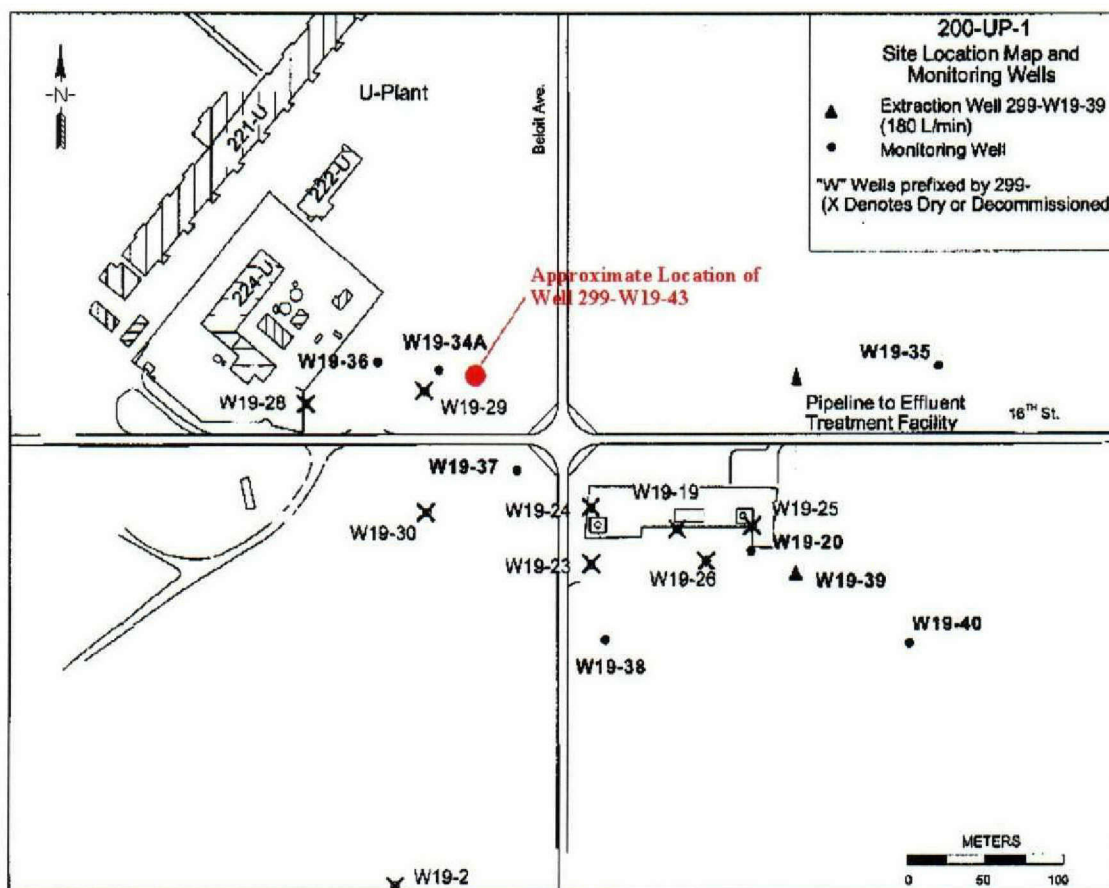


Figure 3-1. Location of new well (from BHI, 2001b).

The borehole was advanced to 274.5 feet using a drive barrel and split-spoon sampling methods; a hard-tool bit was used to advance the borehole from 274.5 feet to total depth. Temporary threaded steel casing was used to keep the borehole open as the borehole was advanced to total depth. Twelve-inch diameter casing was used to a depth of 50 feet; eight-inch diameter casing was used to total depth. Split-spoon soil samples enclosed in Lexan liners were recovered at various intervals as the borehole was advanced through the section, according to the project sampling and analysis plan (MSE, 2001b). The samples were

submitted to Battelle Labs, the laboratory subcontracted by MSE for the laboratory analysis. In addition to the split-spoon samples, soil grab samples were collected at 10-foot intervals from cuttings for laboratory soil-moisture analysis. These were also submitted to Battelle for analysis.

Stratigraphic and lithologic descriptions were recorded as the borehole was advanced to total depth. Three primary stratigraphic rock-units were described that included, from youngest to oldest, the Hanford formation, Plio-Pleistocene Unit, and Ringold Formation. Several subunits were recognized within each of the primary units. These units included Unit 1 and Unit 2 of the Hanford formation, Palouse Soil and Caliche of the Plio-Pleistocene Unit, and the Upper Ringold and Unit E Gravels of the Ringold Formation. A detailed stratigraphic column of these units including all split-spoon sampling intervals; grab sample points; depths of temporary casing; and various geophysical logs was compiled.

3.2.1 Soil Chemical and Physical Properties

The analysis of the soil chemistry and physical properties included identifying the major mineral composition; analysis of the grain coatings and precipitates present in the soil matrix; determination of the grain size distribution; and surface area of the sediments. The measurements for soil chemical and physical properties are listed in Table 3-1.

3.2.2 Porewater Chemistry

The porewater analysis included determination of the major ions in solution, alkalinity, dissolved CO₂ in the unsaturated zone (via soil gas sampling), and pH. The measurements for porewater analysis are listed in Table 3-2.

3.3 SOIL GAS INVESTIGATION

Dissolved CO₂ and alkalinity control the concentration of carbonate species, including uranyl carbonate complexes, in the porewater by affecting the pH of solution. Since it is not feasible to measure pH in the unsaturated zone porewater, dissolved CO₂ must be determined from measurements of the CO₂ concentration in the soil gas.

The investigation of CO₂ gas in the unsaturated zone consisted of field measurements of CO₂ concentration, analytical confirmatory work on CO₂ concentration, and isotope composition. Field measurements were completed for depths from 80 to 253 feet-below ground surface (ft-bgs) while drilling using a cable-tool drilling rig. The soil-gas sampling intervals are described in Table 3-3. Soil-gas samples were submitted to the University of Waterloo Environmental Isotope Laboratory, also working under subcontract to MSE, for analysis. However, inappropriate sampling containers compromised the quality of the analytical results received from this laboratory for the turn around time. The CO₂ investigation on the upper section of the unsaturated zone (ground surface to 43 ft-bgs) was completed using a cone penetrometer; the intervals sampled are described in Section 3.3.1 Summary of CPT Soil Gas Sampling.

To enable the collection of this data, MSE developed the "Subsurface CO₂ Sampling System", which was subsequently used to collect the soil-gas data during the borehole drilling. Because of MSE's use of this innovative system at the Hanford Site, DOE-RL was able to claim an additional deployment during FY01.

3.3.1 Summary of CPT Soil Gas Sampling

MSE subcontracted Applied Research Associates, Inc. (ARA) to provide CPT support for soil gas sampling and additional data acquisition in the UP-1 Operable Unit at the Hanford Site 200 West Area. The scope of work was to acquire data (i.e., soil gas samples, pore pressure, conductivity (for soil moisture estimation), sleeve friction, and tip stress) from the surface to at least 100 ft-bgs in the area near well 299-W19-43. Up

to three boreholes were planned for acquiring the CPT data. In the end, however, the CPT was not able to achieve the 100 ft performance depth.

Three borehole locations were positioned 15-ft to the south of well 299-W19-43 and 10-ft apart, as described in the Description of Work for this activity prepared by MSE (MSE, 2001e). The CPT tools consisted of a cone "sipper" and the basic tool head for acquiring pore pressure, conductivity (soil moisture), sleeve friction, and tip stress. For the first borehole, soil gas samples were acquired every 5-ft starting 5-ft bgs and at a depth of approximately 43-ft bgs, the depth achieved before refusal. While extracting from the hole, the cone "sipper" and one length of rod were lost down the hole approximately 8-ft bgs. After attempts to recover the equipment failed, ARA pushed to a depth of 40.8-ft bgs and backfilled with bentonite granules to a depth of approximately 10-ft bgs.

At the second borehole location ARA setup the basic CPT tool head for acquiring pore pressure, conductivity, sleeve friction, and tip stress. ARA pushed the basic tool head to a depth of 63.5-ft bgs before meeting with refusal. Like the previous push, resistance was encountered at about 41-ft bgs. The second hole was backfilled with bentonite granules to a depth of approximately 8.5-ft bgs.

Instead of moving to the third borehole location, ARA attempted another push at the second borehole location, approximately 2-ft from the first attempt. This time the cone "sipper" was used. Unfortunately, ARA was only able to push down to 42.41-ft bgs before meeting refusal. During the push MSE acquired soil gas samples at 20-ft, 40-ft, and 42.41-ft bgs. This hole was backfilled with bentonite granules to a depth of approximately 8.5-ft bgs.

It was decided that additional pushes would most likely have similar results. The remaining upper portions of the boreholes were abandoned with cement and tagged as per the subcontract technical representative (STR) request.

3.4 GEOPHYSICAL LOGGING

To compliment the geologist observations and the analytical laboratory data, high-resolution spectral gamma and neutron moisture data were acquired from 50 to 257 ft-bgs in well 299-W19-43. The purpose for these data was to better define the distributions of the soil moisture and gamma emitting isotopes between the soil sample intervals.

The results of the logging effort are presented and discussed further in Section 7.2. Under subcontract to MSE, Duratek completed the logging efforts during off-hours to prevent interference with the drilling activities.

The spectral gamma logging was completed using standard logging procedures including those described in *American Society for Testing and Materials (ASTM) D 5753-95e1* and *ASTM D 6274-98* (total gamma). Data acquisition was completed in a continuous logging mode at a rate that ensured the data are valid on an interval of at least 1 foot. The standard energy windows for potassium (K), uranium (U), and thorium (Th) were recorded and plotted. Other gamma-emitting isotopes of interest that were also addressed by the spectral gamma logging are shown in Table 3-4.

Neutron soil-moisture logging was completed using standard logging procedures, including those described in *ASTM D 5753-95e1*. Data acquisition was completed in a continuous logging mode, following the procedures outlined in Sections 8.2 through 8.4 of *ASTM D 6031-96*. The logging proceeded at a rate that ensured the data are valid on an interval of at least 1 foot. The 8-inch Duratek calibration coefficients were used for the soil-moisture logs as described in the moisture log analysis and summary provided by Duratek for this effort. A copy of the summary is included in Appendix A. However, as stated later in Section 7, there are discrepancies between the neutron soil-moisture data and laboratory measurements of soil moisture.

Table 3-1. Soil Chemical and Physical Property Measurements

Parameter	Measurement Method	Reference
Sediment Mineralogy, to include grain coatings and precipitates*	Optical Mineralogical Analysis	Methods of Soil Analysis, Part I, Chapter 8
	X-ray Analysis	Methods of Soil Analysis, Part I, Chapter 12
Shape Factor of Soil Particles*	Optical Mineralogical Analysis	Methods of Soil Analysis, Part I, Chapter 8
Grain Size Distribution	Sieve Analysis	Methods of Soil Analysis, Part I, Chapter 15
Surface Area*	BET Analysis	Methods of Soil Analysis, Part I, Chapter 16
Soil Organic Matter	Combustion	Methods of Soil Analysis, Part III, Chapter 34
Specific Density	Pycnometer Method	Methods of Soil Analysis, Part I, Chapter 14
Bulk Density	Core Method	Methods of Soil Analysis, Part I, Chapter 13
Speciation of Uranium bound to Soil Matrix*	Dissolution of Metals	Methods of Soil Analysis, Part III, Chapter 3
Identifying the Main Sorbent(s) of Uranium*	Optical Mineralogical Analysis	Methods of Soil Analysis, Part I, Chapter 8
	Electron Microscope	NA
Surface Charge Density of the Main Sorbent(s) of Uranium.	Literature Values	Langmuir, 1997
Percent Soil Moisture (Field)	"Speedy" Soil Moisture	ASTM D 4944-89
Percent Soil Moisture (Lab)	Laboratory Measurement	ASTM D 4959-89 (1994)
Percent Soil Moisture (Borehole)	Neutron Moisture Log	ASTM D 5220-92

Table 3-2. Porewater Chemistry Measurements

Parameter	Measurement Method	Reference
Major Anions (SO ₄ , Cl)	Laboratory Analysis by Ion Chromatography	EPA SW-846, Method 9056
Total Recoverable Metals (Ca, Mg, Na, K)	Laboratory Analysis by Inductively Coupled Plasma Furnace	EPA SW-846, Preparation Method 3005A, ICP Method 6010B
Iron Speciation	Laboratory Analysis by Colorimetric	EPA Standard Methods 3500-Fe D
Speciation of Uranium	Laboratory Specific Analysis	NA
pH of Porewater-Vadose Zone	Computed from Alkalinity and Soil Gas CO ₂ pressure	
pH of Porewater-Saturated Zone	Electrometric Method	EPA SW-846, Method 9040B
Alkalinity (Forms) of Porewater	Titration	EPA Standard Method 2320B
Dissolved CO ₂ -Vadose Zone	Field Measurement of Partial Pressure of Soil Gasses.	
Dissolved CO ₂ -Saturated Zone	Calculated from pH and Alkalinity	
Carbon Isotopic Compositions	Gas Chromatograph - Isotope Ratio Mass Spectrometry	

Table 3-3. Soil Gas Sample Intervals

Sampling Depth (Feet)	Rock Unit	General Lithology
80	Hanford – Unit 2	Medium to Coarse Sand
135	Hanford – Unit 2	Fine Sand
170	Hanford – Unit 2	Sandy Silt
194	Caliche	Calcareous Silty Sand
207	Upper Ringold	Silt
217	Upper Ringold	Sandy Silt
228	Upper Ringold	Sandy Silt
253	Unit E Gravels	Sandy Gravel

Table 3-4. Gamma-emitting isotopes addressed in addition to standard K, U, and Th isotopes

Cs-137	Co-60	Pu-238	Pu-239	Pu-240
Eu-152	Eu-154	Eu-155	Ra-226	Ra-228
Na-22	Tc-99	Th-228	Th-232	U-233
U-234	U-235	U-238		

4 FISCAL YEAR 2002 ACTIVITIES

The activities accomplished during FY02 are briefly described in this section. These include:

- Completion of the laboratory analyses of the soil and soil gas samples obtained during the drilling of well 299-W19-43;
- Review information from previous reports and summarize inventory of the wastes disposed of in the 216-U1/U2 Cribs;
- Incorporation/update of the data and information from the geologic logging, soil moisture testing, geophysical measurements, hydrogeologic information and the analyses of the soil and soil gas samples collected from the borehole into the geochemical model;
- Evaluation of the processes and geochemical reactions that are important to the mobility of uranium within the unsaturated and saturated soils;
- Completion of the work plans for the calibration and validation of the geochemical model;
- Completion of first iteration of the geochemical model;
- Completion of the initial laboratory batch testing for calibration of the geochemical model;
- Initiation of the procurements to support the validation tasks; and
- Completion and submittal of an FY02 status report.

4.1 LABORATORY AND FIELD MEASUREMENTS

The analyses of the laboratory studies of the soil, soil moisture, and gas samples obtained from the borehole drilled in the 200 West Area were completed. Petrographic studies of thin sections made from the soil samples were completed. In addition, the carbon dioxide data from the soil-gas field studies were analyzed as they pertain to the formation moisture pH (see Section 7). Additionally, the stratigraphic columns showing the results of the sampling and analysis originally prepared in FY01 were updated to reflect the new information that has been acquired during FY02. These stratigraphic columns are included with this report and referenced as data plates. All of the data plates have the stratigraphic units, graphic lithologic log, and geologist's observations included for reference and continuity between each plate.

Data and information from the geologic logging, soil moisture testing, borehole geophysical measurements, hydrogeologic information, and analyses of the soils and gas samples collected from the borehole were incorporated into the geochemical model. The information obtained from the data was used to evaluate the processes and recognize geochemical reactions that are important to the mobility of uranium within the unsaturated and saturated soils associated with the groundwater contamination from the 216-U1/U2 Cribs in the 200 West Area at the site.

4.2 PRELIMINARY GEOCHEMICAL MODEL AND SENSITIVITY ANALYSIS

A preliminary geochemical model was compiled and a sensitivity analysis conducted. The purpose for the sensitivity analysis was to evaluate the limitations of the available data and determine which geochemical

model parameters are relevant to this study in terms of adsorption of uranium to the soils. The parameters that were investigated in the sensitivity analysis include the surface complexation structural model, the concentration of both surface sites and UO_2^{+2} in solution; the variations in the CO_2 concentration; and the effects of additional ions in solution. The results from the sensitivity analysis are summarized in a separate report titled *Hanford Uranium Mobility Geochemical Modeling: Sensitivity Analysis* issued May 17, 2002 (MSE, 2002a) and in Section 8.1 of this report.

Based on the results from the sensitivity analysis, the first iteration of the geochemical model/description of the uranium transport in the unsaturated and saturated soils for this project was developed during FY02. The model takes into account variations in the types of soils, soil chemistry, and groundwater chemistry at the site.

4.3 GEOCHEMICAL MODEL CALIBRATION AND VALIDATION

The work plans for both the geochemical model calibration and validation tasks were finalized by MSE. The plans were reviewed and approved by BHI and DOE-RL. The model calibration is being completed through a series of batch tests to determine the amount of uranium adsorption to the Hanford soils over a range of pH values. The results of the batch testing will be used to optimize the geochemical model parameters. The batch tests were conducted in an atmosphere with a controlled carbon dioxide concentration.

Water obtained from the Columbia River upstream of the Vernita Bridge on the north side of the Hanford site was used for the batch testing. This was done for two reasons: the process waters that were discharged to the cribs were originally from the Columbia River; and the use of Columbia River water also eliminated any issues associated with using groundwater from the Hanford site due to contamination and focused the efforts of the study on conducting the batch tests.

The soil samples collected during the FY01 drilling activities were transferred to MSE for use in the model calibration batch testing and for later use in the model validation study. The batch testing for the model calibration was conducted at the Mike Mansfield Advanced Technology Center in Butte, Montana. The model calibration batch testing results are further detailed in Section 9.

The planning and procurement tasks for the validation of the geochemical model were also initiated. The validation work will be accomplished through additional laboratory studies using contaminated water from the well drilled in FY01. Once completed, the uranium adsorption/desorption data will be compared to the results predicted using the geochemical model.

4.4 216-U1/U2 CRIBS WASTE DISPOSAL INVENTORY

Information from previous reports and documentation from the Hanford site pertaining to the inventory of the wastes disposed of in the 216-U1/U2 Cribs was compiled and reviewed. In addition, the reviews helped to determine and/or estimate the pH and chemistry of the waste stream discharged to the cribs. This information has been summarized in a separate report (MSE, 2002c).

5 FISCAL YEAR 2003 ACTIVITIES

This section has been intentionally left blank and will be completed following the FY03 activities.

6 FISCAL YEAR 2004 ACTIVITIES

This section has been intentionally left blank and will be completed following the FY04 activities.

7 RESULTS

The project results for the laboratory and field work to date are presented in this section. The initial geochemical modeling results are presented in Section 8.

7.1 FIELD OBSERVATIONS OF LITHOLOGY

Generally, the lithology of the section consists of sands, gravels, silts, and calcareous dominated deposits. Saturated sediments were found to occur 257 ft bgs. A detailed lithologic description is presented for each major stratigraphic unit and subunit. Additionally, these observations are presented graphically on Plate 1.

7.1.1 Hanford formation

The Hanford formation near 299-W19-43 is approximately 181 feet in thickness and consists of two units of unconsolidated sediments (Unit 1 and Unit 2) that make up the primary thickness of the vadose zone. Unit 1 is approximately 67 ft thick and Unit 2 is approximately 114 ft thick.

7.1.1.1 Hanford Unit 1

Unit 1 extends from the ground surface to approximately 67 ft bgs. Sediments of the Hanford formation are generally coarser grained than underlying sediments of Unit 2 and consist generally of a series of unconsolidated fining-upward sequences of gravels, sands, and silts.

This unit is a highly permeable facies that varies between very fine to coarse-grained sands, silty sands (generally very fine to medium grained), gravelly sand (fine to coarse grained sands), and minor interbeds of silt. Generally, the sand fraction consists of grains that range between 50 percent to 70 percent basalt and 30 percent to 50 percent felsics (quartz and feldspars) with trace muscovite and biotite. Gravels are generally basaltic (fine to coarse gravels with rare cobbles to 4 inches in diameter) and occasionally coated with a variable coating of calcium carbonate. Subsurface moisture was described in the field as dry to damp. Damp sediments were generally found to be associated with the finer grained material (silts). A weak to strong reaction with hydrochloric acid (1 Normal) began in sediments eight feet below existing grade and continued through the unit. This indicates that the sands and silts have variable amount of calcium carbonate cement within the matrix. Sands are especially calcareous near 52 feet, 54 feet, and 58 feet below existing grade. Oxides of iron often stain mafic minerals (e.g., biotite); partings associated with interlaminated silts and fine sands are commonly stained, especially near 29 feet below existing grade.

Three split-spoon samples and nine grab samples were recovered from Unit 1. These included two split-spoon samples (MSE core samples 101 and 102) and one split-spoon sample recovered for Bechtel Hanford for waste designation. Nine grab samples were collected to quart-size tins to determine moisture content.

7.1.1.2 Hanford Unit 2

Unit 2 of the Hanford formation extends from 67 ft bgs to 181 ft bgs. Sediments of the Hanford Unit 2 formation are generally finer grained than overlying sediments of Unit 1 and consist typically of interstratified sands and silts that make up a series of fining-upward sequences. Unit 2 sediments become more silty and clayey toward the base of the unit. There is an unconformity between this unit and the underlying Plio-Pleistocene Unit.

The Hanford Unit 2 consists of a sequence of fine to coarse-grained sands with interstratified silty sands and silt that occurs below a gravelly sand (medium to coarse grained) associated with the base of Unit 1. Sands immediately below the base of Unit 1 are similar to those described in Unit 1 and consist of

approximately 70 percent basalt and 30 percent felsics. These sands become more felsic with depth and generally contain 25 percent basalt and 75 percent felsics near 159 feet and 90 percent felsics by 161 feet. Generally, sediments of Unit 2 become damp below 70 feet. Sands, interbedded silts and clays below 155 feet become slightly more calcareous and exhibit a strong reaction with hydrochloric acid compared to sediments stratigraphically above. However, scattered carbonate nodules and accretions were observed near 68 feet and strong reactions with hydrochloric acid were observed between 77 feet and 80 feet. Scattered and infrequent gravels associated with a medium to coarse-grained sand near 70 feet are partially coated with carbonate-rich clay. A clastic dike was observed between 159 feet and 161 feet. This sedimentary feature consisted of calcareous medium sand penetrating a plastic clay. Iron oxide stains and alteration of mafics are rare and were observed in a sand interval between 156 feet and 159 feet.

Unit 2 becomes clayey and silty with interbeds of very fine sand near 168 feet. This lithology is often laminated and becomes calcareous near 180 feet with calcareous accretions or possibly calcareous rip-up clasts associated with the contact of the underlying Plio-Pleistocene Unit. Severe iron-oxide alteration observed in silts near 182 feet associated with laminations and partings. Unit 2 forms an unconformable and erosional contact with the underlying Plio-Pleistocene Unit. This contact occurs near 181 feet.

Four split-spoon samples (MSE core samples 103 through 106) and eleven grab samples (quart-size tins for moisture) were recovered from Unit 2.

7.1.2 Plio-Pleistocene Unit

The Plio-Pleistocene Unit near 299-W19-43 is approximately 24.4 feet in thickness, extending from 181 ft bgs to 205.4 ft bgs. It consists of two subunits: Palouse Soils and Caliche.

7.1.2.1 Palouse Soil

Palouse Soil extends from 181 ft bgs to 186 ft-bgs. The sediments consist of dry to damp calcareous silts that are well laminated and have a moderate to strong reaction with hydrochloric acid. This unit contains approximately 10 percent to 15 percent fine sand, 80 percent silt, and 5 percent clay. Occasional iron-oxide stringers and stain along partings and possible root traces were observed. These silts are five feet in thickness and grade to a silty and gravelly very fine to coarse-grained calcareous sand near 186 feet (top of Caliche).

A single split-spoon sample was recovered from the Palouse Soil (MSE Core Sample 107).

7.1.2.2 Caliche

Silty and gravelly calcareous sand was picked as the top of the Caliche near 186 ft bgs and extends to a depth of 205.4 ft bgs. This sand (very fine to coarse grained that includes 15 percent fine to coarse gravels and 15 percent silt) is well cemented with calcium carbonate from 186 ft bgs 196 ft bgs. These sands are commonly stained with oxides of iron and alteration to clay is throughout the matrix and grade into calcareous silty sands near 196 feet with common calcium carbonate nodules and stringers.

Dry to slightly moist calcareous silty sands make up the primary thickness of the Caliche Unit and occur between 196 feet and 205.4 feet. Calcareous stringers and accretions are common in this unit that consists of approximately 80 percent fine to medium sand and 20 percent silt. Calcium carbonate cemented root casts are common between 201 feet and 202 feet. Basalt content of sand fraction ranges from 25% to 45% with the balance composed primarily of quartz. These silty sands become less calcareous toward the contact with the underlying Upper Ringold near 205.4 feet where they grade to weakly laminated silt. Laminar partings are coated with calcium carbonate near the contact with the Upper Ringold Formation and calcium carbonate nodules are common near the contact. Non-calcareous stringers (possibly gypsum) occur in these silty sands near 204 feet. These silty and calcareous sands form an unconformable contact with the underlying silts of the Upper Ringold Formation that occurs near 205.4 feet.

Nine split-spoon samples were recovered from the Caliche Unit (MSE Core Samples 108 through 116).

7.1.3 Ringold Formation

Two units of the Ringold Formation were recognized and described as borehole 299-W19-43 was advanced. These units included the silts and silty sands of the Upper Ringold and sandy gravel of the Unit E Gravels. Approximately 90 feet of Ringold sediments were described between 205.4 feet and total depth (295.72 feet).

7.1.3.1 Upper Ringold

Upper Ringold extends from 205.4 ft bgs to 251.5 ft bgs. The sediments in the Upper Ringold consist of 46.1 feet (205.4 feet to 251.5 feet) of silt, sandy silt, and silty sand (236.5 feet to 251.5 feet). Laminated and damp calcareous silt occurs near 208 feet with infrequent oxides of manganese visible along partings; carbonate content, associated with partings, rapidly decreases below 210 feet. The unit is bioturbated near 209 feet (calcium carbonate filled burrow) and grades to sandy silt near 219 feet with common stains of iron oxides and scattered carbonate-rich accretions near 214 feet and 216 feet. Convolutional silty clay occurs near 223 feet that grades into sandy silt near 225 feet and silty sand near 237 feet and becomes less calcareous below 210 feet. No reaction with hydrochloric acid near 230 feet. Silty sand is the dominant lithology from 237 feet to 251.5 feet. This sand is very fine to medium grained (10 percent basalt grains and 90 percent felsics) with about 20 to 40 percent silt and has no reaction with hydrochloric acid. Trace amounts of muscovite and chloritized biotite are present. Sand fraction increases to approximately 95 percent near 243 feet and becomes very fine to fine grained with approximately 5 percent silt. Unit becomes slightly moist near 250 feet.

Five split-spoon samples were recovered from the Upper Ringold (MSE Core Samples (117 through 121) and five grab samples (quart-size tins) were recovered to be analyzed for moisture.

7.1.3.2 Unit E Gravels

Unit E Gravels consist of sandy gravel and silty sandy gravels from 251.5 feet to total depth of borehole 299-W19-43. This unit becomes saturated near 257 feet.

Gravels consist of fine to coarse with minor amount to 4-inches in diameter. Gravel ranges from 50 percent near 252 feet and increases to approximately 65 percent by 255 feet. Gravels are dominantly quartzites and meta-igneous. Silt increases from five percent near 252 feet to approximately 10 percent near 255 feet and 15 percent near 268 feet. Sand content decreases from 45 percent near 252 feet to 25 percent near 255 feet. Sand fraction is fine to coarse grained (60 percent to 80 percent fine to medium) and consists of 5 percent to 10 percent basalt grains and 90 percent to 95 percent felsics with trace muscovite. No reaction with hydrochloric acid observed.

Gravels commonly coated with fines that include blackish-gray oxides of manganese and iron-oxide stains (reddish-orange). Intergranular filling also includes flecks and blebs of non-calcareous material (possibly calcium sulfate, similar in appearance and color to calcium carbonate but no reaction with hydrochloric acid observed) and small sooty (blackish-gray) nodules likely rich in oxides of manganese. Slight chloritization of mafics occurs between 260 feet and 270 feet.

Three split-spoon samples were recovered from the Upper Ringold (MSE Core Samples (122 through 124) and one grab sample (quart-size tin) was recovered to be analyzed for moisture.

7.2 GEOPHYSICAL LOGGING DATA

The results of geophysical logging are discussed in this section. The logs acquired include natural gamma, spectral gamma, and neutron soil moisture. The natural gamma log is presented graphically on Plate 1; the spectral gamma logs are shown on Plate 2, and the neutron soil-moisture log is presented on Plate 3. The logs were placed on the data plates that contain information similar or relevant to the type of information contained in the individual geophysical logs. For example, the spectral gamma logs are shown with the XRF data. This allows for a comparison between the results and can be used as a means of cross checking.

Some general observations on the response of the logs to observations made during drilling are presented followed by specific discussions of select intervals. Because the geophysical logs begin at 50 ft-bgs and continue to the water table (257 ft bgs), the observations of the log responses do not include the near surface portion of the well (0 to 50 ft-bgs).

7.2.1 General Geophysical Log Observations

A comparison of the geophysical logs to the lithologic log for well 299-W19-43 indicates the neutron soil moisture and natural gamma data are good indicators of grain size. Finer grained materials tend to retain more moisture than coarse grained materials, resulting in the positive neutron soil-moisture response in these intervals. Additionally, the finer grained sediments generally have silts and some clay minerals. These tend to be composed of the more felsic minerals, which contain potassium, some of it in the form of potassium-40, the most dominant naturally occurring gamma emitting isotope found in nature.

An example of the relationship between the neutron soil-moisture data, the natural gamma data, and the fine-grained materials noted on the lithologic log is observed from 50 to 53 ft-bgs. In this interval, fine sands interbedded with silt were observed during drilling. These zones of interbedded silt exhibit increased soil moisture and increased natural gamma activity.

A second example of the relationship between the neutron soil moisture data, the natural gamma data and the observed lithology can be seen in the interval from 58 to 64 ft-bgs. This interval was described as sand with coarse gravels. The neutron log indicates that no significant soil moisture exists in this interval and the natural gamma count decreases noticeably in this interval.

A general observation with respect to the natural gamma activity is related to the source of the gamma emissions as observed from the spectral gamma data on Plate 2. The natural gamma count appears to be primarily a function of the potassium-40 in the sediments, which typically is around 15 pCi/g for these sediments. The potassium-40 spectral gamma data for correlates well with the x-ray-florescence (XRF) data for potassium as shown on Plate 2. *[Note, the XRF data, which are discussed in detail in Section 7.3, are presented as percentages of the total soil composition while the spectral gamma data are presented in picoCuries per gram (pCi/g).]* This correlation is particularly evident in the Plio-Pleistocene unit from 180 to 205 ft.

The spectral gamma and XRF data for uranium do not correlate as well as for potassium. Two distinct features found in the plot of the uranium concentrations from the XRF data are not reflected in the spectral gamma data. These are the marked increase in the uranium concentration observed at approximately 170 ft and the general decrease in the uranium concentration observed for the Plio-Pleistocene unit. A possible explanation for these discrepancies between the data is that while the small amount of uranium in the soils is detectable with the spectral gamma log, the still smaller changes in the uranium concentrations may not be detectable with the spectral gamma log.

The thorium data from the spectral gamma tend to correlate with the thorium XRF data better than the uranium data. The change in thorium concentrations observed from the XRF data in for the Plio-Pleistocene unit is also observed in the spectral gamma data for thorium in this same interval.

7.2.2 Hanford Unit Geophysical Log Responses

The Hanford Unit is described on the lithologic log from ground surface to 181 ft-bgs. It includes both the Hanford Unit 1 (ground surface to 67 ft-bgs) and Hanford Unit 2 (67 to 181 ft-bgs). Within this interval, two distinct zones are observed in the geophysical log data marked primarily by a change in the soil moisture.

From 50 to 143 ft-bgs the soil moisture indicated by the neutron soil-moisture log shown on Plate 3 is typically 4% by volume. However, discrete zones ranging in thickness from 2 to 4 ft are observed approximately every 10 ft with soil moisture increasing to as much as 8% by volume. The total gamma count for this interval shown on Plate 1 is relatively uniform, ranging from 250 to 300 counts per second (cps). Slight increases in the total gamma count are observed which correlate with the zones of increased soil moisture. The total gamma count for this interval appears to be dominated by the potassium-40 in the sediments, which typically is around 15 pCi/g. The uranium activity is around 2 pCi/g and the thorium activity is around 1 pCi/g.

The interval from 143 to 181 ft-bgs is characterized by a noticeable increase in the soil moisture. The average soil moisture reported from the neutron log in this interval is approximately 8% by volume as compared the 4% by volume for the interval above (50 to 143 ft-bgs). The discrete zones of increased soil moisture observed in the upper interval are also present within this interval, however, these zones have significantly higher soil moisture, some as much as 14% by volume as reported by the neutron log, and occur more frequently (approximately every 5 ft) and range in thickness from 4 to 5 ft.

In the interval from 143 to 181 ft-bgs, the total gamma count has more variability than the interval above (50 to 143 ft-bgs) with low values typically around 250 cps and several zones showing total gamma counts up to 350 cps. The total gamma count in this interval (143 to 181 ft-bgs) appears to vary due to changes in the uranium and thorium activity more than in the interval above (50 to 143 ft-bgs). For example, the interval from 166 to 181 ft-bgs is associated with an increase in thorium activity, while a decrease in the total gamma count observed from 155 to 158 ft-bgs appears to be related to an observed decrease in the uranium and thorium activities.

7.2.3 Plio-Pleistocene Geophysical Log Responses

The Plio-Pleistocene unit is composed of two subunits; the Palouse soils (181 to 186 ft-bgs), and a caliche layer (186 to 205 ft-bgs). These two subunits have distinct geophysical signatures. The Palouse soils are characterized by an increased total gamma count from approximately 300 cps to 350 cps. This increase is related to the uranium and thorium activity. Additionally, the Palouse soils exhibit a decrease in potassium-40 activity. The neutron soil-moisture data indicates the soil moisture above the Palouse soils is approximately 14% by volume and then it decreases rapidly in the Palouse soils to 4% by volume at the base of the unit.

The caliche layer is characterized by a significant decrease in the total gamma count to around 200 cps from the overlying Palouse soils. This change is related to a decrease in the potassium-40 and thorium activities. The soil moisture increases at the top of the caliche to about 12% by volume compared to the 4% soil moisture by volume observed in the overlying Palouse soils. The soil moisture decreases in the caliche layer to 4% at the base of the unit.

7.2.4 Upper Ringold Geophysical Log Responses

The Upper Ringold formation from 205 to 220 ft-bgs, directly below the caliche layer of the Plio-Pleistocene, is characterized by a significant increase in soil moisture to approximately 15% by volume. This interval also exhibits an increase in the total gamma count (350 cps) over the total gamma count observed for the caliche layer. This increase is associated with an increase of the potassium-40 and

thorium. The uranium activity for these soils appears to be steadily decreasing from 2 pCi/g to 1 pCi/g. Two zones of increased soil moisture characterize the remaining portion of the Upper Ringold formation that was logged: the first at 225 ft-bgs and the second at 235 ft-bgs. The remaining sediments have soil moisture levels less than 4% by volume. The total gamma count observed for these sediments increases slightly at 235 ft-bgs, possibly associated with thorium.

7.3 LABORATORY ANALYSES OF SOIL SAMPLES

Split-spoon samples and grab samples obtained during the drilling of well 299-W19-43 were submitted to Battelle Labs in Richland, Washington for analysis of the sediment, one-to-one sediment to water extracts (Rhoades, J.D., 1996), and groundwater according to the methods outlined in Table 3-1 and Table 3-2. The results of these analyses are presented and discussed in the following sections.

7.3.1 Physical Properties and Soil Chemistry

The physical properties of the soils measured in the laboratory included bulk density; particle density; surface area; and particle size (sieve analysis). The results of the physical property analyses are presented in Table 7-1 and shown on Plate 1.

The soil chemistry analyses included bulk mineralogy measured using x-ray diffraction (XRD), the elemental composition of the soil determined from x-ray-fluorescence (XRF), the carbon content of the soil (this includes total carbon, inorganic carbon, and organic carbon). The results of the soil chemistry analyses are presented in Table 7-2, Table 7-3, and Table 7-4 respectively. The results of the XRD and carbon analyses are also shown graphically on Plate 1. The XRF data are shown graphically on Plate 2.

7.3.1.1 Bulk Density and Particle Density

The bulk density and particle density presented in Table 7-1 and shown on Plate 1 were measured from core sub-samples taken during drilling. The average bulk density for the soils is 1.85 g/cc, a slight increase in the bulk density is observed for the Plio-Pleistocene unit. The average particle density, also shown on Plate 1, is 2.65 g/cc, which is the density of quartz. The XRD data (which are discussed below) indicate that quartz is the dominant mineral found in the soils, which agrees with the particle density data. From the bulk density and particle density, the average formation porosity can be calculated using Equation 6 below.

$$\theta = 1 - \frac{\rho_B}{\rho_P} \quad \text{Equation 6}$$

Where θ is the porosity of the formation, ρ_B is the bulk density of the soil, and ρ_P is the particle density of the soil.

The average formation porosity calculated using Equation 6 is 30%. This is a typical value for sandy soils and well with in the expected range of 25% to 50% given for sandy soils (Freeze and Cherry, 1979).

The particle surface area of the soils was measured using Brunauer, Emmett, and Teller (BET) (Carter et al, 1986) analysis for the core samples; these data are presented in Table 7-1 and graphically on Plate 1. The average surface area measured for the samples is 11.40 m²/g. Also include in Table 7-1 are surface areas measurements obtained using the ethylene glycol monoethyl ether (EGM) method (Carter et al, 1986). Originally, this method was to be applied to radioactive samples. When the samples were determined to be non-radioactive, these measurements were made as a reference in case future work required this type of measurement process.

7.3.1.2 Particle Size Analysis

A sieve analysis was conducted on the core samples. The results are listed in Table 7-2. Also listed are the percentages of gravel, sand, silt, and clay as determined by the laboratory for each of the soil types. The results of the analyses indicate that the soils are generally composed of a sand sized fraction, typically comprising 50% to 95% of the sample. At 188 ft the soil is dominated by a gravel fraction and at two intervals, (171 – 182, and 206 to 210 ft) the soils are primarily silt.

It should be noted that although the results from the laboratory do not always total to 100% for the soil composition, the results are close enough to reasonably determine the soil type. As the results indicate, one size fraction is typically dominant in each soil sample.

The results of the sieve analysis were used to estimate saturated hydraulic conductivities for the soils. Both the Hazen method (Fetter, 1988) and the Krumbein and Monk method (Krumbein and Monk, 1943) were used for these estimates. The results are plotted on Plate 1 along with the geometric mean of the results from the two estimations. The estimated saturated hydraulic conductivity is generally between 1×10^{-2} cm/sec and 1×10^{-3} cm/sec for the Hanford units, it decreases to 1×10^{-3} cm/sec and lower in the Plio-Pleistocene unit and then increases to 1×10^{-2} cm/sec again thin the Ringold unit. The discrepancy between the results obtained from the two methods may be due to the inherent assumptions contained in the individual methods.

7.3.1.3 Elemental Composition of Soil from X-Ray-Florescence (XRF)

The results from the XRF analysis of the soil composition are presented in Table 7-3 and shown graphically on Plate 2. The soil composition is relatively uniform in the Hanford units. The data indicate that silicon; most probably in the form of a silicate mineral, composes the bulk of the sediment. Iron is also found in the soils in abundance, ranging from 3% to 10% by weight. There is a slight increase in the iron content in the Plio-Pleistocene unit. Aluminum is also abundant in the soils, typically comprising approximately 10% to 12 % by weight. In the Plio-Pleistocene unit, aluminum decreases slightly. The composition of the Ringold unit appears to be similar to the Hanford units with some minor variation.

7.3.1.4 Bulk Mineralogy from X-Ray Diffraction (XRD)

The bulk mineralogy of the soils was determined using x-ray diffraction (XRD). The results are presented in Table 7-4 as the relative intensities of the major reflections to the Quartz 3.34 Angstrom (\AA) reflection. These results are also shown graphically on Plate 1. This is a relative indicator of mineral abundance. The XRD data indicate that quartz is the dominant mineral assemblage in the soils, making up approximately 60% or more of the soil. Feldspars (primarily plagioclase and potassium feldspar) make up most of the remaining portion of the soils. Other minerals present in the soils in lesser amounts include calcite, amphibole, chlorite, mica, and other phyllosilicates.

The composition of the clay fraction (note: this is the clay sized particles and not the clay minerals) taken from the XRD data is presented in Table 7-5. The clay-sized fraction of the soil is primarily composed of smectite, chlorite, mica, and quartz.

7.3.1.5 Soil Carbon Content

The total carbon content of the soil was analyzed in addition to determining the organic and inorganic carbon content of the soil. The results are presented in Table 7-6. The results of the carbon analyses are also presented graphically on Plate 1.

The primary form of carbon in the soils is inorganic carbon. The total soil carbon content ranges from 0.03% to 6.57% with the median value equal to 0.34%. The organic carbon content of the soils ranged from none to 0.45%. The median organic carbon content is 0.05%. The inorganic carbon, which makes up

most of the carbon in the soils, ranges from none to 6.11%. The median value for the inorganic carbon is 0.30%.

Table 7-1. Laboratory analytical results for soil chemistry and physical properties

Sample Description	Approximate Depth (ft)	Bulk Density (g/cm ³)	Average Particle Density (g/cm ³)	BET Surface Area (m ² /g)	EGM Surface Area (m ² /g)
MSE-CORE-101B	21.5	1.67	3.17	12.70	
MSE-CORE-102B	51.4	2.02	2.64	3.39	
MSE-CORE-103B	81.6	2.00	2.62	3.32	20.16
MSE-CORE-104B	111.3	1.89	2.44	4.44	
MSE-CORE-105B	141.5	1.83	2.55	3.89	
MSE-CORE-106B	171.5	1.64	2.60	15.25	
MSE-CORE-107A	182.4	1.78	2.19	6.40	
MSE-CORE-108A	185.1	1.85	2.76	6.76	
MSE-CORE-108B	186.1	2.00	3.46	12.36	
MSE-CORE-109A	187.6	1.98	2.55	11.39	
MSE-CORE-109B	188.8	1.94	2.40	17.87	
MSE-CORE-110A	189.5	1.88	2.74	16.71	
MSE-CORE-110B	190.6	1.89			
MSE-CORE-111 RS	192.1		2.50	22.99	
MSE-CORE-111A	192.6	1.88	2.72	23.55	58.85
MSE-CORE-111B	193.6	1.94	2.84	19.69	
MSE-CORE-112B	195.8	1.94	2.57	16.03	
MSE-CORE-113B	198.3	1.93	2.81	15.74	
MSE-CORE-115A	202.6	1.95	2.87	16.71	
MSE-CORE-116B	206	1.97	2.57	17.09	
MSE-CORE-117B	208.6	1.78	2.49	12.13	
MSE-CORE-118B	209.8	1.77		12.39	
MSE-CORE-118 RS	210.4		2.49		
MSE-CORE-119B	231.4	1.39	2.51	4.06	
MSE-CORE-120B	246.5	1.73	2.56	3.57	11.92
MSE-CORE-122A	261.5	2.41	2.74	3.56	
MSE-CORE-123A	271.5	2.20	2.58	3.03	3.18

Table 7-2. Laboratory analytical results for soil particle size measurements

Sample Description	Depth (ft)	Percent Passing Sieve #:							Soil Composition (wt %)			
		10	18	35	60	140	200	270	Gravel	Sand	Silt	Clay
MSE-CORE-101B	21.5	99.4	93.7	46.5	19.5	12.9	11.5	10.1	0.6	89.3	4.8	5.3
MSE-CORE-102B	51.4	100.0	98.4	80.8	48.3	21.0	17.0	14.8	0.0	85.2	6.0	3.4
MSE-CORE-103B	81.6	99.2	94.7	68.3	31.6	18.7	16.2	13.9	0.8	85.3	7.1	1.7
MSE-CORE-104B	111.3	99.8	98.5	96.1	93.9	63.0	44.6	31.4	0.2	68.5	17.5	3.7
MSE-CORE-105B	141.5	100.0	100.0	99.9	97.0	49.5	31.6	22.8	0.0	77.2	8.2	4.1
MSE-CORE-106B	171.5	100.0	100.0	99.9	99.9	99.7	99.2	93.8	0.0	6.2	73.9	8.6
MSE-CORE-107A	182.4	100.0	100.0	99.9	99.8	98.7	95.5	86.4	0.0	13.6	57.7	4.1
MSE-CORE-108A	185.1	95.8	94.7	89.3	77.6	55.6	45.5	32.7	4.2	63.1	28.0	5.3
MSE-CORE-108B	186.1	94.3	91.8	87.2	76.8	55.8	44.4	35.7	5.7	58.6	18.8	8.3
MSE-CORE-109A	187.6	93.4	91.0	87.8	77.7	60.6	50.8	39.8	6.6	53.6	28.2	8.5
MSE-CORE-109B	188.8	55.4	55.4	48.8	43.5	36.6	32.4	29.0	44.6	26.4	10.4	2.6
MSE-CORE-110A	189.5	78.1	68.0	58.6	44.2	25.6	18.8	14.5	21.9	63.6	6.0	6.8
MSE-CORE-111 RS	192.1	93.1	86.5	74.8	58.0	32.7	21.0	13.0	6.9	80.1	8.3	3.4
MSE-CORE-111A	192.6	87.0	79.5	70.3	57.0	36.5	29.8	23.8	13.0	63.2	10.4	11.1
MSE-CORE-111B	193.6	81.8	69.8	60.0	48.8	29.4	23.4	20.3	18.2	61.6	8.4	7.8
MSE-CORE-112B	195.8	88.6	83.0	76.1	64.4	47.5	42.5	38.2	11.4	50.4	23.5	13.3
MSE-CORE-113B	198.3	95.7	91.4	83.4	66.9	53.9	42.2	41.6	4.3	54.1	11.0	7.9
MSE-CORE-115A	202.6	93.1	89.7	81.5	68.0	48.7	40.2	33.9	6.9	59.3	11.4	13.6
MSE-CORE-116B	206.0	99.8	99.7	99.3	98.8	98.2	98.0	97.3	0.2	2.6	87.4	4.2
MSE-CORE-117B	208.6	100.0	100.0	100.0	99.9	99.5	99.4	98.4	0.0	1.6	89.6	7.6
MSE-CORE-118 RS	210.4	95.7	95.5	95.5	95.5	95.0	91.4	78.6	4.3	17.1	61.7	9.0
MSE-CORE-119B	231.4	100.0	100.0	100.0	99.9	83.2	53.2	28.3	0.0	71.6	24.5	1.7
MSE-CORE-120B	246.5	97.0	96.6	94.0	86.4	41.6	29.0	23.8	3.0	73.1	17.0	5.5
MSE-CORE-122A	261.5	100.0	58.7	33.3	18.3	7.8	6.1	5.0	0.0	95.0	6.4	2.9
MSE-CORE-123A	271.5	100.0	79.6	70.4	51.3	17.1	14.4	13.2	0.0	86.8	2.4	2.1

Table 7-3. Bulk chemical analysis of soils from XRF

Sample Description	Depth (ft)	Weight %																		
		Na ₂ O	MgO	Al ₂ O ₃	SiO ₂	P ₂ O ₅	SO ₃	Cl	K ₂ O	CaO	TiO ₂	MnO	Fe ₂ O ₃	SrO	BaO	NiO	CuO	ZnO	ZrO ₂	UO ₃
MSE-CORE-101B	21.5	2.723	3.647	13.453	60.544	0.683	0.370	0.048	1.491	6.394	1.783	0.137	9.846	0.042	0.089	0.003	0.002	0.007	0.021	0.001
MSE-CORE-102B	51.4	2.790	1.790	13.349	68.459	0.605	0.375	0.045	2.340	3.097	0.446	0.052	3.188	0.040	0.093	0.002	0.002	0.004	0.021	0.001
MSE-CORE-103B	81.6	2.561	2.752	13.425	70.278	0.619	0.418	0.046	2.457	3.018	0.502	0.056	3.393	0.042	0.105	0.002	0.002	0.001	0.018	0.001
MSE-CORE-104B	111.3	1.968	3.631	13.283	67.026	0.595	0.392	0.045	2.381	3.293	0.584	0.064	4.100	0.038	0.086	0.003	0.002	0.006	0.032	0.002
MSE-CORE-105B	141.5	2.359	3.813	14.347	67.839	0.631	0.409	0.047	2.405	3.512	0.621	0.077	4.357	0.045	0.107	0.003	0.003	0.006	0.034	0.001
MSE-CORE-106B	171.5	1.294	4.808	16.205	62.647	0.621	0.400	0.047	2.738	3.624	0.734	0.075	5.383	0.027	0.090	0.004	0.004	0.008	0.035	0.003
MSE-CORE-107A	182.4	1.914	3.946	13.535	65.856	0.618	0.424	0.048	2.321	2.751	0.684	0.066	4.264	0.038	0.099	0.004	0.003	0.006	0.048	0.002
MSE-CORE-108A	185.1	2.116	3.797	13.359	61.292	0.563	0.323	0.042	1.811	6.693	1.138	0.085	5.769	0.046	0.067	0.004	0.003	0.007	0.049	0.001
MSE-CORE-108B	186.1	1.294	2.735	9.548	37.703	0.801	0.414	0.046	1.233	22.308	1.283	0.169	5.576	0.039	0.058	0.003	0.003	0.006	0.030	0.001
MSE-CORE-109A	187.6	1.766	3.830	10.776	54.696	0.676	0.400	0.047	1.647	11.954	1.143	0.102	5.858	0.040	0.063	0.004	0.003	0.006	0.036	0.001
MSE-CORE-109B	188.8	0.687	3.697	4.768	24.488	0.895	0.422	0.044	0.756	40.530	0.645	0.119	3.371	0.038	0.039	0.002	0.002	0.003	0.015	0.001
MSE-CORE-110A	189.5	1.685	4.012	10.751	45.319	0.898	0.370	0.047	1.056	16.818	1.748	0.133	7.753	0.043	0.072	0.003	0.002	0.008	0.023	0.001
MSE-CORE-111 RS	190.6	1.914	4.327	10.550	47.494	0.824	0.400	0.046	1.072	17.998	1.401	0.119	7.116	0.041	0.063	0.002	0.003	0.007	0.023	0.001
MSE-CORE-111A	192.1	1.968	4.095	13.434	53.484	1.037	0.390	0.049	1.319	9.692	2.237	0.154	10.651	0.038	0.074	0.004	0.003	0.010	0.030	0.001
MSE-CORE-111B	192.6	2.265	4.858	13.516	56.094	0.722	0.395	0.049	1.329	10.083	1.796	0.130	8.367	0.041	0.068	0.003	0.003	0.008	0.025	0.001
MSE-CORE-112B	195.8	0.795	2.918	7.016	31.320	1.219	0.355	0.043	0.915	30.969	0.924	0.079	5.018	0.036	0.047	0.003	0.003	0.005	0.021	0.001
MSE-CORE-113B	198.3	1.995	3.780	10.984	51.915	0.818	0.397	0.048	1.254	14.454	1.404	0.103	6.841	0.042	0.067	0.002	0.002	0.007	0.023	0.001
MSE-CORE-115A	202.6	1.483	3.797	10.361	46.139	1.007	0.378	0.047	1.136	19.169	1.238	0.094	6.473	0.040	0.058	0.003	0.003	0.006	0.024	0.001
MSE-CORE-116B	206.0	2.197	5.239	13.075	59.267	0.637	0.376	0.045	2.406	6.273	0.732	0.087	5.219	0.072	0.150	0.005	0.003	0.007	0.033	0.001
MSE-CORE-117B	208.6	2.467	4.443	15.588	62.754	0.661	0.409	0.048	2.923	3.190	0.842	0.113	5.501	0.073	0.161	0.006	0.004	0.007	0.031	0.001
MSE-CORE-118 RS	209.8	2.372	4.841	14.669	63.182	0.637	0.410	0.048	2.779	4.417	0.737	0.100	5.336	0.055	0.127	0.005	0.004	0.006	0.030	0.003
MSE-CORE-119B	231.4	2.238	2.470	12.437	74.949	0.610	0.365	0.044	1.954	2.001	0.503	0.049	3.306	0.039	0.075	0.002	0.002	0.004	0.033	0.001
MSE-CORE-120B	246.5	2.831	1.757	12.061	80.254	0.608	0.375	0.046	2.057	1.716	0.404	0.046	2.793	0.045	0.089	0.002	0.001	0.001	0.022	0.001
MSE-CORE-122A	261.5	3.491	2.653	14.121	73.380	0.660	0.419	0.048	1.812	3.974	0.574	0.073	4.321	0.041	0.076	0.002	0.004	0.006	0.018	0.001
MSE-CORE-123A	271.5	3.370	2.205	13.579	73.808	0.628	0.408	0.047	2.106	2.948	0.573	0.064	4.057	0.049	0.095	0.003	0.002	0.005	0.027	0.001

Table 7-4. Bulk mineralogical results from XRD analysis of soils

Sample Description	Depth (ft)	Relative Intensities of Major Reflections of Minerals to the Quartz 3.34 Å Reflection (Qualitative Indicator of Mineral Abundances)							
		Quartz	Plagioclase	K-Spar	Calcite	Amphibole	Chlorite	Mica	Clay (Represents Phyllosilicates)
MSE-CORE-101B	21.5	1	0.86	0.14	0.00	0.01	0.01	0.05	0.02
MSE-CORE-102B	51.4	1	0.39	0.19	0.02	0.02	0.01	0.06	0.01
MSE-CORE-103B	81.6	1	0.29	0.15	0.01	0.02	0.01	0.05	0.01
MSE-CORE-104B	111.3	1	0.20	0.08	0.05	0.11	0.00	0.05	0.01
MSE-CORE-105B	141.5	1	0.32	0.12	0.01	0.07	0.01	0.05	0.01
MSE-CORE-106A	170.6	1	0.13	0.04	0.02	0.02	0.02	0.12	0.02
MSE-CORE-107A	182.4	1	0.16	0.05	0.00	0.06	0.01	0.07	0.01
MSE-CORE-108A	185.1	1	0.40	0.05	0.04	0.16	0.02	0.07	0.01
MSE-CORE-108B	186.1	1	0.42	0.06	0.34	0.14	0.02	0.08	0.01
MSE-CORE-109B	188.8	1	2.44	0.34	2.73	0.08	0.09	0.24	0.03
MSE-CORE-110A	189.5	1	0.68	0.43	0.39	0.05	0.02	0.05	0.01
MSE-CORE-111A	192.6	1	0.57	0.09	0.39	0.06	0.01	0.03	0.01
MSE-CORE-111B	193.6	1	1.77	0.33	0.00	0.15	0.00	0.03	0.03
MSE-CORE-112B	195.8	1	1.16	0.18	1.16	0.14	0.01	0.09	0.02
MSE-CORE-113B	198.3	1	0.86	0.12	0.20	0.11	0.02	0.05	0.01
MSE-CORE-115B	203.6	1	0.60	0.08	0.38	0.08	0.02	0.05	0.04
MSE-CORE-116B	206.0	1	0.32	0.12	0.02	0.07	0.07	0.05	0.01
MSE-CORE-117B	208.6	1	0.36	0.14	0.02	0.07	0.04	0.03	0.01
MSE-CORE-118B	209.8	1	0.53	0.08	0.08	0.07	0.04	0.09	0.01
MSE-CORE-119B	231.4	1	0.16	0.07	0.00	0.02	0.01	0.03	0.01
MSE-CORE-120B	246.5	1	0.14	0.06	0.00	0.02	0.01	0.04	0.01
MSE-CORE-122A	261.5	1	0.24	0.06	0.00	0.03	0.00	0.01	0.00
MSE-CORE-123A	271.5	1	0.28	0.18	0.00	0.01	0.00	0.03	0.01

Table 7-5. Bulk mineralogical results from XRD analysis of clay fraction in soils

Sample Description	Approximate Depth	Relative Intensities of Major Reflections of Minerals to the Quartz 3.34 Å Reflection (Qualitative Indicator of Mineral Abundances)							
		Smectite	Chlorite	Mica	Kaolinite	Quartz	Feldspar	Amphibole	Calcite
MSE-CORE-101B	21.5	na	na	na	na	na	na	na	na
MSE-CORE-102B	51.4	0.81	0.77	1	Y	Y	tr	Y	
MSE-CORE-103B	81.6	0.4	0.64	1.00	Y	Y	tr	Y	
MSE-CORE-104B	111.3	0.49	0.67	1	Y	Y	tr	Y	
MSE-CORE-105B	141.5	0.74	1.01	1.00	Y?	Y	Y		
MSE-CORE-106A	170.6	0.82	0.58	1	Y	Y	Y		tr
MSE-CORE-107A	182.4	0.67	0.59	1.00	Y	Y	tr	Y	
MSE-CORE-108A	185.1	tr?	0.46	1	Y	Y	Y	Y	Y
MSE-CORE-108B	186.1	tr?	Y	Y		tr?	tr	?	Y1
MSE-CORE-109B	188.8		Y	Y		Y	Y		Y1
MSE-CORE-110A	189.5		Y	Y	Y	Y	Y		Y1
MSE-CORE-111A	192.6	tr	Y	Y	Y?	Y	Y	Y	Y1
MSE-CORE-111B	193.6	tr	Y	Y		Y	Y	tr	Y1
MSE-CORE-112B	195.8	tr	1.44	1		Y	Y		Y
MSE-CORE-113B	198.3		Y	Y		Y	Y		Y1
MSE-CORE-115B	203.6	tr?	Y	Y		tr	tr		Y1
MSE-CORE-116B	206.0	4.18	2.6	1	Y	Y	Y	Y	
MSE-CORE-117B	208.6	2.8	1.76	1	Y	Y	Y	Y	
MSE-CORE-118B	209.8	1.92	0.96	1.00	Y	Y	Y	Y	
MSE-CORE-119B	231.4	1.12	0.64	1.00	Y	Y	Y	Y	
MSE-CORE-120B	246.5	0.44	2.19	1	Y?	Y	Y	Y	
MSE-CORE-122A	261.5	tr	3.35	1.00		Y	Y	Y	Y
MSE-CORE-123A	271.5	tr	4.65	1	?	Y	Y	Y	

Y – Mineral present in minor amounts
 tr – Mineral present in trace amounts
 ? – Uncertainty in measurement
 na – Not analyzed

Table 7-6. Laboratory analytical results for soil carbon content

Sample Description	Approximate Depth (ft)	Total Carbon (wt %)	Organic Carbon (wt%)	Inorganic Carbon (wt%)
MSE-CAN-001	5	0.66	0.21	0.45
MSE-CAN-002	10	0.35	0.05	0.30
MSE-CAN-003	15	0.07	0.02	0.05
MSE-CAN-004	20	0.24	0.05	0.19
MSE-CAN-005	25	0.11	0.03	0.08
MSE-CAN-023	215	0.03	0.01	0.02
MSE-CORE-101B	21.5	0.13	0.04	0.09
MSE-CORE-102B	51.4	0.34	0.04	0.30
MSE-CORE-103B	81.6	0.25	0.02	0.23
MSE-CORE-104B	111.3	0.29	0.04	0.25
MSE-CORE-105B	141.5	0.25	0.03	0.22
MSE-CORE-106B	171.5	0.54	0.07	0.47
MSE-CORE-107A	182.4	0.26	0.05	0.21
MSE-CORE-108A	185.1	0.67	0.07	0.60
MSE-CORE-108B	186.1	2.67	0.15	2.52
MSE-CORE-109A	187.6	1.77	0.08	1.69
MSE-CORE-109B	188.8	6.57	0.45	6.11
MSE-CORE-110A	189.5	2.51	0.04	2.49
MSE-CORE-111 RS	192.1	0.44	0.06	0.36
MSE-CORE-111A	192.6	2.15	0.07	2.08
MSE-CORE-111B	193.6	0.67	0.05	0.62
MSE-CORE-112B	195.8	4.59	0.15	4.44
MSE-CORE-113B	198.3	1.56	0.08	1.48
MSE-CORE-115A	202.6	2.70	0.03	2.67
MSE-CORE-116B	206	0.30	0.00	0.30
MSE-CORE-117B	208.6	0.11	0.01	0.10
MSE-CORE-118B	209.8	1.65	0.34	1.31
MSE-CORE-119B	231.4	0.05	0.02	0.03
MSE-CORE-120B	246.5	0.05	0.05	0.00
MSE-CORE-122A	261.5	0.07	0.03	0.04
MSE-CORE-123A	271.5	0.05	0.03	0.02

7.3.2 Soil Moisture and Sediment-Water Extract Chemistry

Soil moisture and one-to-one sediment to water extracts obtained from selected soil cores were analyzed for: pH; Eh; conductivity; alkalinity; cations and anions, uranium, and carbon concentrations. Results for these analyses are presented in this section in addition to a discussion of the soil moisture in the soils.

7.3.2.1 Soil Moisture

The soil moisture data, shown on Plate 3, were obtained from two different sample types and from the neutron moisture log. The first soil moisture data presented in Table 7-7 and identified as "can" samples are from grab samples taken during drilling and placed immediately into tin cans that were sealed. These

samples were specifically acquired for a soil moisture determination. The second set of soil moisture data shown in Table 7-7 is from sub-samples taken from the core samples. These two data sets were combined and plotted on Plate 3 along side the neutron soil-moisture data and soil moisture data obtained from the CPT electrical conductivity data.

The volumetric soil moisture was calculated from the weight percent soil moisture measured in the laboratory. It appears that these values differ from the volumetric soil moisture determined using the neutron-soil moisture log by a factor of bulk density. This discrepancy needs to be resolved through reexamination of the procedures used by each vender. This will be completed in FY03. However, the general trends in soil moisture are similar between the data sets.

In the Hanford unit where the measurements overlap (50 to 60 ft bgs), the neutron soil-moisture data and soil-moisture data from the CPT conductivity measurements are offset by approximately 10%, with CPT data being greater.

The data from both the neutron soil-moisture log and the laboratory show a significant increase immediately below the Plio-Pleistocene unit at approximately 205 to 230 ft. This general level of correlation between the data suggests the measurements are representative of the trends in subsurface soil moisture conditions.

7.3.2.2 Sediment-Water Extract pH, Eh, Conductivity, and Alkalinity

The results of the sediment-water extract pH, Eh, conductivity, and alkalinity measurements are presented in Table 7-8 and shown graphically on Plate 3. The pH shown was measured in the laboratory under atmospheric conditions and ranges from 6.7 to 8.1: the average pH value measured in the laboratory was 7.7. The pH values measured in the laboratory will be discussed in Section 7.4 as they compare to the pH values determined from the carbon dioxide measurements. The alkalinity was determined from the total inorganic carbon in the soil moisture. The assumption was made that for the pH range, the inorganic carbon would be in the form of bicarbonate (HCO_3^-). The equivalents of inorganic carbon were determined for each sample and expressed as the carbonate alkalinity value in terms of milli-equivalents per liter. This approach was taken because the alkalinity values determined from the titration data were not repeatable.

7.3.2.3 Carbon Concentrations of Sediment-Water Extract

The total carbon concentrations and organic carbon concentrations were measured for the sediment-water extract. The inorganic carbon concentration was calculated by subtracting the organic carbon concentration from the total carbon concentration. The results of the carbon analysis are also included in Table 7-8.

7.3.2.4 Cations and Anions of Sediment-Water Extract

In addition, the sediment-water extracts were analyzed for cations (see Table 7-9) and anions (see Table 7-10) concentrations. The cation analysis included calcium (Ca^{+2}), potassium (K^+), magnesium (Mg^{+2}), and sodium (Na^+). The anion analysis included fluorine (F^-), chloride (Cl^-), bromide (Br^-), nitrate (NO_3^-), phosphate (PO_4^{-3}), and sulfate (SO_4^{-2}).

Table 7-7. Soil moisture data

Sample Description	Approximate Depth (ft)	Soil Moisture (Wt%)	Bulk Density (g/cm3)	Calculated Soil Moisture (vol%)	Neutron Soil Moisture (vol%)
MSE-CAN-001	5.0	4.27	1.9	8.1	N/A
MSE-CAN-002	10.0	3.47	1.9	6.6	N/A
MSE-CAN-003	15.0	2.92	1.9	5.5	N/A
MSE-CAN-004	20.0	5.21	1.9	9.9	N/A
MSE-CAN-005	25.0	3.13	1.9	5.9	N/A
MSE-CAN-006	30.0	4.51	1.9	8.6	N/A
MSE-CAN-007	40.0	2.8	1.9	5.3	N/A
MSE-CAN-008	50.0	2.49	1.9	4.7	0.72
MSE-CAN-009	60.0	2.78	1.9	5.3	3.01
MSE-CAN-010	70.0	2.57	1.9	4.9	2.62
MSE-CAN-011	80.0	2.48	1.9	4.7	2.86
MSE-CAN-012	90.0	3.64	1.9	6.9	3.72
MSE-CAN-013	100.0	2.89	1.9	5.5	2.49
MSE-CAN-014	110.0	5.06	1.9	9.6	3.79
MSE-CAN-015	120.0	3.54	1.9	6.7	5.52
MSE-CAN-016	130.0	4.69	1.9	8.9	4.13
MSE-CAN-017	140.0	3.93	1.9	7.5	4.12
MSE-CAN-018	150.0	7.22	1.9	13.7	4.84
MSE-CAN-019	160.0	22.31	1.9	42.4	14.95
MSE-CAN-020	170.0	9.92	1.9	18.8	6.39
MSE-CAN-021	180.0	15.5	1.9	29.5	12.51
MSE-CAN-022	206.5	17.45	1.9	33.2	13.9
MSE-CAN-023	215.0	18.94	1.9	36.0	15.93
MSE-CAN-024	220.0	12.29	1.9	23.4	4.54
MSE-CAN-025	241.0	5.1	1.9	9.7	2.63
MSE-CAN-026	250.0	8.6	1.9	16.3	6.57
MSE-CAN-027	260.0	5.34	1.9	10.1	17.53
MSE-CORE-101A	20.5	3.83	1.72	6.6	N/A
MSE-CORE-101B	21.5	3.46	1.67	5.8	N/A
MSE-CORE-102A	50.5	3.19	1.85	5.9	1.71
MSE-CORE-102B	51.4	2.77	2.02	5.6	2.53
MSE-CORE-103A	80.6	1.96	1.88	3.7	2.55
MSE-CORE-103B	81.6	2.02	2	4.0	2.59
MSE-CORE-104A	110.6	3.68	1.83	6.7	3.77
MSE-CORE-104B	111.3	7.32	1.89	13.8	4.21
MSE-CORE-105A	140.5	7.68	1.63	12.5	3.38
MSE-CORE-105B	141.5	4.65	1.83	8.5	3.92
MSE-CORE-106A	170.6	5.17	1.65	8.5	5.04
MSE-CORE-106B	171.5	19.54	1.64	32.0	10.2
MSE-CORE-107A	182.4	12.01	1.78	21.4	9.62
MSE-CORE-107B	183.4	11.51	1.5	17.3	6.3
MSE-CORE-108A	185.1	6.71	1.85	12.4	3.96
MSE-CORE-108B	186.1	12.75	2	25.5	6.47
MSE-CORE-109A	187.6	9.84	1.98	19.5	10.59
MSE-CORE-109B	188.8	9.03	1.94	17.5	11.29
MSE-CORE-110A	189.5	6.33	1.88	11.9	11.13
MSE-CORE-110B	190.6	10	1.89	18.9	5.7
MSE-CORE-111 RS	192.1	7.49	1.89	14.2	9.01
MSE-CORE-111A	192.6	9.64	1.88	18.1	9.04
MSE-CORE-111B	193.6	5.79	1.94	11.2	8.92
MSE-CORE-112A	194.8	9.02	1.84	16.6	8.21

Sample Description	Approximate Depth (ft)	Soil Moisture (Wt%)	Bulk Density (g/cm3)	Calculated Soil Moisture (vol%)	Neutron Soil Moisture (vol%)
MSE-CORE-112B	195.8	11.12	1.94	21.6	7.66
MSE-CORE-113A	197.3	7.77	1.85	14.4	7.04
MSE-CORE-113B	198.3	6.39	1.93	12.3	5.2
MSE-CORE-114A	200.6	6.43	1.82	11.7	5.32
MSE-CORE-114B	201.5	7.44	1.89	14.1	5.54
MSE-CORE-115A	202.6	8.8	1.95	17.2	5.82
MSE-CORE-115B	203.6	6.24	1.84	11.5	5.28
MSE-CORE-116A	205.4	14.62	1.92	28.1	15.25
MSE-CORE-116B	206.0	18.83	1.97	37.1	14.15
MSE-CORE-117A	207.7	20.33	1.87	38.0	13.56
MSE-CORE-117B	208.6	18.95	1.78	33.7	14.19
MSE-CORE-118A	209.3	17.8	1.68	29.9	15.12
MSE-CORE-118B	209.8	12.43	1.77	22.0	16.03
MSE-CORE-118 RS	210.4	0		0.0	14.16
MSE-CORE-119A	230.3	7.73	1.36	10.5	3.52
MSE-CORE-119B	231.4	4.69	1.39	6.5	10.29
MSE-CORE-120A	245.6	5.36	1.99	10.7	2.45
MSE-CORE-120B	246.5	4.88	1.73	8.4	2.76
MSE-CORE-122A	261.5	10.03	2.41	24.2	17.53
MSE-CORE-122B	260.5	14.37	2.19	31.5	17.53
MSE-CORE-123A	271.5	12.58	2.2	27.7	17.53
MSE-CORE-123B	270.5	12.77	1.85	23.6	17.53

Table 7-8. Laboratory results of sediment-water extract chemistry and physical properties

Sample Description	Depth (ft)	pH	Eh (mV)	Conductivity (uS/cm)	Carbonate Alkalinity (meq/L)	Total Carbon (%)	Organic Carbon (%)	Inorganic Carbon (%)	Uranium Concentration (ug/L)
MSE-CORE-101B	21.5	7.4	334.9	212		16.97	3.74	13.24	59.68
MSE-CORE-102B	51.4	7.8	354.0	193	1.17	17.36	3.32	14.04	<32.13
MSE-CORE-103B	81.6	7.5	418.9	148	0.90	14.35	3.53	10.82	<51.31
MSE-CORE-104B	111.3	7.8	369.0	238	1.01	16.39	4.23	12.17	20.59
MSE-CORE-106A	170.6	7.6	408.9	487	1.25	20.91	5.93	14.98	9.63
MSE-CORE-108A	185.1	7.9	346.6	260	1.32	19.37	3.50	15.87	157.20
MSE-CORE-108B	186.1	7.5	384.6	291	1.46	24.23	6.72	17.51	239.78
MSE-CORE-110A	189.5	8.0	351.4	224	1.35	18.68	2.50	16.18	66.86
MSE-CORE-112B	195.8	8.0	380.6	299	1.32	21.00	5.18	15.82	131.58
MSE-CORE-113B	198.3	8.0	373.2	214	1.09	17.43	4.36	13.08	162.04
MSE-CORE-116B	206.0	8.0	384.9	284	1.19	19.35	5.06	14.29	<4.87
MSE-CORE-118B	209.8	8.1	403.3	230	1.21	18.85	4.28	14.57	<7.64
MSE-CORE-119B	231.4	6.7	427.2	70	0.27	10.74	7.48	3.26	<21.50
MSE-CORE-120B	246.5	6.8	460.2	231	0.31	8.21	4.54	3.67	<20.69
MSE-CORE-122A	261.5	7.7	372.4	320	0.65	11.17	3.34	7.83	37.58
MSE-CORE-123A	271.5	8.0	372.8	196	0.88	12.13	1.59	10.54	<7.53

Table 7-9. Laboratory results for cation concentrations in the sediment-water extracts

Sample Description	Approximate Depth (ft)	Concentration (meq/L)			
		Ca ²⁺	K ⁺	Mg ²⁺	Na ⁺
MSE-CORE-101B	21.5	0.408	0.1	0.169	0.921
MSE-CORE-102B	51.4	0.465	0.105	0.23	0.772
MSE-CORE-103B	81.6	0.395	0.093	0.26	0.57
MSE-CORE-104B	111.3	0.759	0.124	0.419	0.764
MSE-CORE-106B	171.5	1.814	0.133	0.92	1.267
MSE-CORE-108A	185.1	0.925	0.103	0.614	0.663
MSE-CORE-108B	186.1	1.643	0.113	1.176	0.829
MSE-CORE-110A	189.5	0.745	0.082	0.627	0.629
MSE-CORE-112B	195.8	1.018	0.087	0.841	0.662
MSE-CORE-113B	198.3	0.778	0.076	0.599	0.576
MSE-CORE-116B	206.0	1.093	0.073	0.814	0.636
MSE-CORE-118B	209.8	0.861	0.085	0.724	0.51
MSE-CORE-119B	231.4	0.158	0.044	0.132	0.287
MSE-CORE-120B	246.5	0.202	0.055	0.124	0.364
MSE-CORE-122A	261.5	1.218	0.153	0.719	0.567
MSE-CORE-123A	271.5	0.766	0.108	0.444	0.365

Table 7-10. Laboratory results for the anion concentrations in the groundwater

Sample Description	Approximate Depth	Concentration (meq/L)					
		F ⁻	Cl ⁻	Br ⁻	NO ₃ ⁻	PO ₄ ³⁻	SO ₄ ²⁻
MSE-CORE-101B	21.5	0.026	0.023	0	0.302	0.004	0.41
MSE-CORE-102B	51.4	0.019	0.208	0.001	0.159	0.003	0.369
MSE-CORE-103B	81.6	0.02	0.057	0	0.073	0.003	0.25
MSE-CORE-104B	111.3	0.023	0.135	0.001	0.218	0.003	0.731
MSE-CORE-106B	171.5	0.019	0.254	0.002	1.79	0.005	1.129
MSE-CORE-108A	185.1	0.014	0.055	0.001	0.54	0.004	0.502
MSE-CORE-108B	186.1	0.019	0.102	0.002	1.069	0.003	1.333
MSE-CORE-110A	189.5	0.046	0.036	0.001	0.471	0	0.275
MSE-CORE-112B	195.8	0.042	0.058	0.002	0.689	0.001	0.604
MSE-CORE-113B	198.3	0.041	0.028	0.001	0.326	0	0.413
MSE-CORE-116B	206.0	0.032	0.064	0.001	0.731	0.001	0.756
MSE-CORE-118B	209.8	0.034	0.041	0.001	0.515	0.001	0.404
MSE-CORE-119B	231.4	0.017	0.021	0.001	0.229	0.004	0.125
MSE-CORE-120B	246.5	0.015	0.029	0.001	0.31	0.004	0.108
MSE-CORE-122A	261.5	0.028	0.11	0	1.903	0	0.132
MSE-CORE-123A	271.5	0.012	0.115	0	0.64	0.003	0.146

7.4 PETROGRAPHIC ANALYSIS OF SOIL SAMPLES

A petrographic analysis of the soil samples was completed by MSE to provide information for determining the amount and composition of the grain coatings. The analysis was completed using grain mounts made from selected core samples. The samples used to make the grain mounts are indicated on Plate 4. To

complete the petrographic analysis, estimates of the percentage of framework and matrix components were made; this was followed by estimates of the composition of the framework, estimate of the percentage of the framework grains with coatings or other alterations, and finally estimates of the grain coating compositions. The framework grains were classified as quartz, feldspar, and other rock fragments. The framework alterations and coatings were classified as goethite-limonite, hematite, clay, carbonate, or magnetite-ilmenite. Observations were also made as to the crystalline nature of the coating (i.e., crystalline or amorphous). A summary of the results of the petrographic analysis is presented as Plate 4.

7.4.1 Hanford Soils

The soils from the Hanford Units are typically unconsolidated rock fragments with some grains of quartz and feldspar. Generally, 25 to 50% of the grains have some type of alteration or coatings. These coatings are dominantly composed of iron in the form of a magnetite or ilmenite with lesser amounts of goethite and limonite. Minor amounts of hematite are also present. There is also some clay and carbonate coatings present, but these generally make up only 25% of the total grain coating. An exception to these observations is near the base of the Hanford Unit 2 directly above the Plio-Pleistocene unit. The entire soil framework is observed to have a coating, which is primarily composed of clay followed by carbonate minerals and hematite. Minor amounts (less than 10% each) of the goethite-limonite and magnetite-ilmenite mineral phases are observed in these sediments.

7.4.2 Plio-Pleistocene Unit

The Plio-Pleistocene unit is characterized by a high degree of consolidation; typically, 30% or more of the soil composition was some form of matrix cement. The framework minerals consisted of quartz and feldspar with lesser amounts of other rock fragments. Due to the high degree of cementation, all of the grains had some form of coating. The coatings were primarily composed of clays and carbonate minerals. Very little iron was observed as a grain coating.

7.4.3 Ringold Soils

The Ringold soils are typically unconsolidated materials composed of primarily quartz grains with lesser amounts of feldspars and other rock fragments. There is very little coating or other alteration of the grains (less than 10%), but where it is present; it is almost entirely a form of iron. The grain coatings and alteration in the Upper Ringold is composed of goethite and limonite with minor amounts of hematite, clay, and magnetite/ilmenite. The Ringold Unit E gravels are characterized by coatings of magnetite/ilmenite and with lesser amounts of goethite/limonite.

7.5 CITRATE-BICARBONATE-DITHIONITE (CBD) EXTRACT RESULTS

Eight soil samples were analyzed using the citrate-bicarbonate-dithionite (CBD) extraction method to determine the amount of extractable aluminum, iron, and manganese oxide in the soils. A literature review indicated that iron oxides and hydroxides are the primary sorbents of uranium in most soils; therefore, an investigation into the amount and type of iron oxides was initiated. In conjunction with the petrographic analysis of the sediments, a technique was needed to determine the total amount of free iron oxides (both crystalline and amorphous) in the sediments. To accomplish this, the CBD extraction method was selected based on literature reviews related to uranium adsorption studies using surface complexation modeling (Loeppert and Inskeep, 1996; Payne, 1999; and Barnett et al, 2002). By applying the relative percentages of the various iron oxides observed in the petrographic study to the amount of free iron oxide extracted from the sediments using the CBD extraction method, the mass of the different iron oxides could be determined. In addition to the amount of iron in the soil, the amount of aluminum and manganese oxides

were also measured. The results of the CBD analysis indicating the relative amounts of Al, Fe, and Mn present in the soils as oxides and hydroxides are presented in Table 7-11.

Table 7-11. Laboratory results from citrate-bicarbonate-dithionate analysis

Sample Description	Approximate Depth (ft)	Concentration (mg/kg) in Soil		
		Al	Fe	Mn
MSE-CORE-101B	21.5	81 (79)	1660 (1500)	68 (112)
MSE-CORE-104B	111.3	124	2980	85
MSE-CORE-106B	171.5	172	3760	56
MSE-CORE-107A	182.4	221	4230	89
MSE-CORE-112B	195.7	169 (75)	1640 (1290)	59 (52)
MSE-CORE-119B	231.4	146 (102)	3850 (2780)	106 (110)
MSE-CORE-120B	246.5	116	2460	77
MSE-CORE-123B	271.5	56	1300	42

Values in parentheses are from the second lab and shown for comparison purposes.

Two independent laboratories following the procedure outlined in Loeppert and Inskeep (1996) completed the CBD analyses. The results compared well, suggesting the analyses were representative of the total free iron in the soils. The results were also compared to those reported by Barnett et al (2002), however, the results reported by Barnett appeared to be an order of magnitude greater than the results obtained from the two laboratories. This may be due to the fact that the samples analyzed by Barnett were taken from an outcrop. Potentially the outcrop material may have been more weathered than the samples acquired from the borehole, resulting in a greater amount of iron oxide weathering products.

7.6 CARBON DIOXIDE SAMPLING RESULTS

The results of the soil gas sampling are presented in Table 7-12 as the average CO₂ concentrations measured in the borehole at discrete depth intervals. These results are also shown on Plate 3. As previously discussed, the CO₂ concentration in the soil gas is a critical parameter in determining uranium sorption. The CO₂ concentrations were measured in the field using a CO₂ analyzer and the soil-gas sampling system designed and built by MSE.

The process used to determine the CO₂ concentration in the soil gas is shown schematically in Figure 7-1. The plot of CO₂ concentration as a function of time is representative of the data obtained at each discrete depth interval. The initial data shown from 0 to approximately 0.20 hours represent measurements made of the CO₂ concentrations of atmospheric air made with the CO₂ meter disconnected from the soil gas sampling system. These data verify that the CO₂ meter is accurately measuring the atmospheric CO₂ concentration, which is approximately 300 ppm. The next series of data from approximately 0.20 to 0.40 hours were obtained with the CO₂ meter connected to the soil gas sampling system, which had not yet been connected to the wellhead. These measurements are also approximately 300 ppm, indicating that the CO₂ meter is correctly measuring the concentrations of CO₂ in the air moving through the soil-gas sampling system. The soil-gas sampling system is then connected to the wellhead and the soil gas is purged from the system and well bore. As the soil gas displaces the atmospheric air in the system, the CO₂ concentrations rise until near steady state conditions are achieved. After the CO₂ concentration have reached a near steady state condition, the system was disconnected from the well head and the meter allowed to measure CO₂ concentrations in atmospheric air, again to show that the system is functioning properly. The CO₂ meter calibration was checked and found to be within the acceptable calibration range following the completion of the measurements.

The measurements of soil gas CO₂ concentrations made under the near steady state conditions were averaged to determine the CO₂ concentration for the depth interval. The measurements (see Table 7-12)

used to determine the average CO₂ concentrations were typically within 3% of the average, which shows a high degree of repeatability for the measurements.

The results show a significant variation in the CO₂ concentration with depth ranging from 4,700 ppm to 21,000 ppm. The average CO₂ concentration measured in the subsurface is 11,200 ppm. These values are two to three orders of magnitude greater than atmospheric CO₂ concentrations, which are typically around 300 ppm. There is a marked decrease in the soil gas CO₂ within the Plio-Pleistocene formation, which is characterized by a calcareous cementation of the sediments.

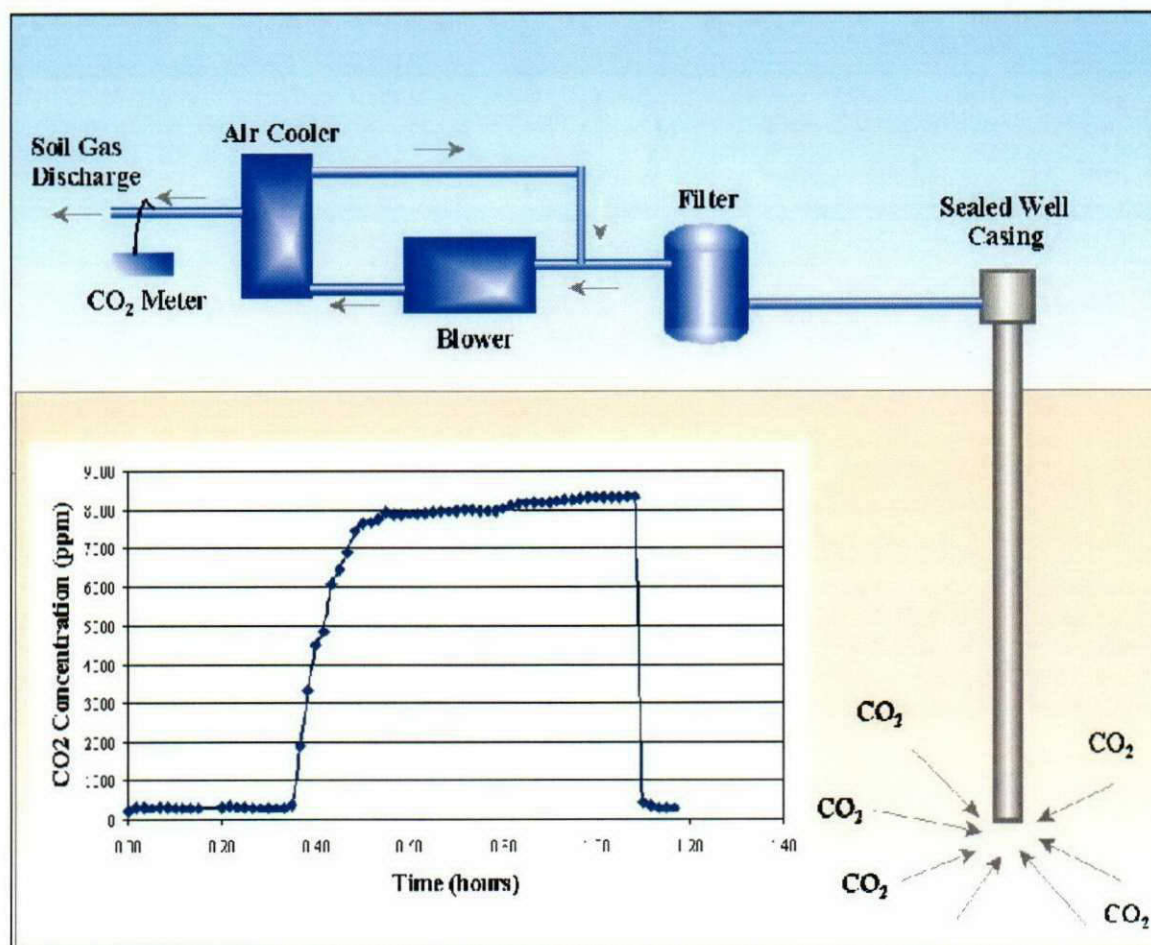


Figure 7-1. A schematic diagram showing the CO₂ concentration measurement system and process.

7.6.1 Calculated pH Values

The pH of the soil moisture was calculated using the measured CO₂ concentrations and the alkalinity of the sediment-water extracts from Equation 5. The results are presented in Table 7-12 and shown graphically on Plate 3. The calculated pH values range from slightly more than 6 to slightly less than 7 and are generally one pH unit lower than the laboratory measurements. This confirms that the pH measurement of soil moisture must not be taken after the samples are exposed to atmospheric CO₂ pressures.

The plot shown in Figure 7-2 clearly shows the importance of in situ pH measurements. The blue line is a plot of uranium sorption as a function of pH. This curve was generated using MINEQL+ V4.5, the model

parameters used were: $\text{Log pCO}_2 = -2.13$, Ionic Strength = 2.10×10^{-3} , $\text{UO}_2^{+2} = 3.7 \times 10^{-6}$ mol/L, and Total $\text{Fe}^{+3} = 1 \times 10^{-3}$ mol/L. The red line shows the frequency distribution of the in situ pH values determined using the CO_2 data and the green line shows the frequency distribution of the laboratory measurements. The uranium sorption in the range of the pH values determined using the CO_2 data ranges from 60% to 80%, while the uranium sorption in the range of the pH values measured in the laboratory is less than 10%.

Table 7-12. Calculated pH values compared to laboratory pH measurements

Approximate Depth (ft)	PCO_2 (ppm)	Alkalinity (meq/L)	pH Calculated	pH Lab Measurement
21.5	4445	1.1	7.1	7.4
51.4	5559	1.17	7.0	7.8
81.6	14299	0.9	6.5	7.5
111.3	17959	1.01	6.5	7.8
170.6	8838	1.25	6.8	7.6
185.1	8405	1.32	6.9	7.9
186.1	8405	1.46	6.9	7.5
189.5	8405	1.35	6.9	8.0
195.8	7971	1.32	6.9	8.0
198.3	7258	1.09	6.9	8.0
206	6544	1.19	7.0	8.0
209.8	9002	1.21	6.8	8.1
231.4	4681	0.27	6.5	6.7
246.5	12699	0.31	6.1	6.8
261.5	12699	0.65	6.4	7.7
271.5	12699	0.88	6.5	8.0

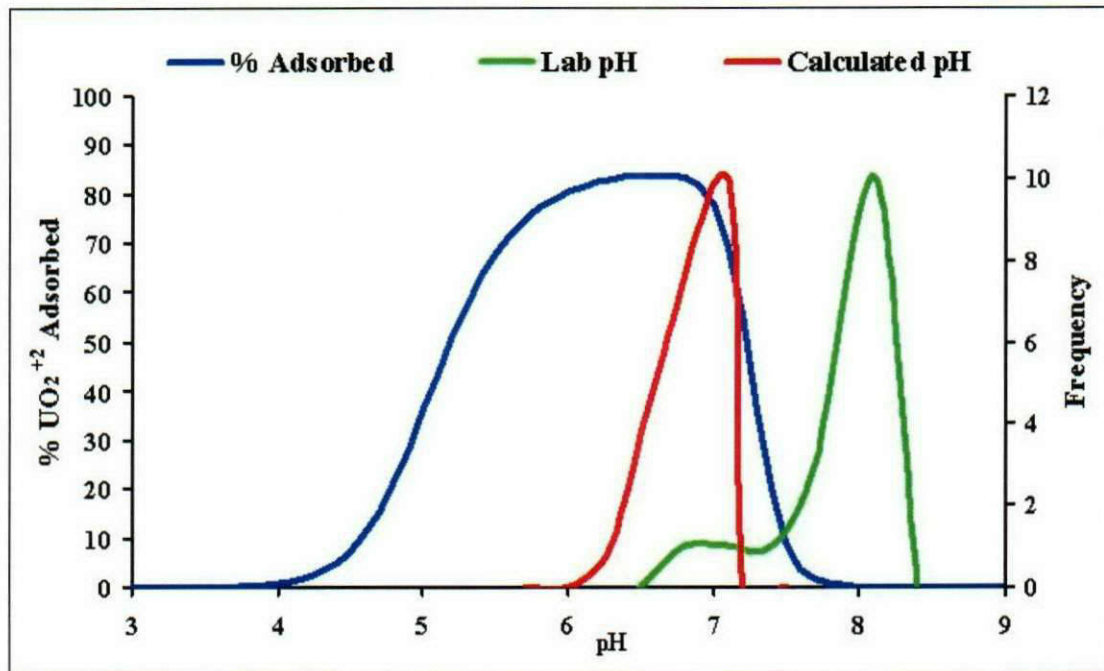


Figure 7-2. Plot of uranium sorption and frequency of pH values from CO2 data and laboratory measurements.

8 GEOCHEMICAL MODELING EFFORTS

The geochemical model parameters, sensitivity analysis of uranyl (UO_2^{+2}) adsorption modeled by MINEQL+[®] v. 4.5, calibration batch testing, and initial geochemical modeling results are discussed in this section. The MINEQL+[®] v. 4.5 (Schecher and McAvoy, 2001) computer software is a Windows[™] based chemical equilibrium modeling system that was derived from the public domain code, MINTEQA2 (Allison et al, 1991). The geochemical model considers UO_2^{+2} is adsorbed to specific sorbing sites, typically composed of metal oxide or hydroxide coatings on the soil matrix. The affinity of the UO_2^{+2} to be adsorbed to the sorbing sites is a function of the ionic strength and pH of the solution; the UO_2^{+2} and carbonate concentrations in solution; and the sorbent surface area and site density.

The primary sorbents of uranium are Fe(III) and Al oxyhydroxides, clays, zeolites, phosphate minerals, and organic matter (Langmuir, 1997). Previous studies have indicated that iron-hydroxide surface sites ($\equiv\text{FeOH}$) dominate UO_2^{+2} complexation in Hanford soils (Barnett et al., 2002). Consequently, MSE assumed that the primary sorbent of UO_2^{+2} in the soils was $\equiv\text{FeOH}$.

MSE chose to use a diffuse layer surface complexation model for the geochemical modeling efforts. The parameters required for the diffuse layer model include: the concentration of available sorbing sites in a given volume of the soil matrix; the surface area of the sorbents exposed to the groundwater; and the thermodynamic equilibrium constants for reactions involving the surface sites and aqueous components. The surface area of the $\equiv\text{FeOH}$ sorbent and concentration of available sorbing sites, were initially taken from a $\equiv\text{FeOH}$ diffuse layer model described by Dzombak and Morel (1990). This model assumes the specific surface area of the sorbent (in this case $\equiv\text{FeOH}$) is $600 \text{ m}^2/\text{g}$; and two types (strong, high affinity and weak, low affinity) of sorbing sites.

The remaining parameters used in the geochemical modeling of UO_2^{+2} adsorption included aqueous component concentrations, CO_2 concentrations, and thermodynamic constants. Results of the sensitivity analysis of UO_2^{+2} adsorption were used to determine which model parameters affected UO_2^{+2} adsorption most.

Calibration of the geochemical model will be completed through a series of laboratory batch tests to compare the measured sorption of UO_2^{+2} to the adsorption predicted by the geochemical model. Initial laboratory batch tests were conducted to provide calibration data. Input parameters for the geochemical model will be adjusted within reasonable bounds in order to produce an acceptable correlation between the predicted and measured data. Because the sorption of uranium to soils is pH dependent, the model results are presented as plots of uranium sorption a function of pH.

8.1 SENSITIVITY ANALYSIS FOR URANIUM SORPTION

This phase of geochemical modeling was conducted to examine how MINEQL+ handles large variations in input parameters and works with an expanded and refined thermodynamic database. MSE investigated the sensitivity of UO_2^{+2} adsorption, as a function of pH, to the following parameters:

1. Changes in the sorption resulting from changes in the concentration of surface sites.
2. Affect of UO_2^{+2} concentrations in solution within a broad range of concentrations ($3.7 \times 10^{-7} \text{ mol/L}$ to 3.7 mol/L) that include those observed for current conditions. Most of the sensitivity analysis was run using a concentration of $3.7 \times 10^{-6} \text{ mol/L}$.
3. Effect of the CO_2 concentration on sorption.

4. Effects of additional ions in solution such as Ca^{+2} , K^{+} , Mg^{+2} , Na^{+} , Al^{+3} , Cl^{-} , F^{-} , NO_3^{-} , PO_4^{-3} , and SO_4^{-2} .

The results of the sensitivity analysis were previously reported in *Hanford Uranium Mobility Geochemical Modeling: Sensitivity Analysis* (MSE, 2002a).

In general, the sensitivity analysis indicated UO_2^{+2} adsorption is proportional to both the surface site density and the concentration of UO_2^{+2} in solution and inversely proportional to the CO_2 concentration in the soils. The addition of Mg^{+2} , F^{-} , PO_4^{-3} , and SO_4^{-2} to the system causes a decrease in UO_2^{+2} adsorption. The decrease in UO_2^{+2} adsorption is more gradual as F^{-} or SO_4^{-2} is added. In contrast, UO_2^{+2} adsorption is drastically decreased because of a slight concentration change of either Mg^{+2} or PO_4^{-3} in the system. The remaining ions (Ca^{+2} , K^{+} , Na^{+} , Al^{+3} , Cl^{-} , and NO_3^{-}) did not significantly affect UO_2^{+2} adsorption over the range of concentrations modeled.

8.1.1 Surface Site Concentration

MINEQL+ allows a finite number of surface sites for adsorption modeling. To examine the sensitivity of the UO_2^{+2} adsorption to surface site concentration, a series of sorption simulations were run. The simulations used a constant UO_2^{+2} concentration and varied the concentration of $\equiv\text{FeOH}$ sorption sites. The model used for the sensitivity analysis calculates the concentration of $\equiv\text{FeOH}$ sorption sites from the total iron concentration. For this portion of the sensitivity analysis, the total iron concentrations ranged from 1 mol/L to 10^{-4} mol/L.

As the number of available surface sites decreases in the soil structure, it follows that the amount of UO_2^{+2} that can be adsorbed onto the soil will also decrease. This is observed in the results shown in Figure 8-1 where the adsorption is plotted for the range of iron concentrations.

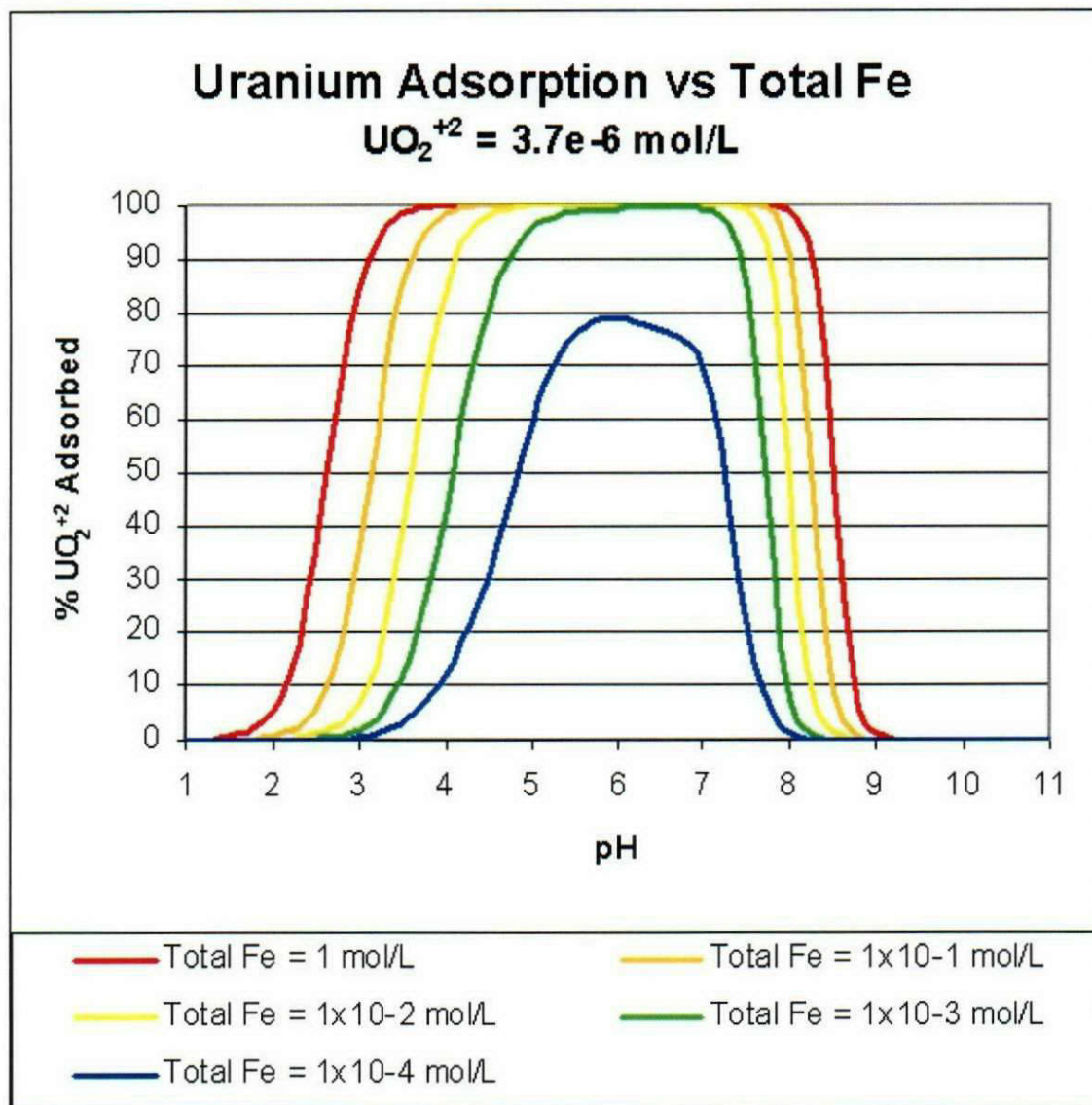


Figure 8-1. UO_2^{+2} adsorption versus total Fe concentration and at a constant pH and constant UO_2^{+2} concentration. Results were generated using the Dzombak and Morel $\equiv\text{FeOH}$ surface complexation model. The UO_2^{+2} concentration used was $3.7 \times 10^{-6} \text{ mol/L}$, the ionic strength was $2.1 \times 10^{-3} \text{ mol/L}$, and the Log $p\text{CO}_2$ was -2.13 .

As the concentration of sorption sites decreases, the percentage of the total uranium adsorbed to the soil also decreases and the pH window that sorption will occur also becomes smaller.

8.1.2 UO_2^{+2} Concentrations in Solution

Another important observation that can be made relevant to the ratio of uranium in solution to the number of sorption sites is shown in Figure 8-2, which is a plot of the of UO_2^{+2} adsorption against the total UO_2^{+2} concentration at a constant pH and total Fe(III).

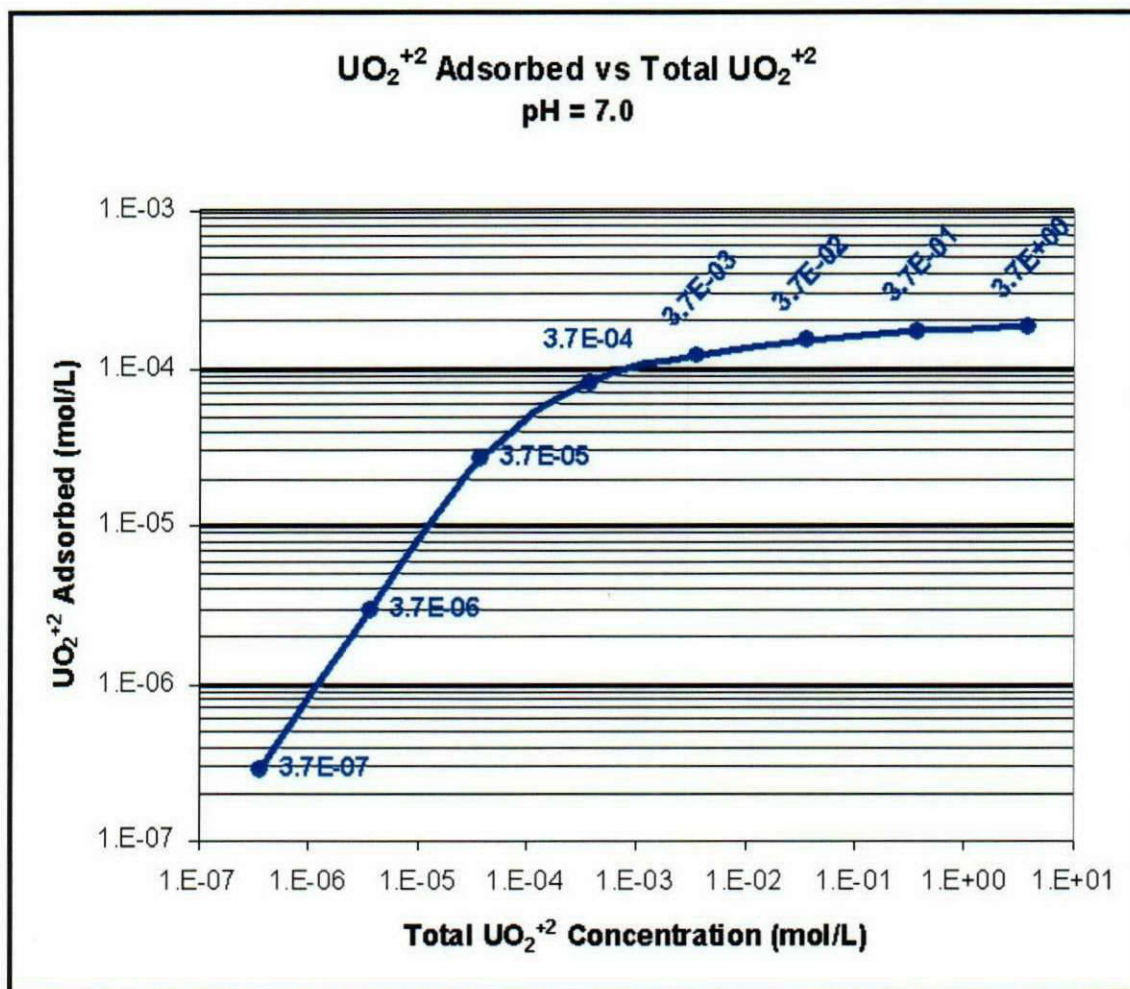


Figure 8-2. UO_2^{+2} adsorption versus total UO_2^{+2} concentration at constant pH and constant total Fe(III). Results were generated using the Dzombak and Morel $\equiv\text{FeOH}$ surface complexation model. The total Fe(III) concentration used was 1×10^{-3} mol/L, the ionic strength was 2.1×10^{-3} mol/L, and the $\text{Log } p\text{CO}_2$ was -2.13 .

Figure 8-2 shows that the ratio of adsorbed UO_2^{+2} to total UO_2^{+2} is not constant over the range of total UO_2^{+2} concentrations shown. This is most likely due to all of the available sorption sites being occupied by UO_2^{+2} and not to changes in the UO_2^{+2} complexation affinity.

8.1.3 Effect of CO_2 Concentrations on Sorption

As previously indicated, UO_2^{+2} is most mobile at the low and high pH ranges and tends to be adsorbed if the pH is near neutral. Since pH is influenced by the concentration of CO_2 in the air (Langmuir, 1997), changes in CO_2 concentration will affect the adsorption of UO_2^{+2} . Figure 8-3 is a plot showing the effect of the CO_2 concentration on UO_2^{+2} adsorption over CO_2 concentrations ranging from 300 ppm ($\text{log } p\text{CO}_2 = -3.5$) to 30,000 ppm ($\text{log } p\text{CO}_2 = -1.5$), which are representative of the concentrations measured in borehole 299-W19-43.

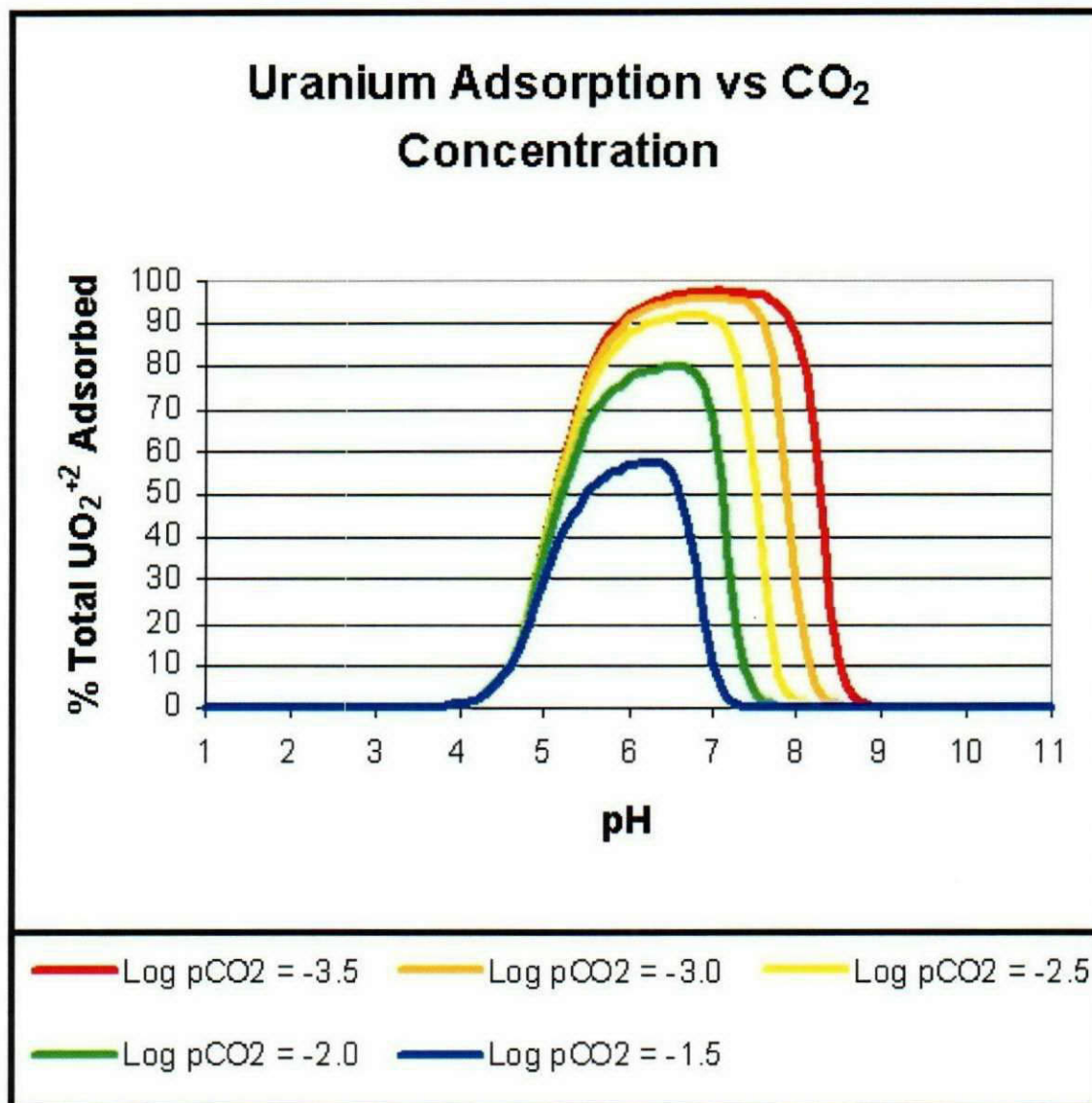


Figure 8-3. Effects of Log pCO₂ values on total percent UO₂⁺² adsorption as a function of pH.

Results were generated using the Dzombak and Morel $\equiv\text{FeOH}$ surface complexation model. The total Fe(III) concentration used was 1×10^{-3} mol/L, the concentration of UO₂⁺² was 3.7×10^{-6} mol/L, and the ionic strength was 2.1×10^{-3} mol/L.

As the concentration of CO₂ increases, the percentage of the total uranium adsorbed to the soil decreases and the pH window that sorption will occur also becomes smaller.

In addition to affecting the solution pH, the dissolved CO₂ forms carbonate complexes with UO₂⁺². The occurrence and abundance of these complexes depends on both the pH and alkalinity of the solution, which are typically functions of the dissolved CO₂. These uranyl-carbonate complexes are orders of magnitude more soluble than UO₂⁺²; thus decreasing the adsorption of uranium to the soil. Important uranyl-carbonate complexes include UO₂CO₃⁰, UO₂(CO₃)₂⁻², and UO₂(CO₃)₃⁻⁴.

8.1.4 Effects of Ions in Solution

The ionic species that significantly affected UO_2^{+2} adsorption based on the sensitivity analysis included: Mg^{+2} , F^- , PO_4^{-3} , and SO_4^{-2} . The results of the simulations in which the concentrations of these ions were varied over a range of concentrations are shown in the following plots (Figure 8-4 through Figure 8-7). The range of concentrations represents those measured in both the Columbia River water and in the Hanford groundwater.

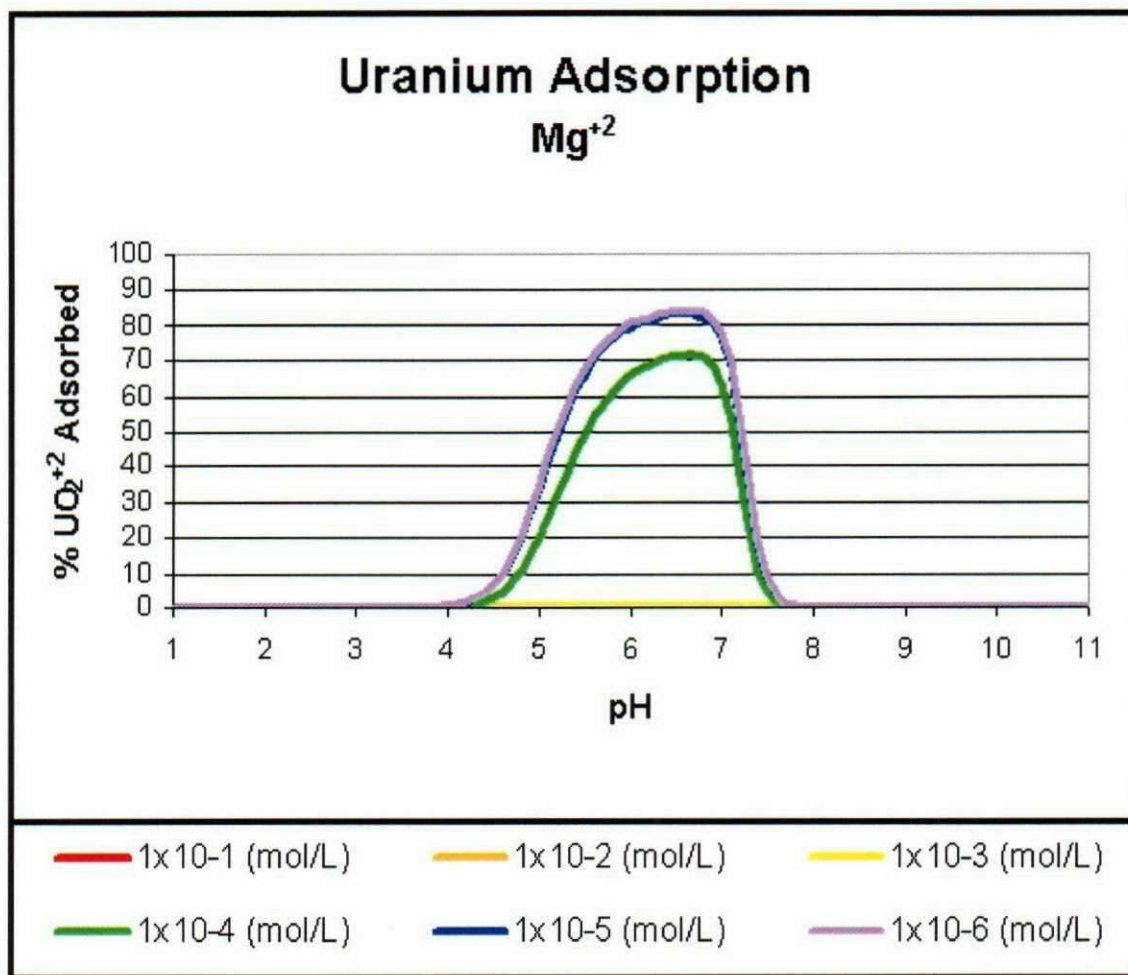


Figure 8-4. Effects on total percent UO_2^{+2} adsorption from the addition of Mg^{+2} to the solution.

Results were generated using the Dzombak and Morel $\equiv\text{FeOH}$ surface complexation model.

The total Fe(III) concentration used was 1×10^{-3} mol/L, the concentration of UO_2^{+2} was 3.7×10^{-6} mol/L, the ionic strength was 2.1×10^{-3} mol/L, and the Log $p\text{CO}_2$ was -2.13 .

Figure 8-4 shows the percent of UO_2^{+2} adsorbed decreasing as the concentration of Mg^{+2} increases. There is a decrease in UO_2^{+2} adsorption of approximately 10% between the 1×10^{-5} mol/L and 1×10^{-4} mol/L Mg^{+2} concentrations. UO_2^{+2} adsorption drastically decreases from about 70% down to almost 0% between the 1×10^{-4} mol/L and 1×10^{-3} mol/L Mg^{+2} concentrations. The decrease in UO_2^{+2} adsorption is a result of the Mg^{+2} competing for the $\equiv\text{FeOH}$ surface sites.

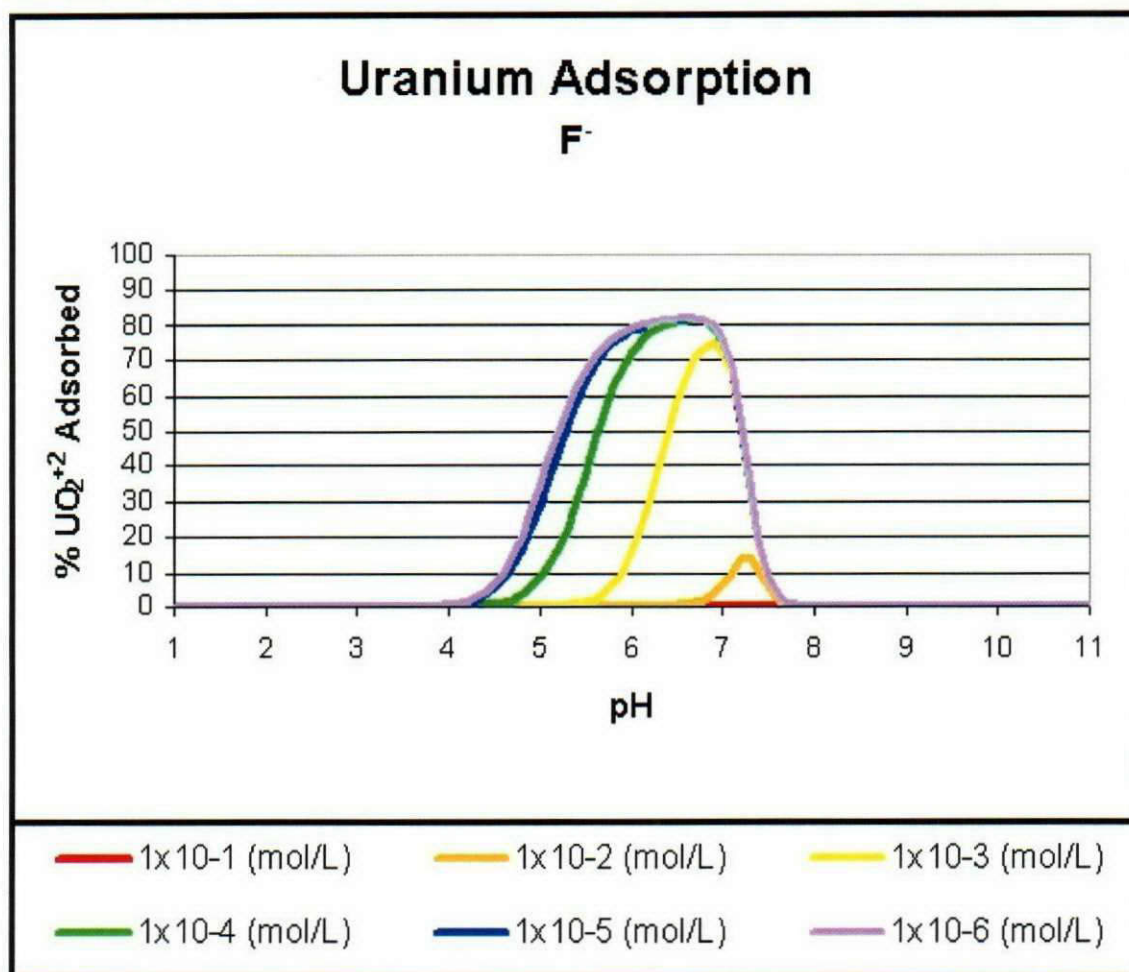


Figure 8-5. Effects on total percent UO_2^{+2} adsorption from the addition of F^- to the solution. Results were generated using the Dzombak and Morel $\equiv FeOH$ surface complexation model. The total $Fe(III)$ concentration used was 1×10^{-3} mol/L, the concentration of UO_2^{+2} was 3.7×10^{-6} mol/L, the ionic strength was 2.1×10^{-3} mol/L, and the $Log pCO_2$ was -2.13 .

Results shown on Figure 8-5 indicate that the presence of F^- in the system can affect the adsorption of UO_2^{+2} . When F^- is added to the system, UO_2^{+2} adsorption decreases and the low-pH UO_2^{+2} adsorption edge shifts to the right, toward higher pH values. Modeling results indicate that uranyl-fluoride species $UO_2F_3^-$, $UO_2F_2(aq)$, and UO_2F^+ are present in the lower pH range, preventing the UO_2^{+2} from adsorbing.

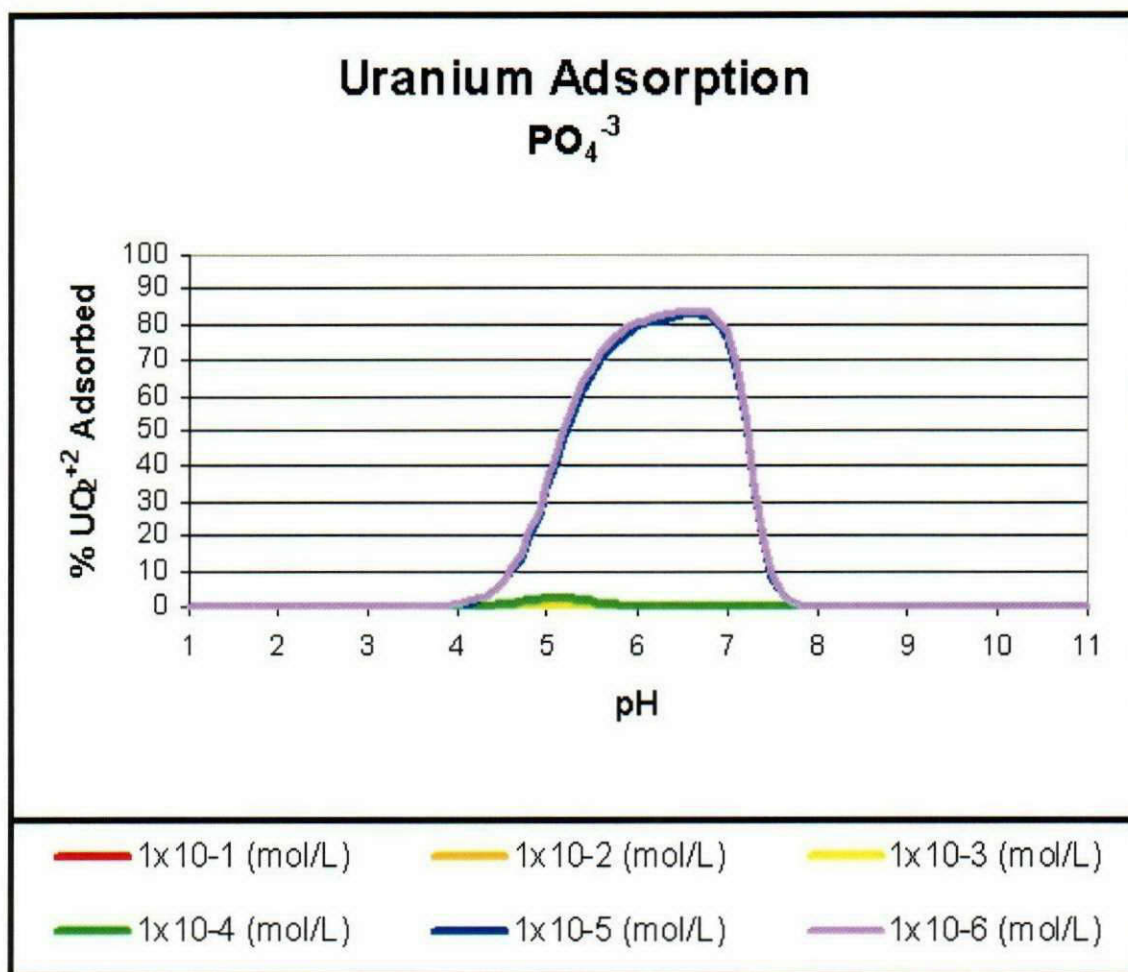


Figure 8-6. Effects on total percent UO_2^{+2} adsorption from the addition of PO_4^{3-} to the solution.
Results were generated using the Dzombak and Morel $\equiv\text{FeOH}$ surface complexation model. The total Fe(III) concentration used was 1×10^{-3} mol/L, the concentration of UO_2^{+2} was 3.7×10^{-6} mol/L, the ionic strength was 2.1×10^{-3} mol/L, and the Log $p\text{CO}_2$ was -2.13 .

The modeling results shown in Figure 8-6 suggest that the presence of PO_4^{3-} in the system can significantly affect the adsorption of UO_2^{+2} . The adsorption of UO_2^{+2} drastically decreases from about 85% down to almost 0% between the 1×10^{-5} mol/L and 1×10^{-4} mol/L PO_4^{3-} . The results also indicate that uranyl-phosphate species ($\text{UO}_2\text{H}_2\text{PO}_4^+$, $\text{UO}_2(\text{HPO}_4)_2^{2-}$, $\text{UO}_2(\text{H}_2\text{PO}_4)_2(\text{aq})$, $\text{UO}_2(\text{H}_2\text{PO}_4)_3^-$, and $\text{UO}_2(\text{H}_2\text{PO}_4)(\text{H}_3\text{PO}_4)^+$ are present in the lower pH range, which act to keep the UO_2^{+2} in solution

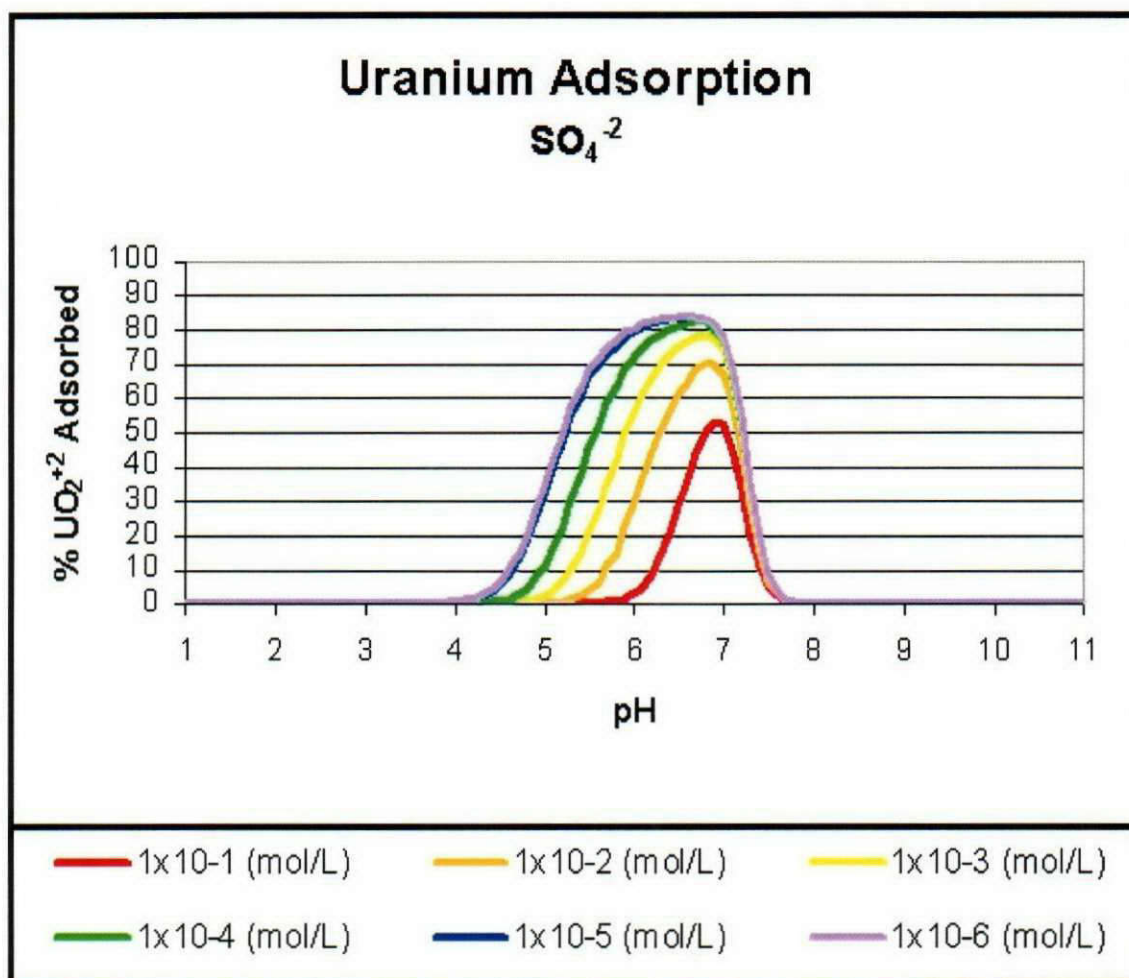


Figure 8-7. Effects on total percent UO_2^{+2} adsorption from the addition of SO_4^{-2} to the solution.
 Results were generated using the Dzombak and Morel $\equiv\text{FeOH}$ surface complexation model.
 The total Fe(III) concentration used was 1×10^{-3} mol/L, the concentration of UO_2^{+2} was 3.7×10^{-6} mol/L, the ionic strength was 2.1×10^{-3} mol/L, and the $\text{Log } p\text{CO}_2$ was -2.13 .

Figure 8-7 shows that the presence of SO_4^{-2} in the system can affect the adsorption of UO_2^{+2} . When SO_4^{-2} is added to the system, UO_2^{+2} adsorption decreases and the low-pH UO_2^{+2} adsorption edge shifts to the right, toward higher pH values. Modeling results indicate that the formation of uranyl-hydroxide, uranyl-sulfate, and uranyl-carbonate species is the primary cause of the decrease in UO_2^{+2} adsorption.

8.2 BATCH TESTS FOR MODEL CALIBRATION

The batch tests to compare the measured sorption of UO_2^{+2} to the adsorption predicted by the geochemical model were completed according to the procedures outlined in *Calibration Plan for Geochemical Model Describing Uranium Transport in the Unsaturated and Saturated Sediments at the 200 West Area of the Department of Energy Hanford Site, Washington* (MSE, 2002b).

8.2.1 Batch Test Solid Phase

The calibration batch tests were completed using five types of soil taken from the core samples acquired from well 299-W19-43 on the Hanford site. The soil samples are described in Table 8-1.

Table 8-1. Summary of soil samples used in model calibration batch tests

Sample	Core	Formation	Description
1	MSE-CORE-101B	Hanford Unit 1	Light brown gray (2.5Y 6/2) to grayish brown (2.5Y 5/2); Medium to coarse grained sand; Subrounded; 40-50% basalt; Quartz is dominant with minor amounts of plagioclase and feldspar and trace pyrite; no visual reaction with HCl; Loose, dry soil; 2-3% magnetite
2	MSE-CORE-104B	Hanford Unit 2	Pale yellow (2.5Y 7/3); very fine to fine grained sand; Rounded to subrounded; 5% basalt; Quartz is dominant; Reddish to reddish-orange staining; Slight reaction with HCl; Little to no moisture; 1% magnetite
3	MSE-CORE-106B	Hanford Unit 2	Very pale brown (10YR 7/3 to 10YR 7/4); Very fine grained silty sand; Rounded to subrounded; 1-2% basalt; Quartz is dominant; Slight to moderate reaction with HCl; Loose to slightly cemented; Little to no moisture; Trace amount of magnetite
4	MSE-CORE-112B	Plio-Pleistocene Caliche	Pale yellow (2.5Y 8/3 to 2.5T 8/4); Silt to very fine grained sand; Subrounded; <1-1% basalt; some quartz; Carbonate present; strong reaction with HCl; Highly cemented but has high transmissivity; trace amount of magnetite.
5	MSE-CORE-119B	Ringold Upper Gravels	Gravel with silty-sand matrix; Matrix is: Light yellow brown (2.5Y 6/3); Silt to very fine grained sand; subrounded; <1-1% basalt; some quartz; No visible reaction with HCl; Loose; Trace amount of magnetite

8.2.2 Batch Test Aqueous Phase

The calibration batch tests were completed using Columbia River Water. The water was spiked with uranyl-nitrate at two concentrations (Low Uranium and High Uranium) to produce the stock solutions used in the initial batch testing. The concentrations were chosen based on the range of dissolved uranium reported for the 200-UP-1 Operable Unit (EPA, 1997). Aliquots of each stock solution were taken and the pH adjusted to obtain seven laboratory solutions ranging in pH from 3 to 9.

The concentration of uranium in the stock solutions was measured in the laboratory and used to calculate the initial concentration of uranium in the soil/water mixtures (see Table 8-2).

Table 8-2. Measured uranium concentrations in initial batch test solutions

		Low Uranium Stock Solution	High Uranium Stock Solution
Stock Solutions	mg/L	0.149	1.28
	mol/L	6.26E-07	5.38E-06
Soil/Water Mixtures	mg/L	0.0745	0.64
	mol/L	3.13E-07	2.69E-06

8.2.3 Batch Test Gas Phase

The batch testing was conducted in a CO₂ controlled atmosphere to simulate the CO₂ concentrations measured during the installation of well 299-W19-43. The CO₂ concentrations selected for the batch testing included 5,000 ppm, 10,000 ppm, and 20,000 ppm. These CO₂ concentrations represented the range of concentrations measured for the samples selected for the batch testing. During the batch testing, the CO₂ concentrations were monitored to ensure the testing conditions were representative of the selected subsurface conditions and to provide data for later geochemical modeling efforts. The measured CO₂ concentrations during the batch testing are presented in Figure 8-8. The average values measured during the batch testing are presented in Table 8-3.

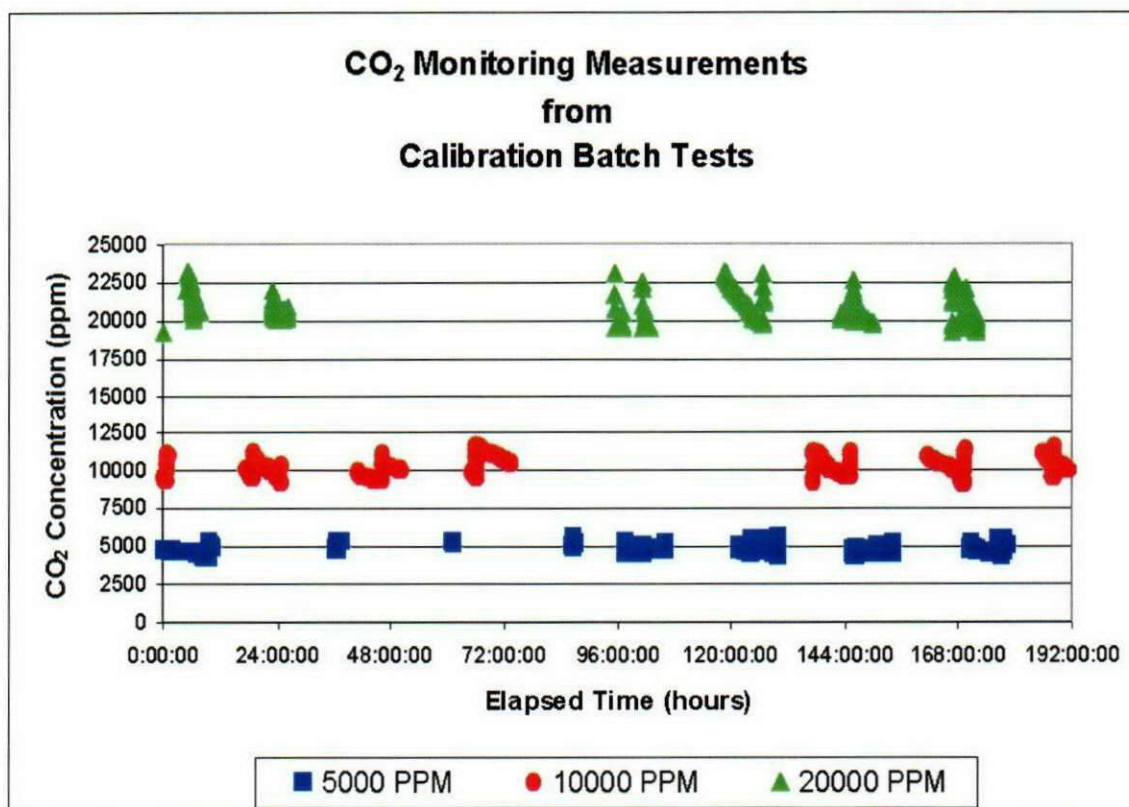


Figure 8-8. CO₂ monitoring measurements acquired during the calibration batch tests.

Table 8-3. Subsurface and batch test CO₂ concentrations

Sample Description	Approximate Depth (ft)	Subsurface CO ₂ Concentration (ppm)	Average Batch Test CO ₂ Concentration (ppm)
MSE-CORE-101B	21.5	3916	4657
MSE-CORE-104B	111.3	17806	20358
MSE-CORE-106B	171.5	8783	10285
MSE-CORE-112B	195.8	7773	10285
MSE-CORE-119B	231.4	5771	4657

8.2.4 Batch Testing

The batch tests were conducted in a glove box to provide the CO₂ concentration control. A picture of the laboratory setup is shown in Figure 8-9. For each batch test, a small quantity of soil was placed in a test tube (approximately 5 grams of soil) and mixed, using a roller table, with Columbia River water (approximately 25 mL) for one day. This was done to equilibrate the soil with the water. The pH adjusted stock solution water (approximately 25 mL) was added to the pre-equilibrated soil/water mixture. The test tubes were gently agitated using the roller table for 2 hours per day for three days. Between rollings, the soil/water mixtures were left open to the glove box atmosphere to equilibrate with the CO₂. The pH of the solution was measured and adjusted if necessary between each rolling. The pH adjustments were made

using HCl and NaOH solutions. After the third rolling, the mixtures were centrifuged and final pH measurements were made. From each soil/water mixture, a subsample of water was extracted. These subsamples were filtered and preserved for laboratory analysis.

Quality control during the batch testing followed the specifications outlined in the calibration test plan. This included duplicate samples; blank samples with water only; and blank samples of spiked water.



Figure 8-9. Batch testing laboratory setup at MSE.

8.3 GEOCHEMICAL MODELING OF BATCH TESTS

The initial geochemical model was designed to simulate conditions of the batch testing. The model parameters for the initial geochemical model were obtained from laboratory analyses, measurements made during the batch tests, and relevant literature values. Laboratory analytical data included concentrations of ionic species in the Columbia River water and the total extractable iron in each soil type. CO_2 concentrations measured during the model calibration batch testing were also used in the initial modeling. Parameters taken from literature included thermodynamic constants, the surface area of the primary sorbent (iron-hydroxide), and the surface site density for the sorbent.

8.3.1 Aqueous Component Concentrations

Concentrations of the ions present in the Columbia River water were determined through laboratory analysis. The aqueous components analyzed for and the corresponding concentrations used in the initial geochemical model are shown in Table 8-4.

Table 8-4. Aqueous component concentrations used in the initial geochemical model

Aqueous Components	Concentration (mg/L)	Concentration (mol/L)
Al ⁺³	NON DETECT	
Ca ⁺²	21	5.24E-04
Cl ⁻	2	5.64E-05
F ⁻	0.1	5.26E-06
Fe ⁺³	NON DETECT	
K ⁺	1	2.56E-05
Mg ⁺²	5	2.06E-04
Na ⁺	3	1.30E-04
NO ₃ ⁻	0.21	1.50E-05
PO ₄ ⁻³	0.03	3.16E-07
Si(OH) ₄ (as Si)	2.7	9.61E-05
SO ₄ ⁻²	13	1.35E-04
Zn ⁺²	0.03	4.59E-07

The ionic strength used in the modeling was calculated from the aqueous components and corresponding concentrations. The ionic strength (*I*) of the solution was calculated using the Davies equation:

$$I = \frac{1}{2} \sum (m_i z_i^2) \quad \text{Equation 7}$$

where *I* is in molal or molar units, *m_i* is the concentration of ion *i*, and *z_i* is the charge of ion *i*. From this, the ionic strength of the solution was calculated to be 1.85x10⁻³ molar.

For each soil sample, an initial high (0.64 mg/L) and low (0.0745 mg/L) uranium concentration were modeled. These were the concentrations of the soil/water mixtures from the batch testing.

8.3.2 Carbon Dioxide Concentrations

As previously discussed in Section 8.2.3, the CO₂ concentrations were measured during the batch testing. The average concentrations of the three target CO₂ concentrations (see Table 8-3) for the batch testing were included in the model as the log of the partial pressure, in atmospheres, of CO₂.

8.3.3 Thermodynamic Data

Equilibrium constants, enthalpy values, and stoichiometric coefficients of the aqueous complexes form the basis of the geochemical model. The thermodynamic database used in the geochemical modeling efforts was derived mainly from the chemical equilibrium modeling program MINEQL+© v. 4.5. In addition to the thermodynamic data included in MINEQL+© v. 4.5, MSE compiled thermodynamic data using information from professionals and recent studies in uranium adsorption. Sources for the thermodynamic database include:

- MINTEQA2 v4.02 (Allison et al., 1991) with updated uranium thermodynamic data;
- *Surface Complexation Modeling: Hydrous Ferric Oxide* (Dzombak and Morel, 1990);
- *Uranium (VI) Interactions with Mineral Surfaces: Controlling Factors and Surface Complexation Modeling* (Payne, 1999);
- *Uranium (VI) Transport Modeling: Geochemical data and Submodels* (Tripathi, 1983);
- *Adsorption of Uranyl Onto Ferric Oxyhydroxides: Application of the Surface Complexation Site-Binding Model* (Hsi and Langmuir, 1985);
- *NIST Critical Stability Constants of Metal Complexes Database, NIST Standard Reference Database 46* (Smith and Martell, 1993);
- *Mixed-Metal Hydroxycarboxylic Acid Complexes - Formation Constants of U(VI) with Fe(III), Al(III), In(III), and Cu(II)* (Manzurola et al., 1989);
- *The Hydrolysis of Cations* (Baes and Mesmer, 1976);
- *Critical Stability Constants, Volume 4: Inorganic Complexes* (Smith and Martell, 1976); and
- *U(VI) Adsorption to Heterogeneous Subsurface Media: Application of a Surface Complexation Model* (Barnett et al., 2002).

8.3.4 Surface Complexation Sorbent Data

The surface complexation sorbent data specifically relates to the description of the sorbent(s) considered in the geochemical model. These data include the sorbent type and structure, surface area, and site density. Iron-hydroxide minerals are being considered the main sorbent for the geochemical modeling.

As previously discussed, studies indicate that iron-hydroxide surface sites ($\equiv\text{FeOH}$) dominate UO_2^{+2} adsorption. Using the CBD analytical results, previously discussed in Section 7.5, and the quantities of soil and groundwater used in the calibration batch samples, the concentrations of adsorbing solid ($\equiv\text{FeOH}$) were calculated for each soil sample and are presented in Table 8-5.

Table 8-5. Solid $\equiv\text{FeOH}$ concentration values for geochemical model

Sample Description	Approximate Depth (ft)	Grams of $\equiv\text{FeOH}$ per Kilogram of Soil (CBD)	Mass (g) of Soil in Batch Sample	Volume (mL) of Groundwater in Batch Sample	Adsorbing Solid ($\equiv\text{FeOH}$) Concentration (g/L)
MSE-CORE-101B	21.5	1.66	5	54	0.154
MSE-CORE-104B	111.3	2.98	5	54	0.276
MSE-CORE-106B	171.5	3.76	5	54	0.348
MSE-CORE-112B	195.8	1.64	5	54	0.152
MSE-CORE-119B	231.4	3.85	5	54	0.356

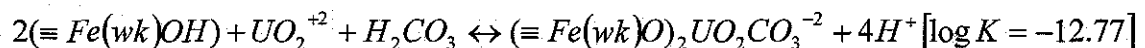
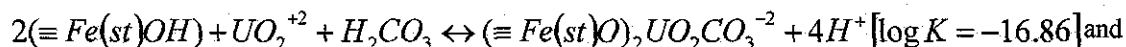
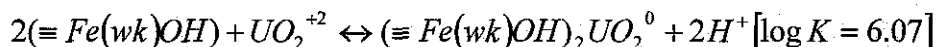
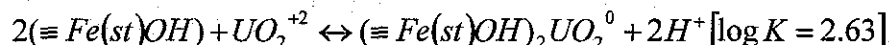
The structure of the sorbent site may be described as either monodentate or bidentate. The terms monodentate and bidentate, when used to describe surface complexation structures, indicate the behavior of the surface in terms of the surface site chemistry (Hiemstra and Riemsdijk, 1998). A monodentate structure is one in which the surface site is treated as a point charge. A bidentate structure treats the site as a distribution of charges, and thus not all of the binding energy that might be available for a point charge is

available in a bidentate structure. The bidentate structure results in increased competition for the surface site by the UO_2^{+2} ion with other ions in solution. At lower pH values, there is an increase in the number of H^+ ions in solution, resulting in less sorption of the uranium at lower pH values. Likewise, at higher pH values, there are fewer surface sites available, again resulting in less sorption of uranium. For the geochemical model, the structure of UO_2^{+2} adsorption to $\equiv FeOH$ sorption site is considered a bidentate one. Several sources have indicated, through laboratory analysis, that a bidentate structure is more likely than a monodentate one (Langmuir, 1997; Hiemstra and Riemsdijk, 1998; and Payne, 1999).

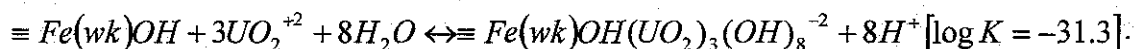
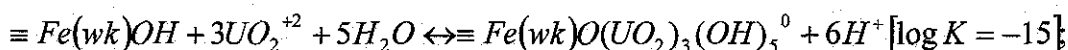
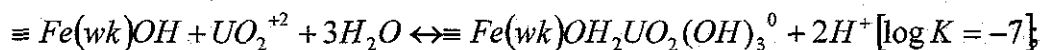
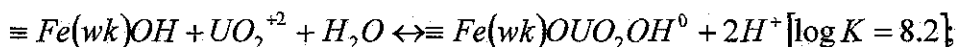
The initial geochemical model followed the $\equiv FeOH$ diffuse layer model described by Dzombak and Morel (1990). The specific surface area of the $\equiv FeOH$ sorbent was modeled as $600 \text{ m}^2/\text{g}$. The model also assumes two types of sorbing sites (strong, high affinity and weak, low affinity). The site densities of the strong and weak sites were 0.005 moles of sites per mole of iron and 0.2 moles per sites per mole of iron, respectively.

8.3.5 Surface Complexation Reactions

As discussed in Section 8.3.3, thermodynamic data for the aqueous reactions were compiled from numerous sources. Thermodynamic constants for the surface complexation reactions describing UO_2^{+2} adsorption to $\equiv FeOH$ sites were also obtained from these sources. For the initial geochemical modeling efforts, only bidentate UO_2^{+2} and uranyl-carbonate surface complexation reactions with strong and weak adsorption sites were considered. The reactions and corresponding thermodynamic constants were:



Additional UO_2^{+2} surface complexation reactions considered for the geochemical modeling efforts include:



9 INITIAL GEOCHEMICAL MODEL EVALUATION

The results of the initial geochemical model as compared to the results from the batch testing are presented in this section. The results are presented as plots of the percent of uranium adsorbed as a function of the pH under which the adsorption occurred for both the model predictions and observed data from the batch tests. The goodness-of-fit between the observed and predicted UO_2^{+2} adsorption data was evaluated quantitatively and qualitatively.

The goodness-of-fit between the results was determined by calculating the root mean squared error (RMSE) according to:

$$RMSE = \left[\frac{1}{(n_d - n_p)} \sum_{i=1}^{n_d} \left(\frac{C - C'}{C_O} \right)^2 \right]^{1/2} \quad \text{Equation 8}$$

Where: n_d is the number of data points, n_p is the number of adjustable parameters, C is the measured concentration, C' is the predicted concentration, and C_O is the initial concentration. The RMSE is a measure of the error between predicted and measured values expressed as a function of the initial concentration.

9.1 BATCH TEST RESULTS

Final uranium concentrations in the batch test samples were measured in the laboratory and the resulting percentages of adsorbed uranium were calculated. Table 9-1 summarizes the data from the batch testing.

Table 9-1. Results of uranium adsorption batch tests

	Low Uranium Stock Solution			High Uranium Stock Solution		
	pH Measured	U Concentration (mg/L) in Solution	% Adsorbed to Soil	pH Measured	U Concentration (mg/L) in Solution	% Adsorbed to Soil
MSE-CORE-101B	5.50	0.009	87.9	5.99	0.2	68.8
	5.94	0.034	54.4	6.19	0.303	52.7
	6.20	0.029	61.1	6.37	0.432	32.5
	6.63	0.067	10.1	6.87	0.571	10.8
	7.39	0.085	-14.1	7.58	0.691	-8.0
	7.75	0.085	-14.1	7.81	0.672	-5.0
	8.39	0.088	-18.1	8.31	0.646	-0.9
MSE-CORE-104B	6.02	0.028	62.4	6.17	0.405	36.7
	6.15	0.041	45.0	6.27	0.467	27.0
	6.38	0.018	75.8	6.36	0.449	29.8
	6.64	0.039	47.7	6.96	1.12	-75.0
	7.33	0.09	-20.8	7.26	1.42	-121.9
	7.97	0.104	-39.6	7.51	1.5	-134.4
	8.78	0.101	-35.6	8.07	0.735	-14.8
MSE-CORE-106B	5.28	0.011	85.2	5.36	0.218	65.9
	5.76	0.02	73.2	5.89	0.363	43.3
	6.18	0.01	86.6	6.40	0.53	17.2
	6.61	0.053	28.9	6.48	0.503	21.4
	7.39	0.08	-7.4	7.38	0.634	0.9

	Low Uranium Stock Solution			High Uranium Stock Solution		
	pH Measured	U Concentration (mg/L) in Solution	% Adsorbed to Soil	pH Measured	U Concentration (mg/L) in Solution	% Adsorbed to Soil
	7.94	0.088	-18.1	7.97	0.674	-5.3
	8.14	0.095	-27.5	9.01	0.682	-6.6
MSE-CORE-112B	6.28	0.084	-12.8	5.98	0.613	4.2
	6.46	0.076	-2.0	6.26	0.493	23.0
	6.45	0.04	46.3	6.32	0.475	25.8
	6.86	0.056	24.8	6.74	0.392	38.8
	7.47	0.054	27.5	7.45	0.444	30.6
	7.34	0.071	4.7	7.67	0.422	34.1
	8.55	0.115	-54.4	8.19	0.503	21.4
MSE-CORE-119B	3.90	0.014	81.2	4.76	0.139	78.3
	4.52	0.006	91.9	4.76	0.062	90.3
	5.54	0.003	96.0	5.54	0.031	95.2
	6.34	0.007	90.6	6.35	0.081	87.3
	7.17	0.051	31.5	7.15	0.503	21.4
	8.32	0.086	-15.4	7.56	0.574	10.3
	8.79	0.086	-15.4	8.71	0.634	0.9
Values in italics were assumed 0% for comparison to modeled values.						

The negative values shown in Table 9-1 indicate that more uranium was in solution at the completion of the batch test than what was initially in the stock solution at the onset of the batch tests. This may be a result of uranium initially in the soil desorbing during the batch testing. Laboratory error is also a possible reason for this discrepancy. Additional studies may confirm the cause of the negative values.

9.2 INITIAL GEOCHEMICAL MODEL RESULTS

The initial conditions of the soil/water mixtures for each batch test were modeled to predict the UO_2^{+2} adsorption. The analytical data from the batch tests were then compared to the predicted data from the geochemical model. The following figures illustrate the most recent results of the geochemical model iterations and the laboratory batch tests.

Discrepancies between the model and laboratory results may be attributed to several factors including over/under estimation of available adsorption sites, errors in thermodynamic constants, and inclusion and/or exclusion of specific chemical reactions. While the RMSE values for the models indicate poor agreement between the modeled and observed values for adsorption, the general shape of the modeled and observed sorption curves in most cases is promising. The results of this preliminary effort will be reexamined, several batch tests rerun and the batch test procedure reviewed to ensure that the modeled geochemical conditions reflected those of the batch test.

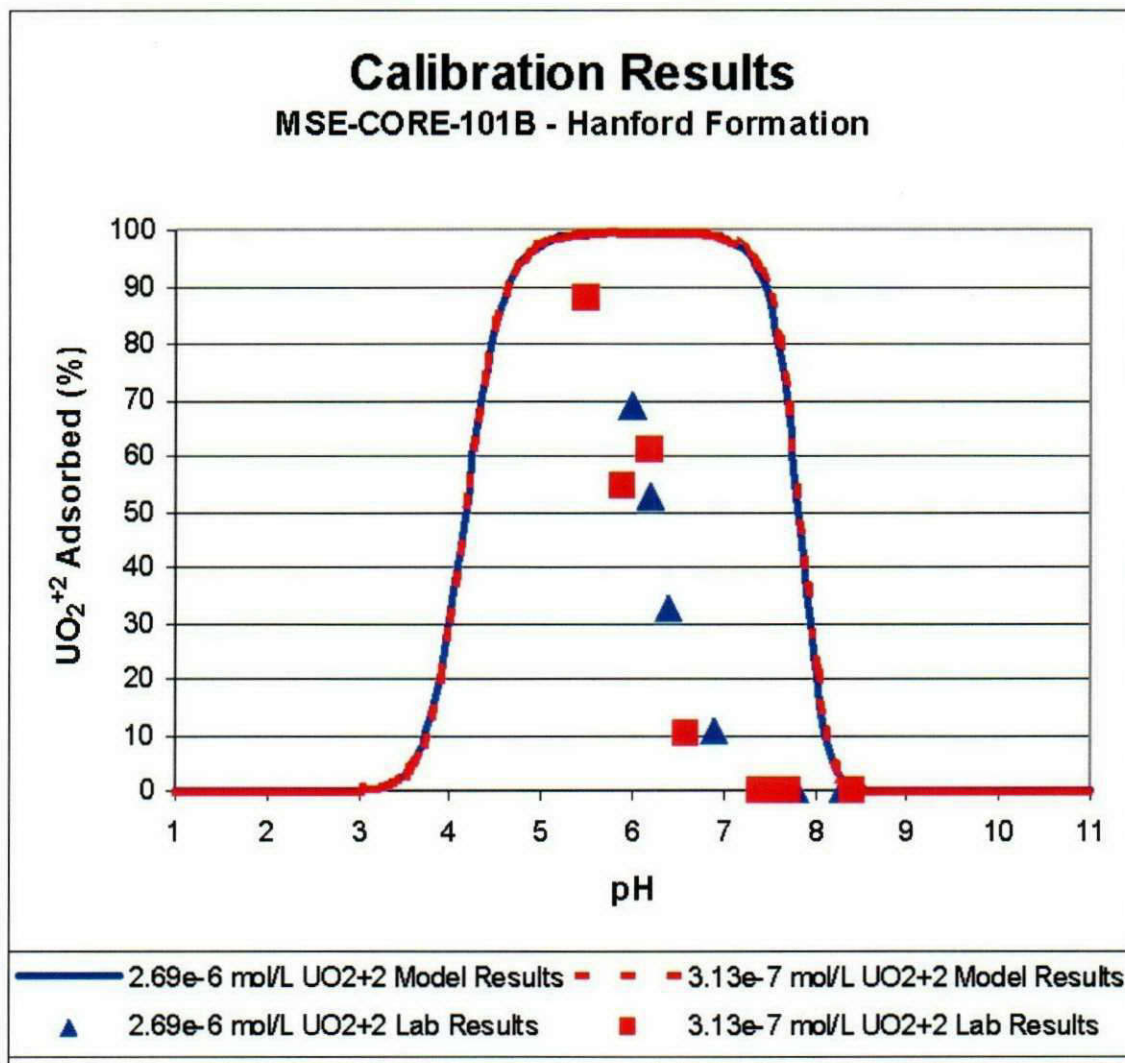


Figure 9-1. Geochemical modeling and batch test results for MSE-CORE-101B. *RMSE between the model and laboratory values was 7.83 for the high uranium concentration and 7.61 for the low uranium concentration.*

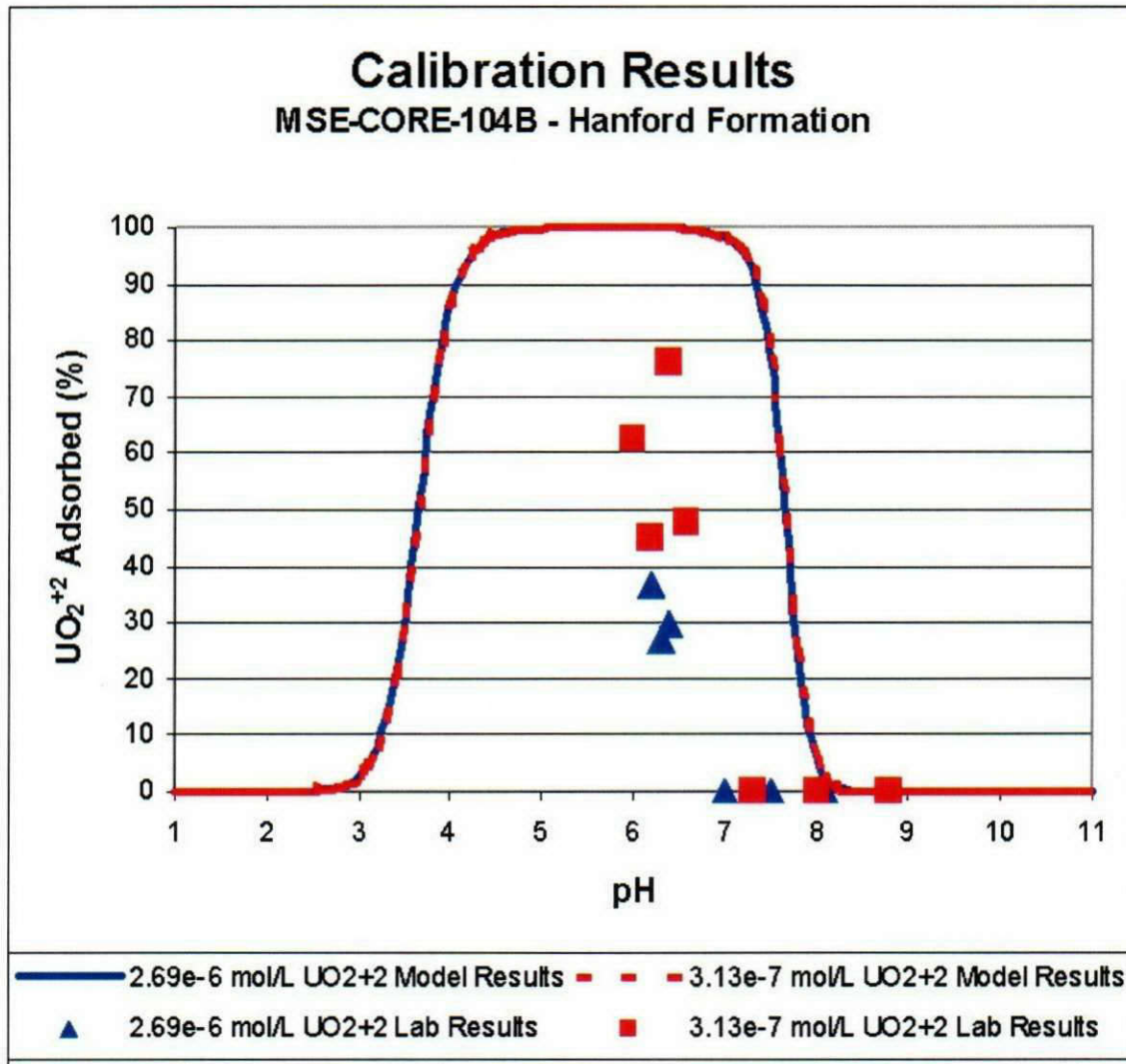


Figure 9-2. Geochemical modeling and batch test results for MSE-CORE-104B. *RMSE between the model and laboratory values was 8.90 for the high uranium concentration and 6.66 for the low uranium concentration.*

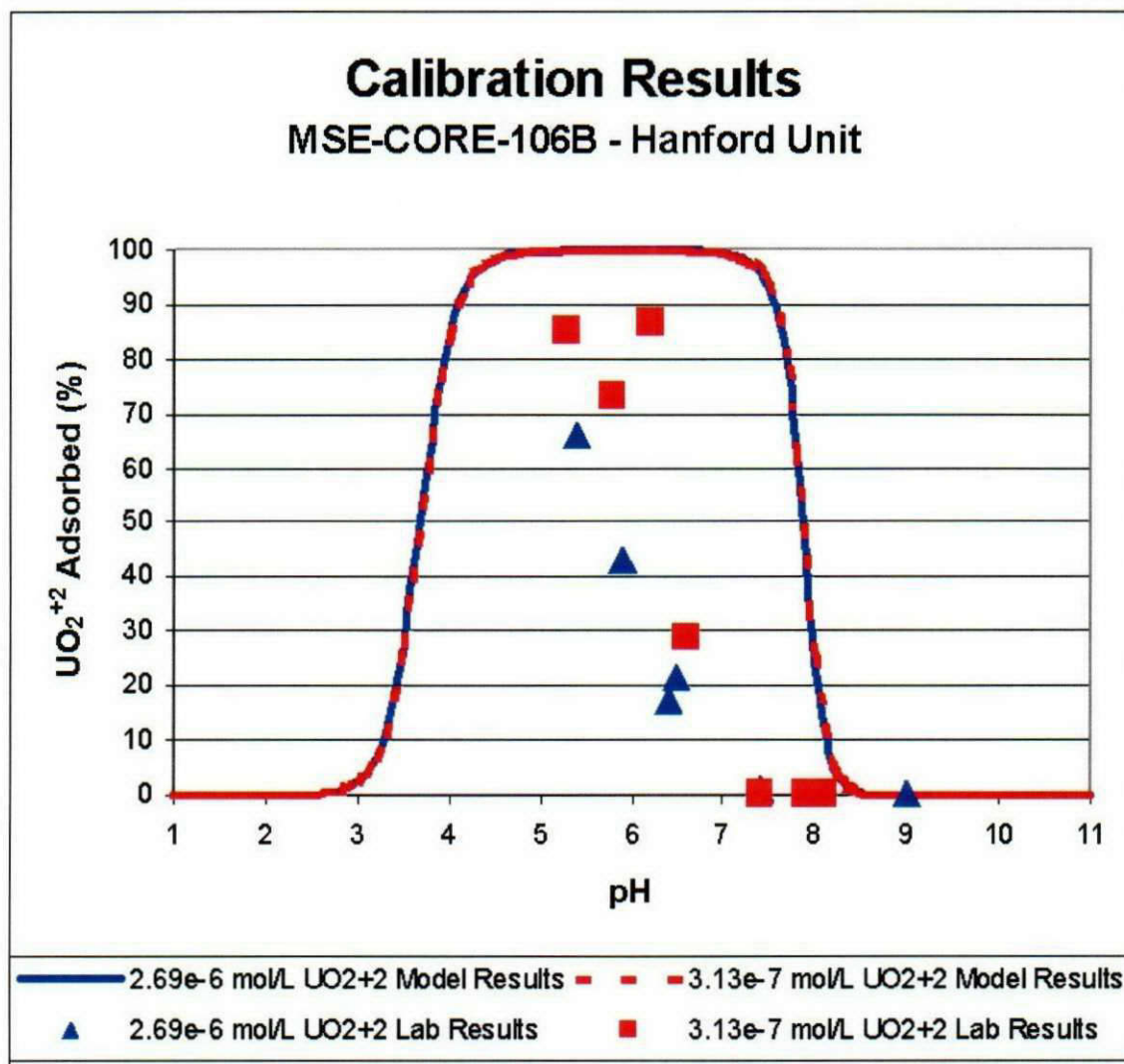


Figure 9-3. Geochemical modeling and batch test results for MSE-CORE-106B. *RMSE between the model and laboratory values was 7.87 for the high uranium concentration and 6.80 for the low uranium concentration.*

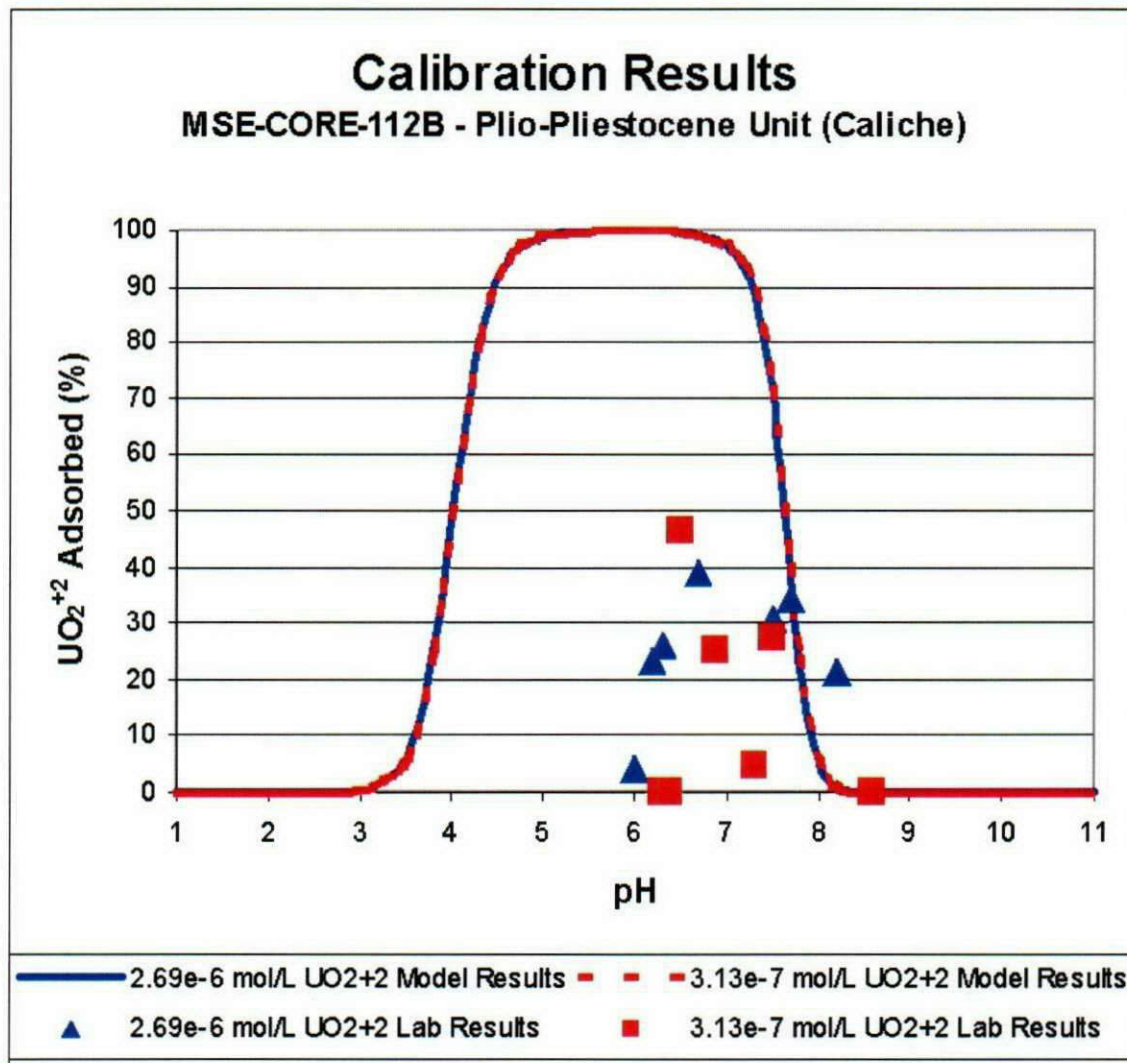


Figure 9-4. Geochemical modeling and batch test results for MSE-CORE-112B. *RMSE between the model and laboratory values was 7.43 for the high uranium concentration and 8.70 for the low uranium concentration.*

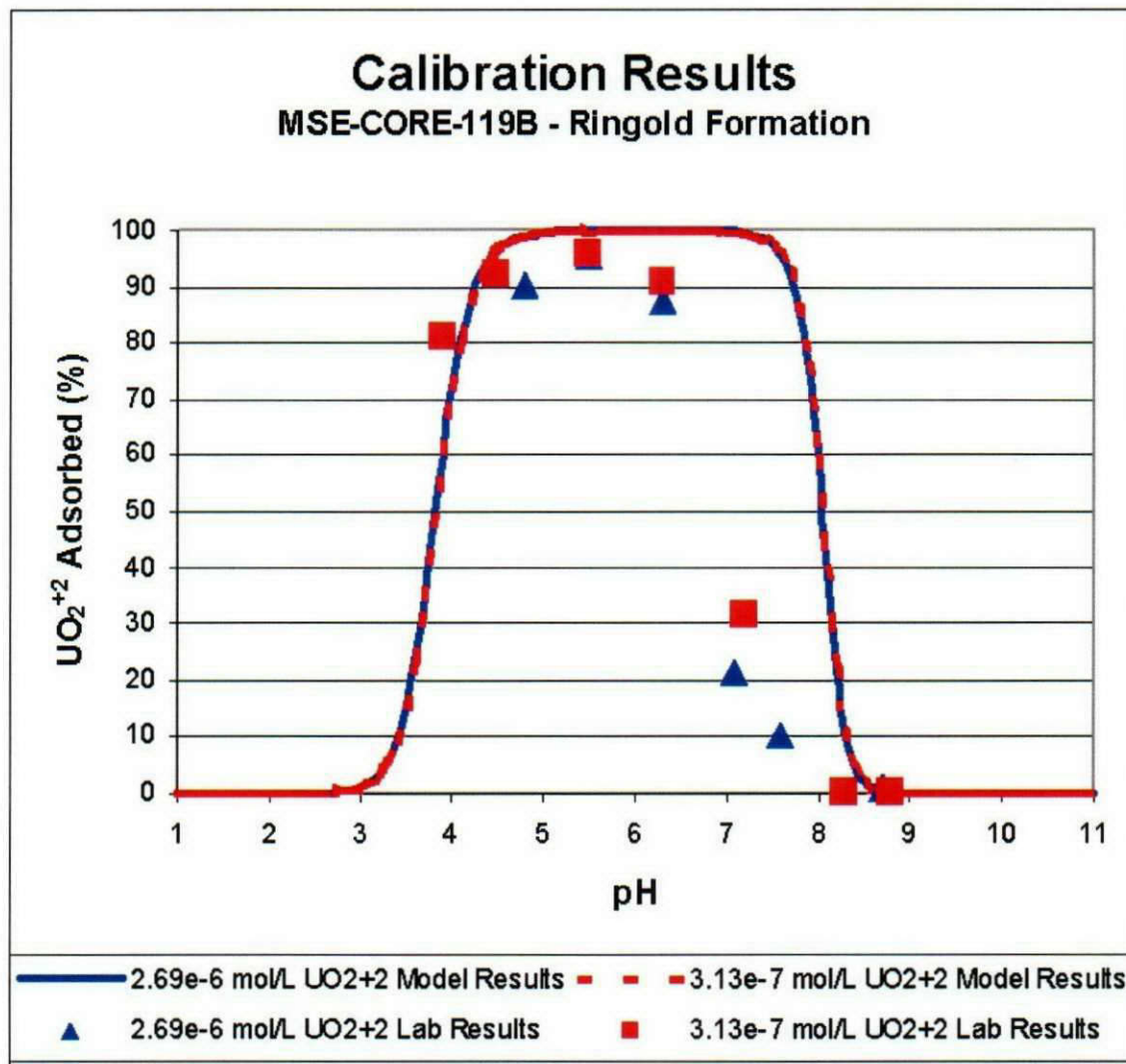


Figure 9-5. Geochemical modeling and batch test results for MSE-CORE-119B. *RMSE between the model and laboratory values was 5.43 for the high uranium concentration and 3.46 for the low uranium concentration.*

10 MODEL PARAMETER OPTIMIZATION/CALIBRATION STATUS

Model parameter optimization will be conducted by MSE. This will be the final step in the calibration process and be completed using FITEQL (Herbelin, & Westall, 1999), which is a computer program for determination of chemical equilibrium constants from experimental data. The calibration data from the batch testing will be used for this effort. The geochemical model parameters that are being considered for optimization include the surface area and surface-site density data for the sorbent. These parameters were initially taken from literature as generally accepted values compiled from a number of studies. However, there is considerable range in some of the values reported in the literature. During the parameter optimization, MSE will ensure the final model parameters are within a range realistic for Hanford conditions. MSE will also reconfirm the assumption that iron oxides are the dominant sorbents of the uranium for the Hanford soils. The results of the subsequent model parameter optimization will be reported in the FY03 Status Report.

11 MODEL VALIDATION STATUS

The model validation process has been initiated. The test plan for model validation has been written by MSE, reviewed, and approved by BHI and DOE-RL. Data will be obtained from an additional set of batch test for this purpose. The validation program may be refined based on results of additional batch tests and other input.

12 PROJECTED OUT YEAR ACTIVITIES

12.1 FY03

The geochemical modeling will be completed, along with the laboratory validation of the model using Hanford soils and groundwater collected from the well drilled in FY01. The site conceptual model will be improved and recommendations will be made for numerical models that can incorporate the description of uranium transport in the unsaturated and saturated materials at the site. In addition, MSE will make recommendations for remedial alternatives based on the refined understanding of the uranium transport in the unsaturated and saturated materials at the site, as well as completing an annual status report for FY03.

Scope that will be accomplished during FY03 includes:

1. Continue to coordinate all efforts with FHI and DOE-RL, and participate in monthly conference calls.
2. Complete additional laboratory analysis associated with calibration batch tests.
3. Complete the laboratory validation batch testing using Hanford soils and groundwater collected from the well drilled in FY01.
4. Complete the validation of the geochemical model.
5. Coordinate with FHI and DOE-RL to meet with personnel at Hanford working on projects in the 200 East and 300 Areas, in order to share information that may be pertinent to all three project efforts.
6. Complete geochemical modeling efforts.
7. Improve/update the current conceptual model for the area of concern.
8. Provide recommendations for numerical models that can incorporate the description of uranium transport in the unsaturated and saturated materials at the site.
9. Provide recommendations for remedial alternatives based on the refined understanding of the uranium transport in the unsaturated and saturated materials at the site.
10. Complete an annual status report.

12.2 FY04

The project will be finalized, and all reporting and closeout efforts for the project will be completed in FY04.

13 REFERENCES

- Allison, Jerry D., David S. Brown, and Kevin J Novo-Gradac, 1991. *MINTEQA2/PRODEFA2, A Geochemical Assessment Model for Environmental Systems: Version 3.0 User's Manual*. Environmental Research Laboratory. Office of Research and Development. U.S. Environmental Protection Agency; Athens Georgia. March 1991.
- ASTM Guide D5753-95e1. *Standard Guide for Planning and Conducting Borehole Geophysical Logging*. American Society For Testing And Materials, West Conshohocken, PA.
- ASTM Guide D6274-98. *Standard Guide for Conducting Borehole Geophysical Logging-Gamma*. American Society For Testing And Materials, West Conshohocken, PA.
- ASTM Test Method D6031-96. *Standard Test Method for Logging In Situ Moisture Content and Density of Soil and Rock by the Nuclear Method in Horizontal, Slanted, and Vertical Access Tubes*. American Society For Testing And Materials, West Conshohocken, PA.
- Baes, C. F. and R. E. Mesmer. 1976, *The Hydrolysis of Cations*. Wiley, New York. 1976.
- Barnett, Mark O., Philip M. Jardine, and Scott C. Brooks., 2002. *U(VI) Adsorption to Hetrogeneous Subsurface Media: Application of a Surface Complexation Model*. Environmental Science & Technology. American Chemical Society. Vol. 36, No. 5. 2002.
- BHI, 1995. *200 West Area Limited Field Investigation*. Bechtel Hanford Inc., Richland Washington. March 1995.
- BHI, 2001a. *Memorandum of Understanding between MSE-technology Applications, Inc. and Bechtel Hanford, Inc for Site access and Quality Assurance, Environmental, Health and Safety Oversight*. Bechtel Hanford Inc., Richland Washington.
- BHI, 2001b. *Sampling and Analysis Instruction for the Installation and Sampling of One New Groundwater Monitoring Well at the 200-UP-1 Operable Unit*, BHI-01540, Rev. 0, Bechtel Hanford Inc., Richland Washington.
- Carter, D.L., Mortland, M.M., and Kemper, W.D., 1986. *Specific Surface*. Part 1: Klute, A. Ed: Soil Science Society of America, Madison, WI: pp 413-423.
- DOE/RL, 1997. *Waste Site Grouping for 200 Areas Soil Investigations* DOE/RL-96-81 Rev. 0. January 1, 1997
- DOE/RL, 1999. *200 Areas Remedial Investigation/Feasibility Study Implementation Plan-Environmental Restoration Program* DOE/RL-98-28 Rev. 0. April 1, 1999
- Dzombak, D.A. and Morel, F.M.M., 1990. *Surface complexation modeling, Hydrous ferric oxide*. Wiley-Interscience, New York 1990
- EPA, 1997. *Declaration of the Record of Decision, Interim Action Record of Decision for the 200 Area UP-1 OU 043623*. February 1997.
- Fetter, C.W., 1988, *Applied Hydrogeology*, 2nd Ed., MacMillian Publishing Company, New York, NY.
- Freeze, R.A., and John A. Cherry, 1979, *Groundwater*, Prentice-Hall, Inc., Englewood Cliffs, N.J. 07632.

- Herbelin, A. L. and John C. Westall, 1999. *FITEQL, A computer program for determination of chemical equilibrium constants from experimental data* Report 99-01. Department of Chemistry, Oregon State University, Corvallis, Oregon 97331.
- Hiemstra, T. and W.H. Van Riemsdijk, 1998. *Surface Structural Ion Adsorption Modeling of Competitive Binding of Oxyanions by Metal (Hydr)oxides*. Journal of Colloid and Interface Science. 210, pages 182-193.
- Hsi, C. K. and D. Langmuir. 1985. *Adsorption of Uranyl Onto Ferric Oxyhydroxides: Application of the Surface Complexation Site-Binding Model*. *Geochimica et Cosmochimica Acta*; 49: 1931-1941. 1985.
- Krumbein, W. C., and Monk, G. D., 1943, *Permeability as a function of the size parameters of unconsolidated sand*: Transaction of the American Institute of Mining, Metallurgical and Petroleum Engineers, v. 151, p. 153-163.
- Langmuir, D. 1997. *Aqueous Environmental Geochemistry*. Prentice Hall, Upper Saddle River, NJ. 1997.
- Loeppert, R. H., and Inskeep, W.P., 1996. *In Methods of Soil Analysis, Part 3*: Sparks, D.L. Ed: Soil Science Society of America, Madison, WI: pp 639-664.\
- Manzurola, E., A. Apelblat, G. Markovits, and O. Levy. 1989. *Mixed-Metal Hydroxycarboxylic Acid Complexes - Formation Constants of U(VI) with Fe(III), Al(III), In(III), and Cu(II)*. Journal of the Chemical Society, Faraday Transactions 1; 85: 373-379. 1989.
- MSE, 2001a. *Multi-Year Implementation and Project Management Plan for Development of a Conceptual Geochemical Model for Uranium Mobility in the Unsaturated Zone and Saturated Sediments at the 200 West Area of the DOE Hanford Site, Washington*. MSE Technology Applications, Butte, Montana
- MSE, 2001b. *Sampling and Analysis Plan for Development of a Conceptual Geochemical Model for Uranium Transport in the Unsaturated and Saturated Sediments at the 200-West Area of the Department of Energy Hanford Site, Washington*. ECCP-11, MSE-Technology Applications, Butte, Montana 59702. June 2001.
- MSE, 2001c. *Data Quality Objectives Summary Report for Development of a Conceptual Geochemical Model for Uranium Mobility in the Unsaturated Zone and Saturated Sediments at the 200 West Area of the DOE Hanford Site, Washington*. MSE Technology Applications, Butte, Montana 59702.
- MSE, 2001d. *Health and Safety Plan for Carbon Dioxide Sampling of the Borehole at the 200 West Area of the Hanford Site in Support of the Uranium Mobility Study in the 200 West Area of the Hanford Site*. MSE Technology Applications, Butte, Montana 59702. 2001.
- MSE, 2001e. *Description of Work: Soil Gas CO₂ Concentration and Soil Moisture Investigation at 200 West Area Hanford Site for the UP-1 Uranium Mobility Investigation*. MSE Technology Applications, Butte, Montana 59702. 2001.
- MSE, 2002a. *Hanford Uranium Mobility Geochemical Modeling: Sensitivity Analysis*. MSE Technology Applications, Inc. Butte, Montana; May 17, 2002.
- MSE, 2002b. *Calibration Plan for Geochemical Model Describing Uranium Transport in the Unsaturated and Saturated Sediments at the 200 West Area of the Department of Energy Hanford Site, Washington*. MSE Technology Applications, Inc. Butte, Montana; May 17, 2002.

- MSE, 2002c. *Waste Inventory Report for the U-Plant in the 200 West Area of the Department of Energy Hanford Site, Washington*. MSE Technology Applications, Inc. Butte, Montana; 2002.
- Pabalan, R. T., Turner, D.R. Bertetti, F.P., and Prikryl, J.D. 1998. *Uranium (VI) sorption onto selected mineral surfaces*. Chapter 3 in Adsorption of Metals by Geomedia. Variables, Mechanisms and Model Applications. E.A. Jenne ed., Academic Press, San Diego CA, 99-130. 1998
- Payne, Timothy Ernest. 1999. *Uranium (VI) Interactions with Mineral Surfaces: Controlling Factors and Surface Complexation Modeling*. Thesis for Doctor of Philosophy from the University of New South Wales. School of Civil and Environmental Sciences. August 1999.
- Rhoades, J.D., 1996. Salinity: *Electrical Conductivity and Total Dissolved Solids*. Part 3: Sparks, D.L. Ed: Soil Science Society of America, Madison, WI: pp 417-435.
- Schecher, William D. and Drew C. McAvoy. 2001 *MINEQL+ A Chemical Equilibrium Modeling System*. Environmental Research Software; Hallowell, Maine. 1998.
- Smith, R. M. and A. E. Martell. 1993. *NIST Critical Stability Constants of Metal Complexes Database, NIST Standard Reference Database 46*. U.S. Department of Commerce, Gaithersburg MD. 1993.
- Smith, R. M. and A. E. Martell. 1976. *Critical Stability Constants, Volume 4: Inorganic Complexes*. Plenum Press, New York. 1976.
- Tripathi, V. S. 1983. *Uranium (VI) Transport Modeling: Geochemical Data and Submodels*. PhD Thesis; Stanford University. 1983.
- Turner, D.R. 1995. *A uniform approach to surface complexation modeling of Radionuclide sorption*. Report CN-WRA 95-001. Center for Nuclear Waste Regulatory Analysis, San Antonio TX. 1995.
- Waite, T.D., J.A. Davis, T.E. Payne, G.A. Waychunas, and N. Xu. 1994. *Uranium (VI) Adsorption to Ferrihydrite: Application of a Surface Complexation Model*. *Geochimica et Cosmochimica Acta*. Vol 58; No 24; pp 5465-5478. 1994.
- WHC, 1988. *U1/U2 Uranium Plume Characterization, Remedial Action Review and Recommendation for Future Action* WHC-EP-0133. June 1, 1988.

Appendix A Duratek Geophysical Logging Reports

Neutron-Neutron Moisture Borehole Survey

Duratek Federal Services

Log Header

Project: 200 UP1

Well: 299-W19-43

Log Type: Moisture Gauge

Borehole Information

Well # <u>C3381</u>	Water Depth <u>none</u> ft	Total Depth <u>255</u> ft
Elevation Reference <u>n/a</u>	Elevation <u>n/a</u> ft	
Depth Reference <u>Ground Surface</u>	Casing Stickup <u>3.7</u> ft	
Casing Diameter <u>10.75 ID</u> in	Depth Interval <u>0 to 50</u> ft	Thickness <u>0.50</u> in
Casing Diameter <u>7.625 ID</u> in	Depth Interval <u>0 to 255</u> ft	Thickness <u>0.50</u> in

Logging Information

Log Type:	Moisture Gauge
Company	Duratek Federal Services
Date/Archive File Name	July 16, 2001 M2W19043
Logging Engineers	<u>J. Kiesler</u> <u>J. Meisner</u>
Instrument Series	RLSM00.0
Logging Unit	RLS-1
Depth Interval	45 to 150 ft Prefix MA98
	130 to 230 ft MA99
	225 to 255 ft MC00
Instrument Calibration Date	July 11, 2001
Calibration Report	WHC-SD-EN-TI-306, Rev. 0

Analysis Information

Company	Three Rivers Scientific
Analyst	Russ Randall
Date	July 18, 2001
Notes	Moisture values range from 3% to 16% for the depths logged. No valid calibration is available for the 11 inch casing diameter from surface to 50 feet. Casing thickness (0.5") applied to depths logged.

RLS Neutron-Neutron Moisture

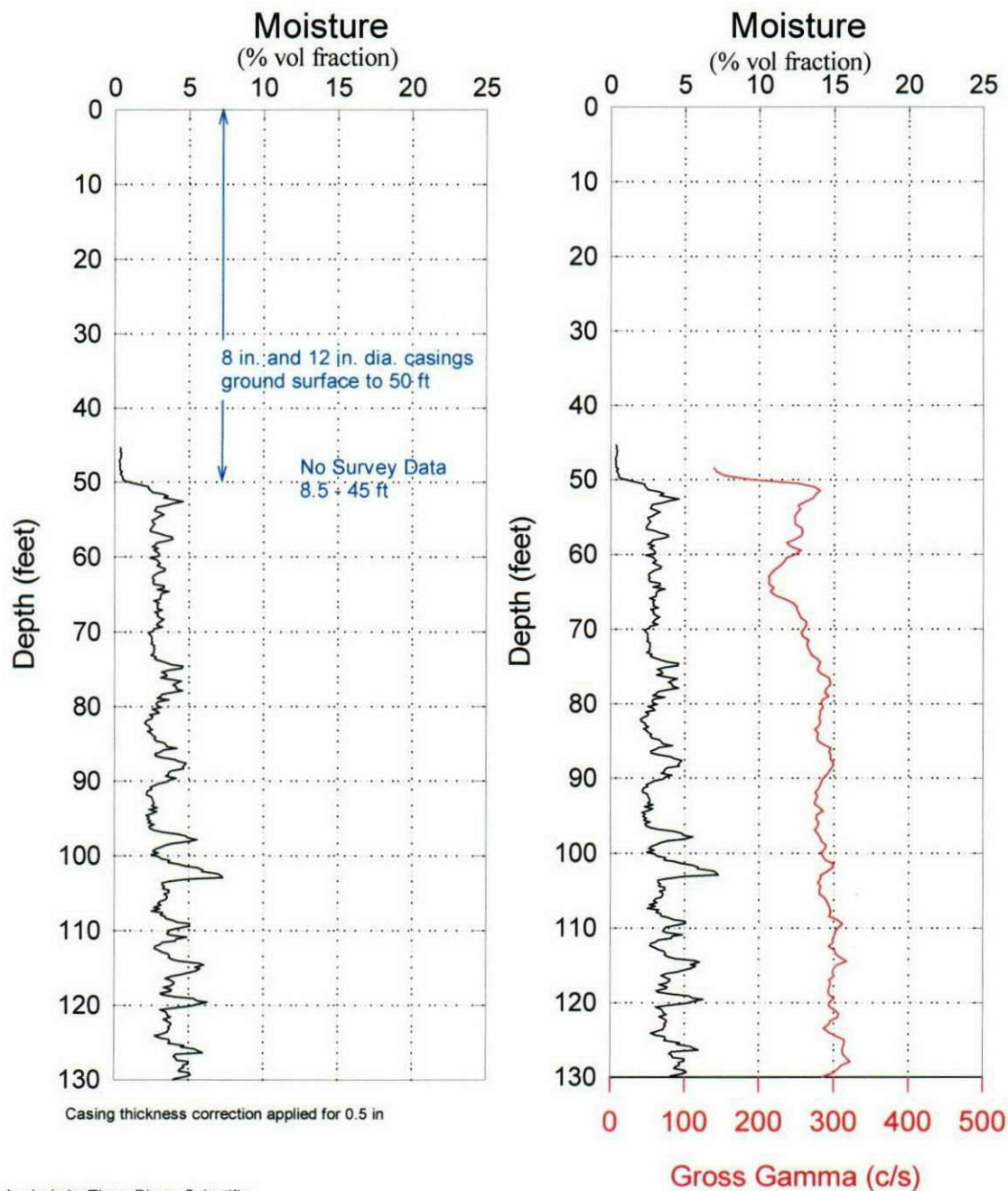
Duratek Federal Services

Project: 200 UP1

Log Date : July 15&16, 2001

Borehole: 299-W19-43

Depth Datum : Ground Surface



Analysis by Three Rivers Scientific

RLS Neutron-Neutron Moisture

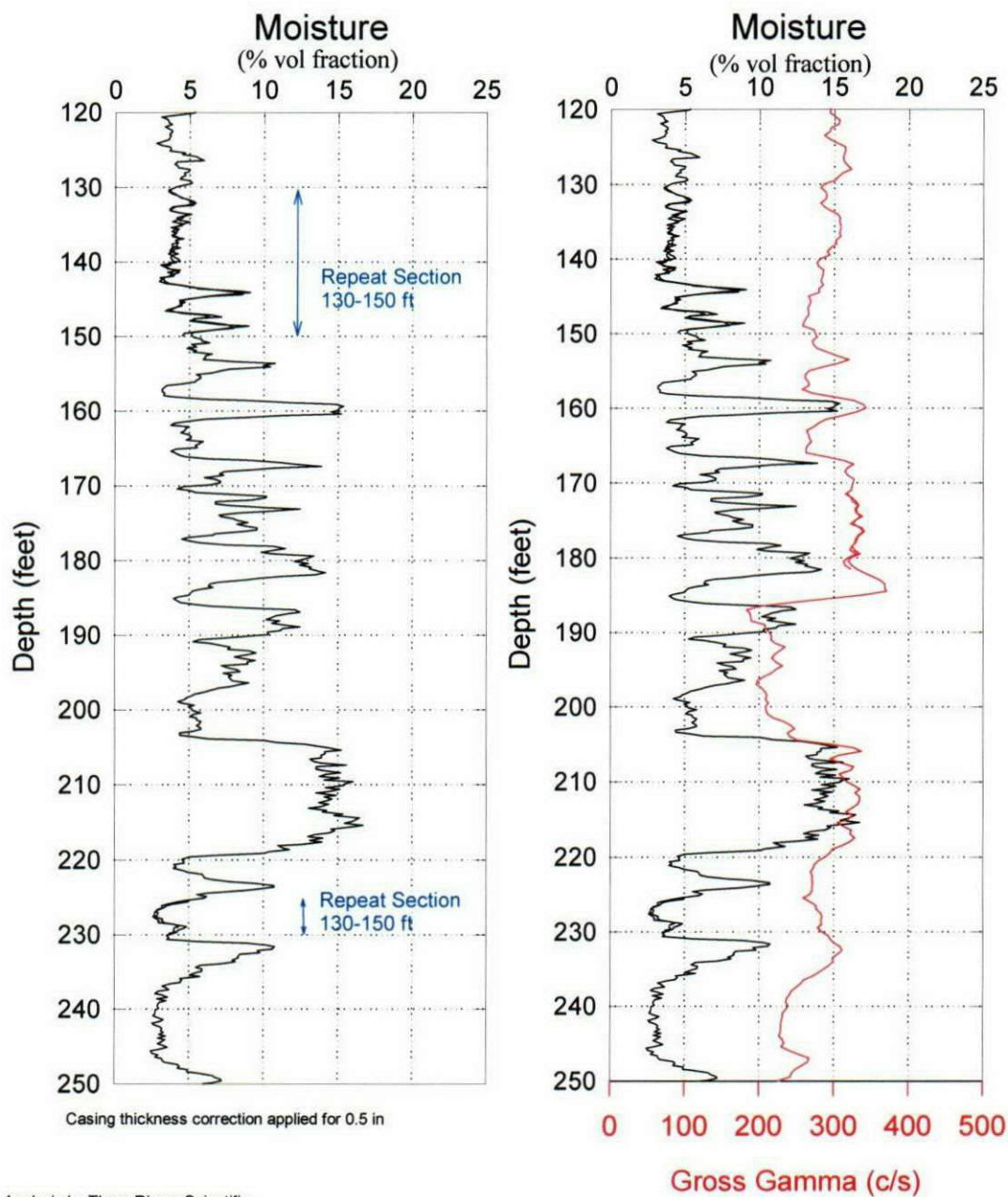
Duratek Federal Services

Project: 200 UP1

Log Date : July 15&16, 2001

Borehole: 299-W19-43

Depth Datum : Ground Surface



Analysis by Three Rivers Scientific

RLS Neutron-Neutron Moisture

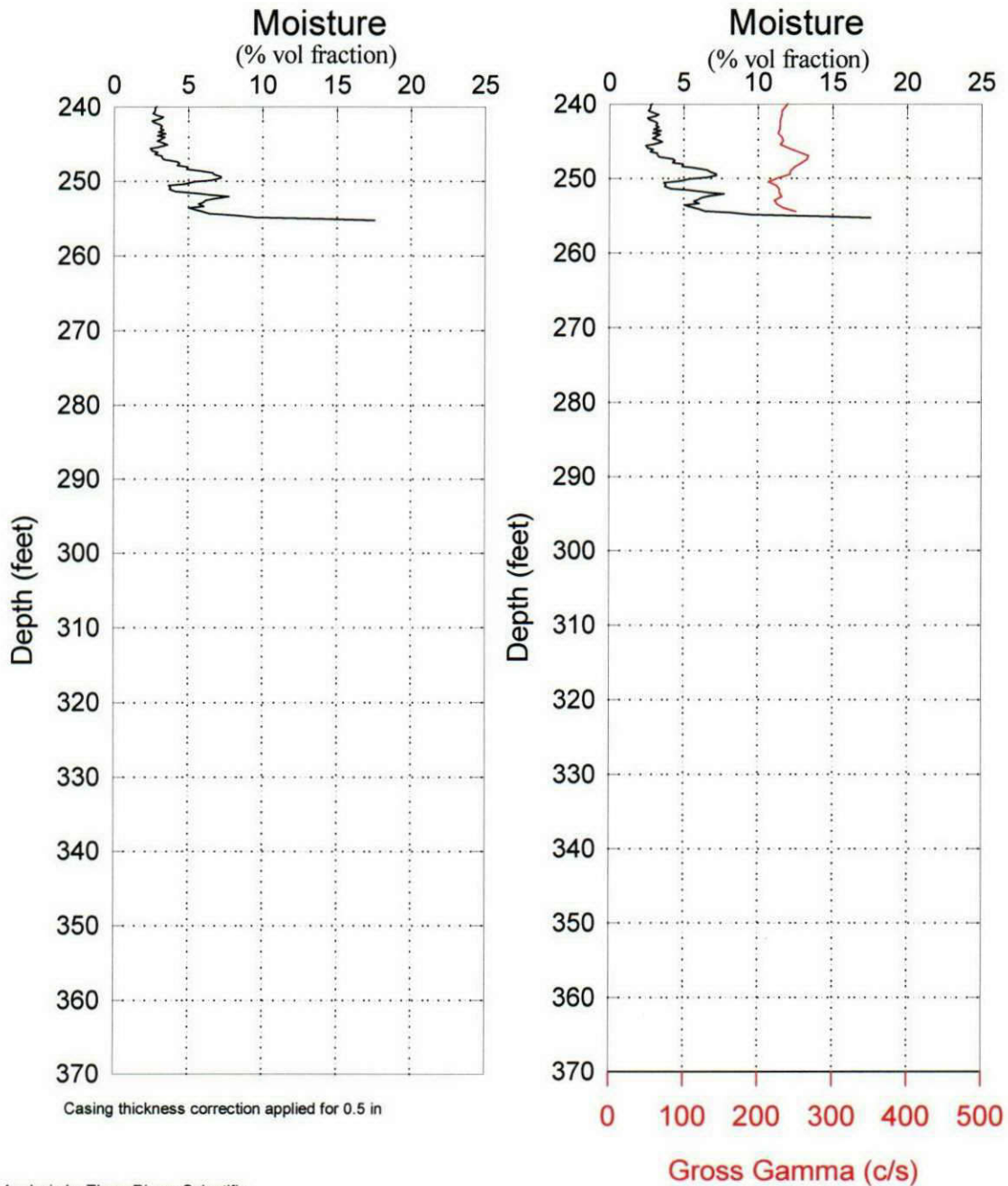
Duratek Federal Services

Project: 200 UP1

Log Date : July 15&16, 2001

Borehole: 299-W19-43

Depth Datum : Ground Surface



Moisture Log Analysis & Summary
Duratek Federal Services

Project: 200 UP1 Well ID: 299-W19-43
Log Type: Moisture Gauge Log Date: July 15&16, 2000

General Notes:

The 8 inch calibration coefficients were used for all logged depths. The 8 inch calibration standard has an 8.64 inch borehole diameter, with .32 inch casing thickness, and the borehole diameter in these log data is 8.625 inches. The depth interval from 0 to 50 feet has both the 8 inch and 10 inch casing. No calibration exists for the 10 inch casing.

Log data were collected with a depth reference of ground surface.

System Performance Verify: The pre- and post-log verification passed performance standards, 0.3% change from start of log to end of log, in the shield verify.

Repeat Interval: Based on the repeat interval from 130 to 150 feet and 225 to 230 feet, the logging system performed according to specifications.

Environmental Corrections: The moisture levels have been corrected for casing thickness (0.5 inch) for all well depths logged. No formation density correction has been applied because density values are not available.

Observations:

The moisture levels show values ranging from 3% to 16% for the depth interval from 50 feet to 255 feet.

A variable moisture structure shows from 75 to 255 feet. Over this depth interval, there is some correlation with the gross gamma signature, and sections with little correlation. Therefore, moisture content is sensitive to physical geologic conditions, while radionuclides variations are representative of mineralogy.

RLS Spectral Gamma Ray Borehole Survey

Duratek Federal Services

Log Header

Project: 200 UP1

Well: 299-W19-43

Log Type: HPGe Spectral Gamma Ray

Borehole Information

Well # <u>C3381</u>	Water Depth <u>none</u> ft	Total Depth <u>255</u> ft
Elevation Reference <u>n/a</u>	Elevation <u>n/a</u> ft	
Depth Reference <u>Ground Surface</u>	Casing Stickup <u>3.7</u> ft	
Casing Diameter <u>10.75</u> ID in	Depth Interval <u>0 to 50</u> ft	Thickness <u>0.5</u> in
Casing Diameter <u>7.625</u> ID in	Depth Interval <u>0 to 255</u> ft	Thickness <u>0.5</u> in

Logging Information

Log Type:	HPGe Spectral Gamma Ray	
Company	Duratek Federal Services	
Date/Archive File Name	July 16, 2001 H2W19043	
Logging Engineers	<u>J. Meisner</u>	<u>J. Kiesler</u>
Instrument Series	RLSG07000S00.0	
Logging Unit	RLS-1	
Depth Interval	48 to 181 ft	Prefix A726
	171 to 255 ft	A727
Instrument Calibration Date	Oct 6, 2000	
Calibration Report	WHC-SD-EN-TI-292, Rev 0.	

Analysis Information

Company	Three Rivers Scientific
Analyst	Russ Randall
Date	July 18, 2001
Notes	<u>No man-made contamination detected. The natural uranium levels are slightly higher than normal Hanford soils.</u>

RLS Spectral Gamma Ray Borehole Survey

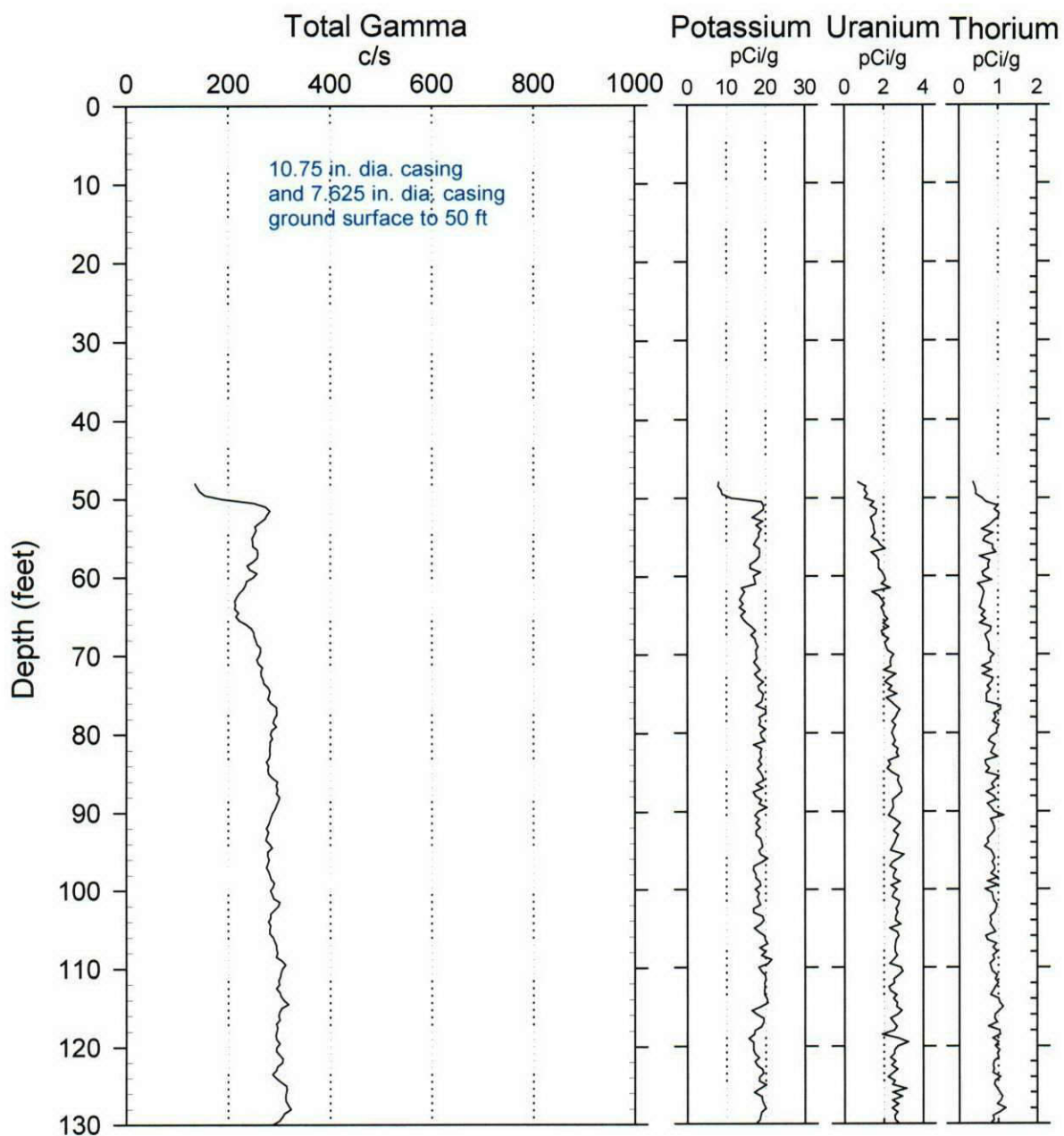
Duratek Federal Services

Project: 200 UP1

Log Date: July 16, 2001

Borehole: 299-W19-43

Naturally Occurring Radionuclides



RLS Spectral Gamma Ray Borehole Survey

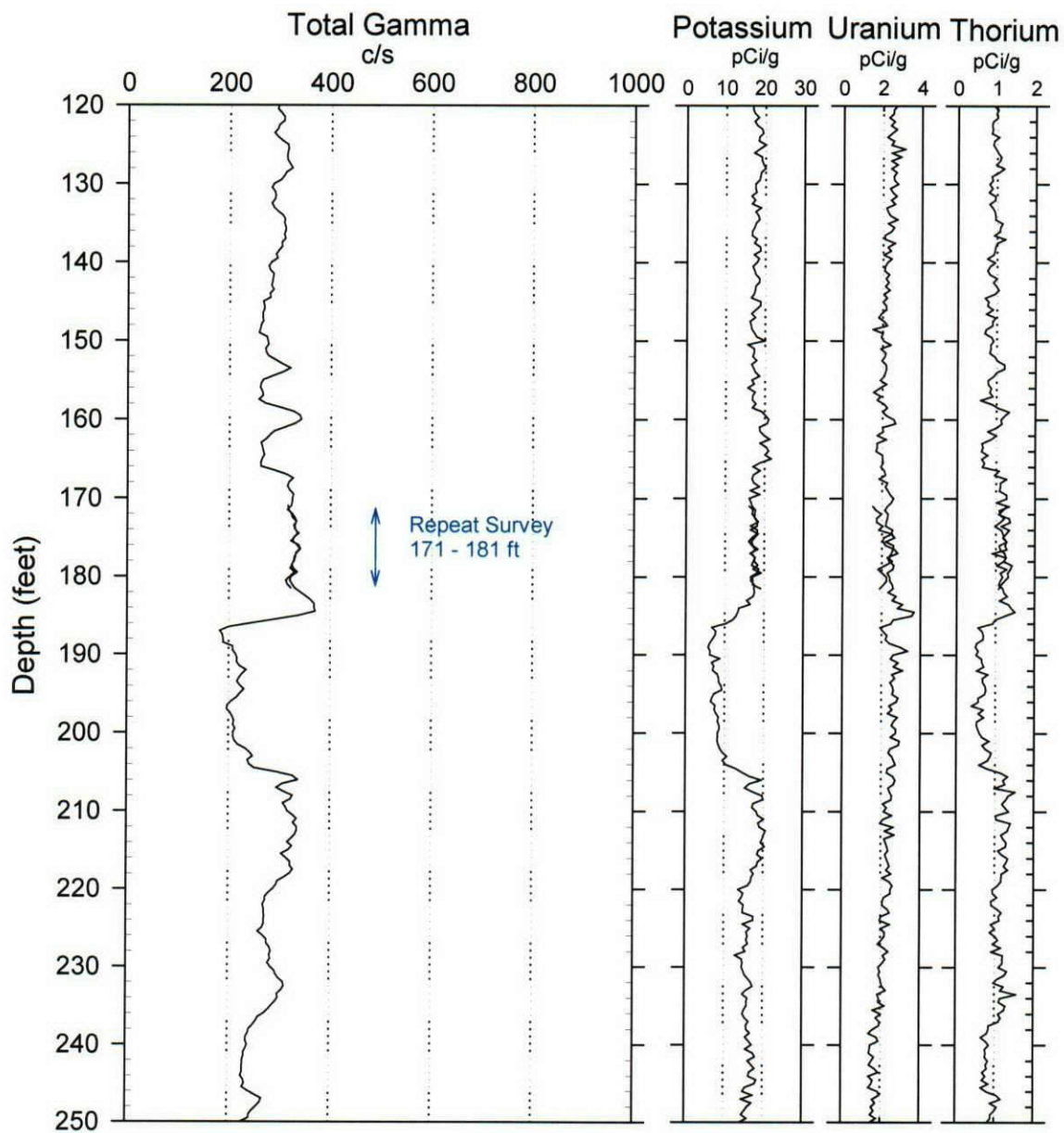
Duratek Federal Services

Project: 200 UP1

Log Date: July 16, 2001

Borehole: 299-W19-43

Naturally Occurring Radionuclides



RLS Spectral Gamma Ray Borehole Survey

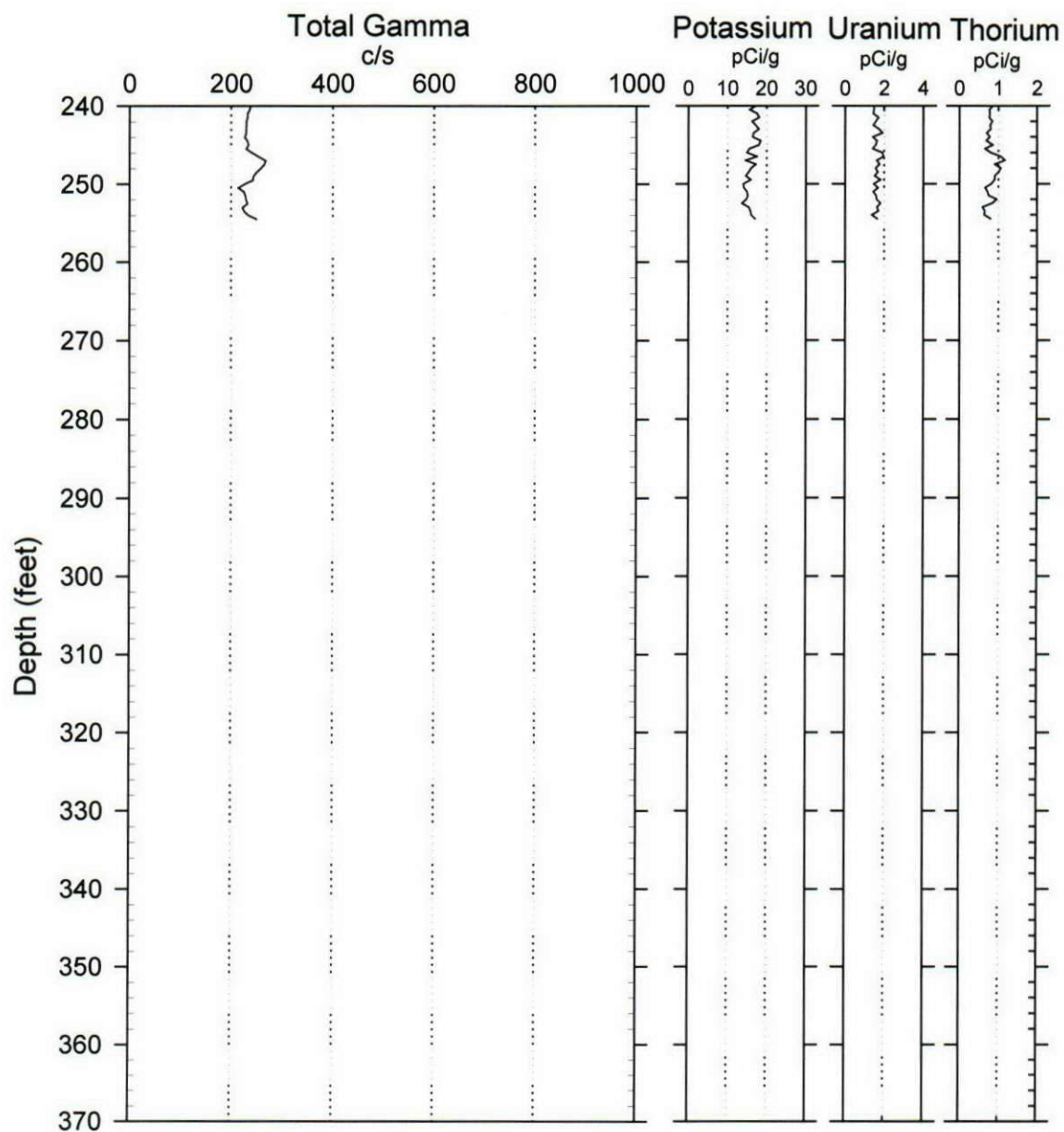
Duratek Federal Services

Project: 200 UP1

Log Date: July 16, 2001

Borehole: 299-W19-43

Naturally Occurring Radionuclides



RLS Spectral Gamma Ray Borehole Survey

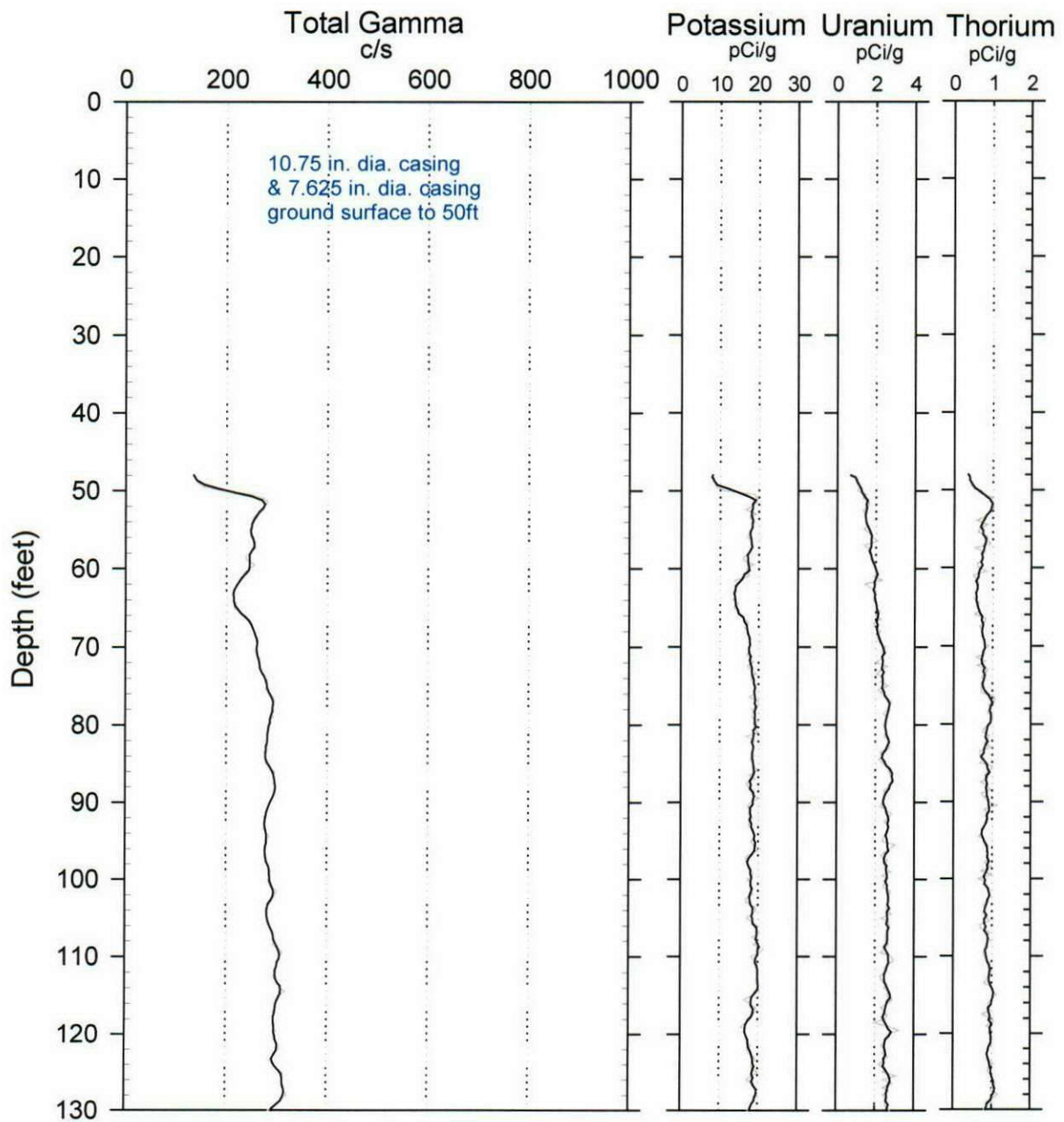
Duratek Federal Services

Project: 200 UP1

Log Date: July 16, 2001

Borehole: 299-W19-43

Naturally Occurring Radionuclides
Stacked



Analysis by: Three Rivers Scientific

RLS Spectral Gamma Ray Borehole Survey

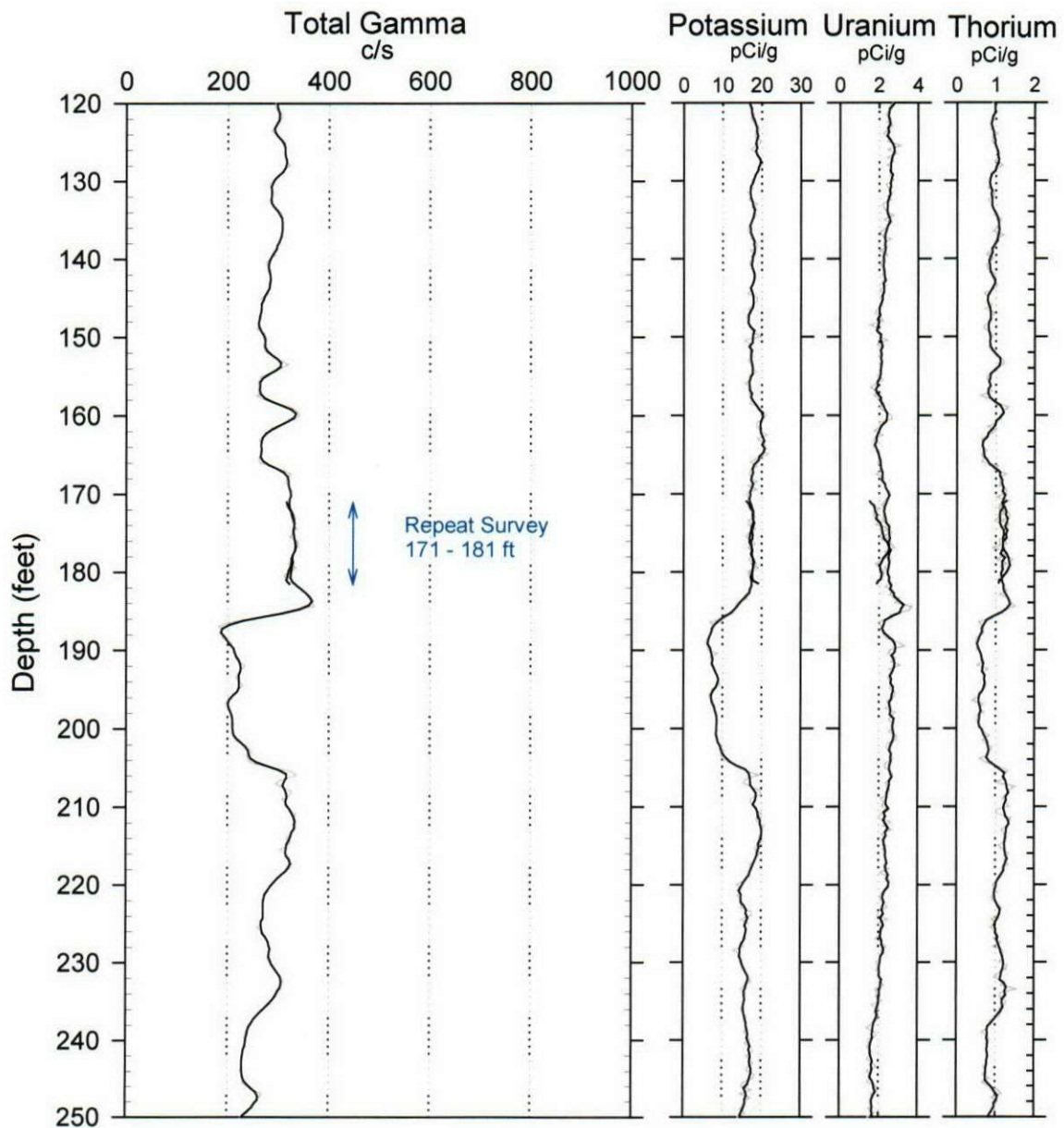
Duratek Federal Services

Project: 200 UP1

Log Date: July 16, 2001

Borehole: 299-W19-43

Naturally Occurring Radionuclides
Stacked



Analysis by: Three Rivers Scientific

RLS Spectral Gamma Ray Borehole Survey

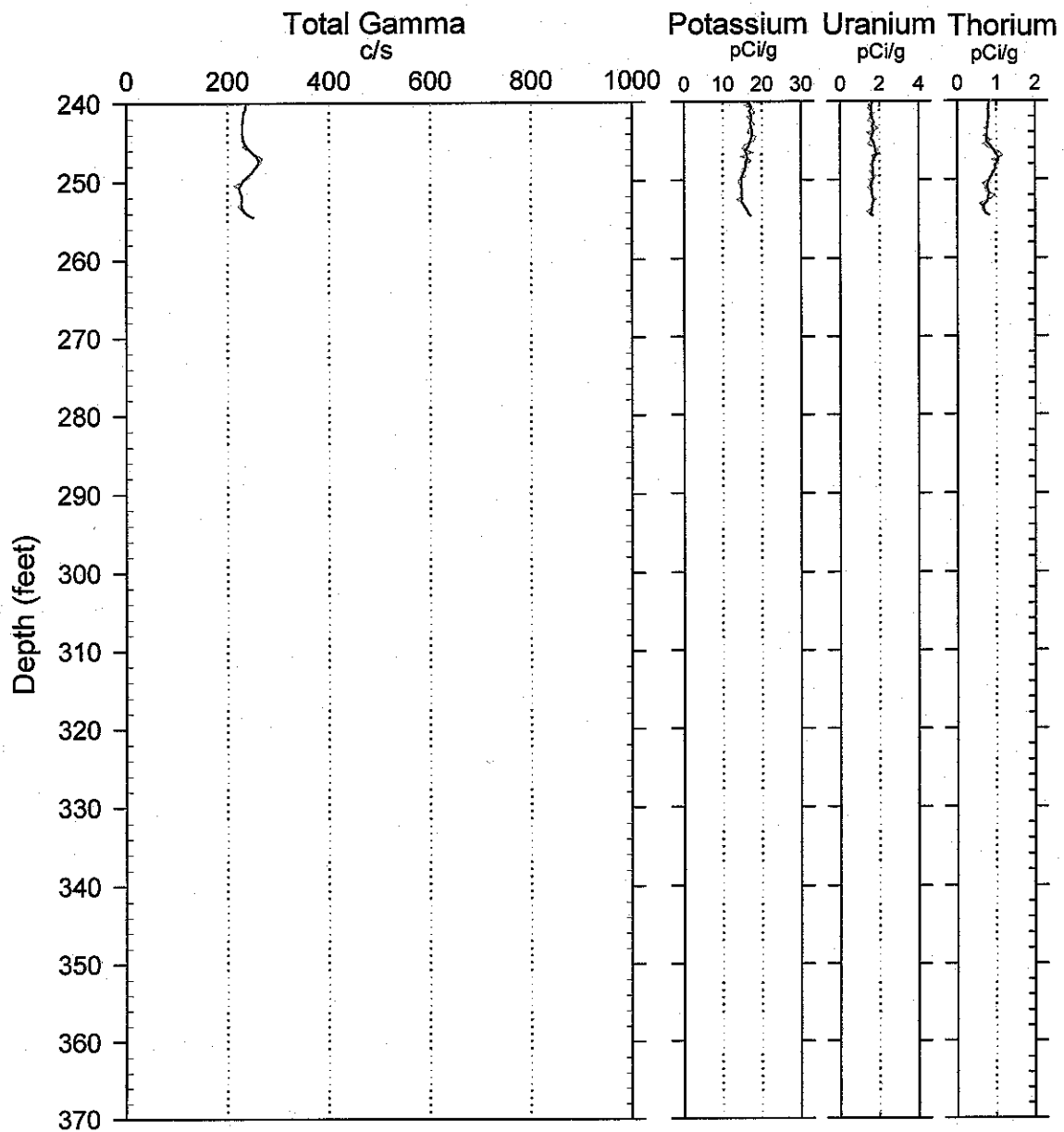
Duratek Federal Services

Project: 200 UP1

Log Date: July 16, 2001

Borehole: 299-W19-43

Naturally Occurring Radionuclides
Stacked



Analysis by: Three Rivers Scientific

Spectral Gamma Ray Log Analysis & Summary
Duratek Federal Services

Project: 200 UP1
Log Type: HPGe Spectral Gamma Ray

Well: 299-W19-43
Log Date: July 16, 2001

General Notes:

Total gamma is a response to geologic concentrations of natural radionuclides. A change in sensitivity of gross gamma to geologic concentrations of natural radionuclides occurs at dual casing change to single casing (50 ft).

Log data collected with a depth reference of ground surface.

System Performance Verify: The pre- and post-log verification passed performance standards; -3.5% and 2.3% changes were observed in the gross for each series run. The FWHM of the 583 keV photo peak was also within specifications for pre- and post-log verification.

Repeat Interval: Based on the repeat interval, the logging system performed as per specifications, for potassium and thorium (see notes below on radon pumping).

Environmental Corrections: All radionuclide concentrations have been corrected for casing attenuation (entire well). No water correction was applied, because water level was not reached. No casing correction was applied to the total gamma due to Compton downscatter interference.

Radionuclides:

No man-made radionuclide contamination was detected. This observation was confirmed using a summing technique for the spectral data. A stacking of spectra was performed to enhance the statistical precision of the KUT signals. Four adjacent spectra are summed and the depth is set at the mid-point of the beginning and ending spectra. This averages spectra over 2 feet vertical depth resolution, which is close to the inherent depth resolution of the gamma instrument. The next sum is performed over the 2nd through 5th spectra. Data processing is then performed over these summed spectra as normal.

The natural uranium concentration is slightly higher than normally observed for Hanford soils. No dis-equilibrium below radon, in the natural uranium series was observed within statistical uncertainty of the collected data. There is some indication of radon pumping causing real changes in uranium and gross. The repeat section experienced 1 hour and 18 minutes delay while refilling the tool with liquid nitrogen. Over this time interval, the uranium and gross did not repeat within statistical precision, but the potassium and thorium did repeat within statistical precision.

The changes in gross gamma from 150 to 255 feet are reflected by changes in potassium, uranium, and thorium; which is indicative of geologic effects. A stack plot is also included. The enhanced statistical precision of the stacked response allows a better view of the changes in KUT causing the changes in gross.

PLATES

Plate 1. Lithologic Data

Plate 2. Sediment Mineralogy

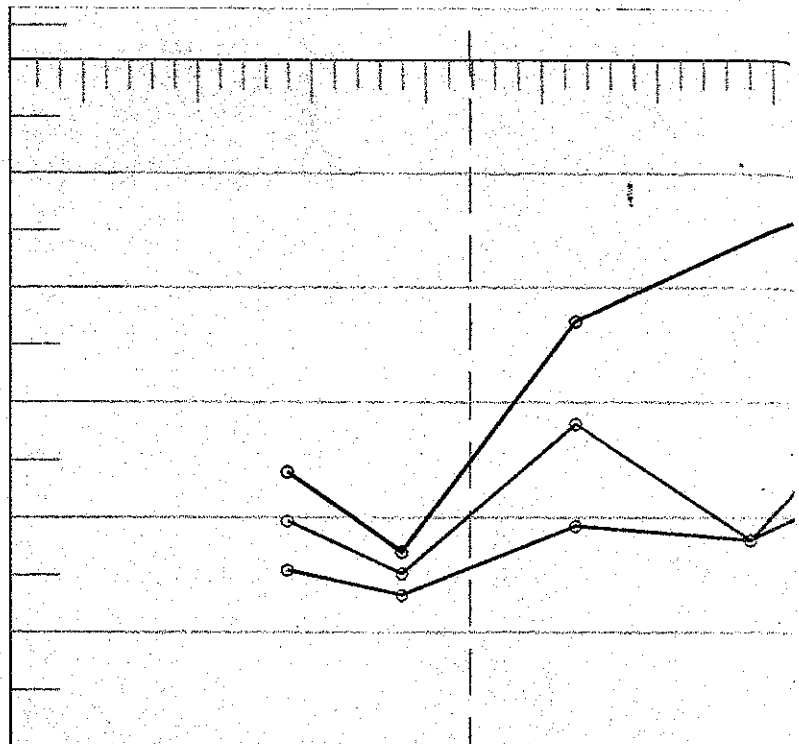
Plate 3. Groundwater Geochemical Data

Plate 4. Petrographic Analysis Data

ohm*m Ohm Meters

Scale 1" = 10'

▼ (257)

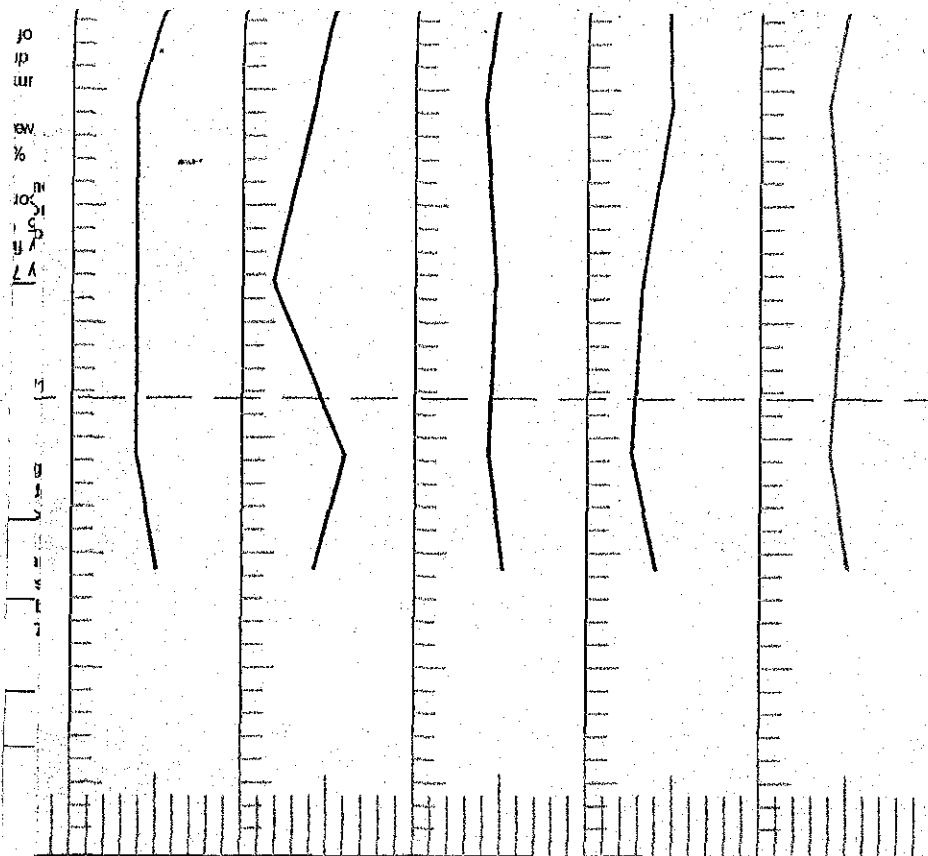


DRAFT ONLY

Plate 1: Lithologic Data

DRAWN BY: J. D. Bane		CHECKED BY:	
APPROVALS		RESPONSIBLE ENG.:	
PROJECT ENG.:		PROJECT MANAGER:	
CHIEF ENG.:			
HSE TECH. DIV. APPLICATIONS, INC. P.O. Box 4078 Burlington, VT 05402		HUM2-0801	
DWG. NO.		SHEET 1 OF 1	
CAD #		GROUP	
SPEC #		SCALE AS NOTED	

THIS DOCUMENT AND DATA AND INFORMATION IS
TO BE KEPT AS CONFIDENTIAL, NEITHER
THE CONTENTS NOR THE RESULTS THEREOF
SHALL BE DISCLOSED IN WHOLE OR IN PART WITHOUT
AUTHORIZATION FROM HSE IN



m²/g Meter Squared Per Gram

ohm*m Ohm Meters

pCi/g Pico Curie Per Gram

Scale 1" = 10'

DRAFT ONLY

Plate 2: Sediment Mineralogy

THIS DOCUMENT AND DATA AND INFORMATION IS
TO BE TREATED AS CONFIDENTIAL. NEITHER
THIS DOCUMENT NOR ANY INFORMATION OR DATA
THEREIN MAY BE REPRODUCED, USED, RELEASED
OR DISCLOSED IN WHOLE OR IN PART, WITHOUT
AUTHORIZATION FROM MSE TA.

DRAWN BY: d. bane

CHECKED BY:

APPROVALS

RESPONSIBLE ENG.:

PROJECT ENG.:

PROJECT MANAGER:

CHIEF ENG.:



TA, INC.
MSE TECHNOLOGY APPLICATIONS, INC.
P.O. Box 4878 (406) 494-7100
Butte, MT 59702

HANFORD SITE - 200 WEST AREA
Sediment Mineralogy
and Stratigraphic Column
BOREHOLE 299-W19-43

DWG. NO.

HUM2-1013

REV.

-

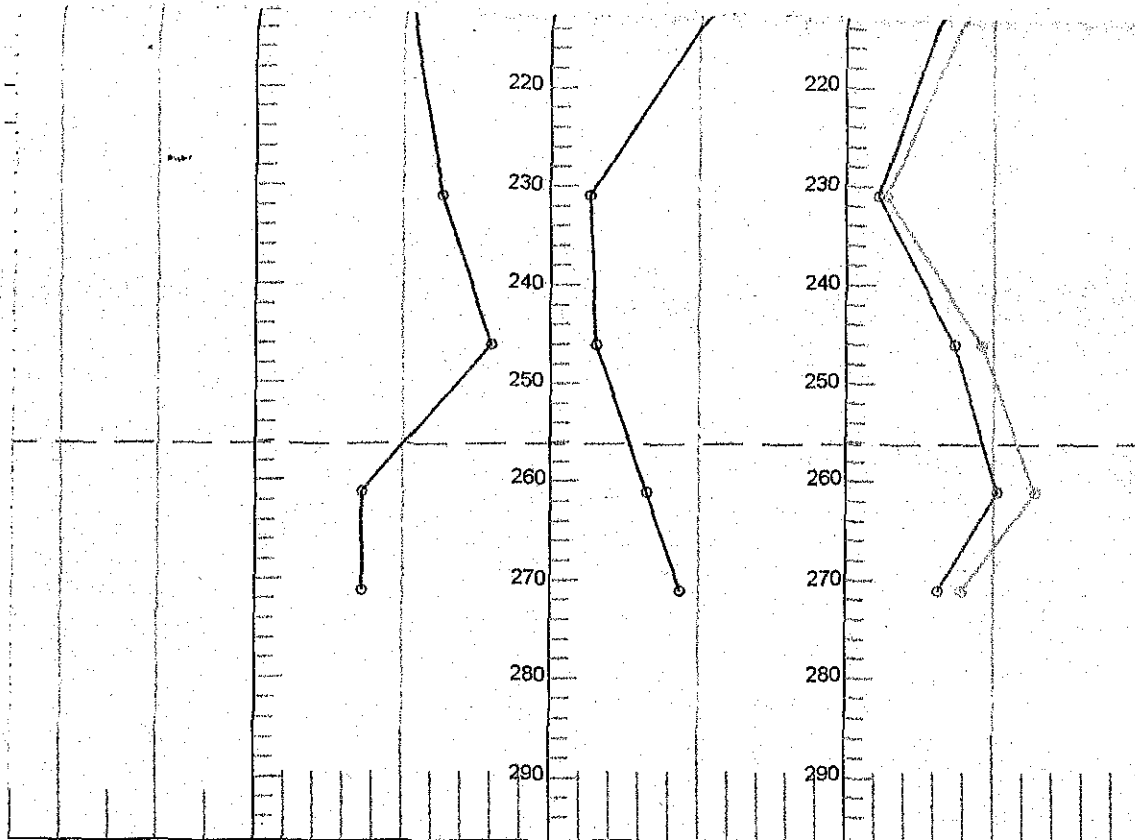
CAD # hum2-1013

SHEET 1 OF 1

GROUP

SPEC # SPEC

SCALE: AS NOTED



CPS Counts Per Second
 g/ccm Grams Per Cubic Centimeter
 m²/g Meter Squared Per Gram
 ohm*m Ohm Meters

Scale 1" = 10'

DRAFT ONLY

Plate 3: Porewater Geochemical Data

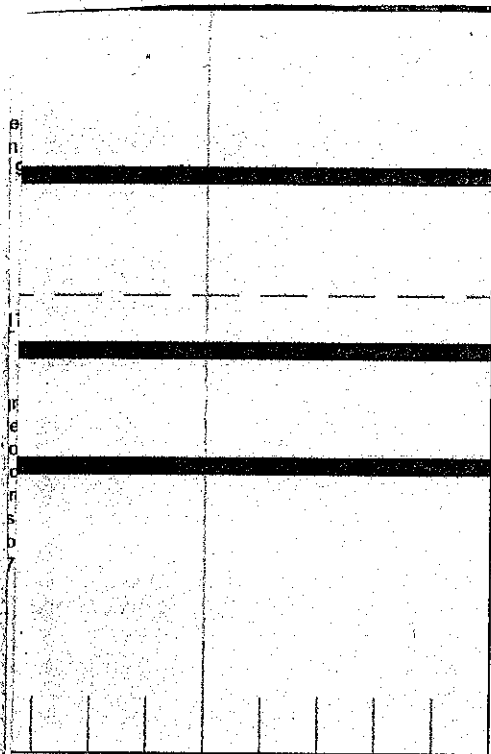
3 SO₄⁻²

THIS DOCUMENT AND DATA AND INFORMATION IS
 TO BE TREATED AS CONFIDENTIAL. NEITHER
 THIS DOCUMENT NOR ANY INFORMATION OR DATA
 THEREIN MAY BE REPRODUCED, USED, RELEASED
 OR DISCLOSED IN WHOLE OR IN PART, WITHOUT
 AUTHORIZATION FROM HSC TA.

DRAWN BY: J. BARR
 CHECKED BY:
 APPROVALS
 RESPONSIBLE ENG:
 PROJECT ENG:
 PROJECT MANAGER:
 CHIEF ENG:

HSC TA, INC.
 HSC TECHNOLOGY APPLICATIONS, INC.
 P.O. Box 4678
 Dulles, VA 20142

HANFORD SITE - 200 WEST AREA Porewater Geochemical Data and Stratigraphic Column BOREHOLE 299-W19-43		
OWG. NO.	REV.	
HUM2-1014	-	
CAD. # HUM2-1014	SHEET 1 of 1	GROUP
SPEC. # SPEC	SCALE: AS NOTED	



▼ (257')

Scale 1" = 10'

DRAFT ONLY

Plate 4: Petrographic Analyses Data

Carbonate ■ Magnetite-Ilmenite⁹

THIS DOCUMENT AND DATA AND INFORMATION IS TO BE TREATED AS CONFIDENTIAL, NEITHER THIS DOCUMENT NOR ANY INFORMATION OR DATA THEREIN MAY BE REPRODUCED, USED, RELEASED OR DISCLOSED IN WHOLE OR IN PART, WITHOUT AUTHORIZATION FROM MSE TA

DRAWN BY: d. bane
CHECKED BY:
APPROVALS
RESPONSIBLE ENG.:
PROJECT ENG.:
PROJECT MANAGER:
CHIEF ENG.:

MSE TA, INC.
MSE TECHNOLOGY APPLICATIONS, INC.
P.O. Box 4078 (406) 494-7100
Butte, MT 59702

HANFORD SITE - 200 WEST AREA
Lithologic Data
and Stratigraphic Column
BOREHOLE 299-W19-43

DWG. NO.	HUM2-0816	REV.	-
CAD #	hum2-0816	SHEET	1 OF 1
SPEC #	SPEC	SCALE:	AS NOTED
		GROUP	